

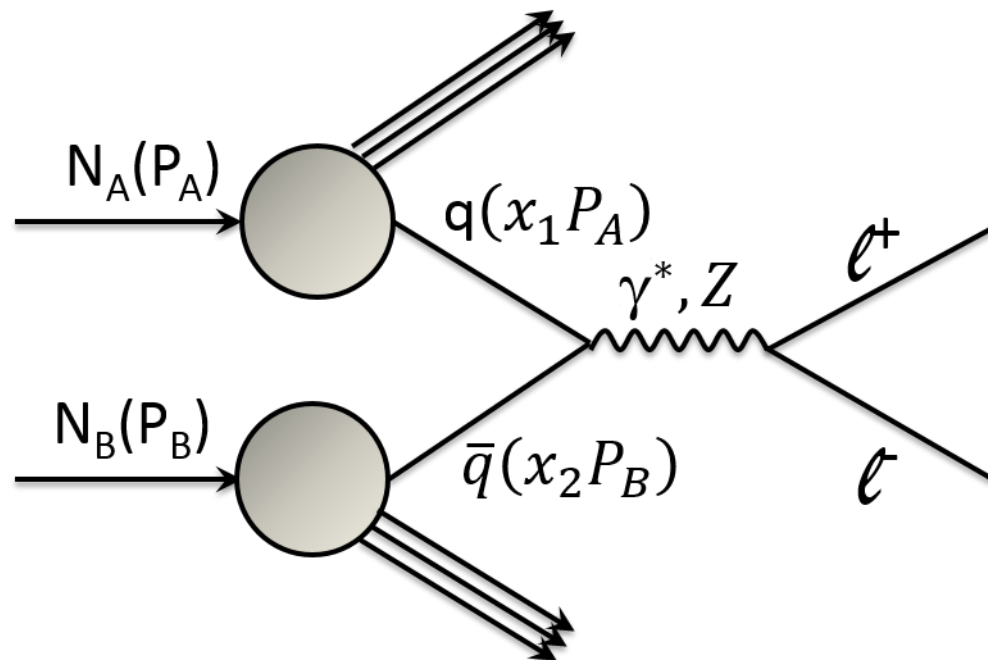
Spinfest 2015

July 13, 2015, Tokai, Ibaraki, Japan

Study of Nucleon Partonic Structure in Drell-Yan Process at J-PARC

Wen-Chen Chang

Institute of Physics, Academia Sinica, Taiwan

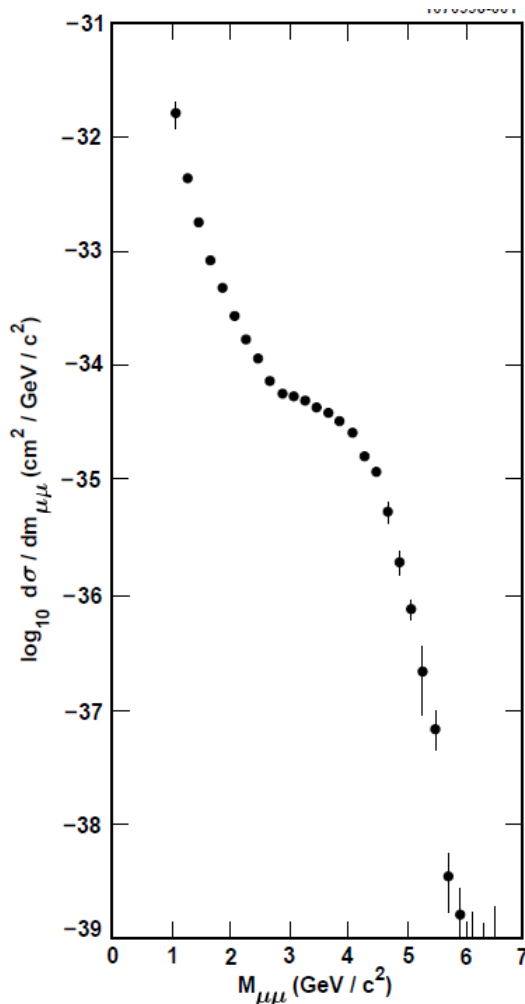


Outline

- **Introduction of Drell-Yan Process:**
 - History & Formalism
 - Success and Failure
 - QCD effect
- **Parton Density Function (PDF)**
 - Flavor asymmetry of sea quarks (E906/SeaQuest Experiment)
 - LHC W, Z production: strangeness and charm
 - RHIC W production: polarization of sea quarks
- **Transverse-Momentum-Dependent Distribution (TMD)**
 - Sivers function (COMPASS Experiment)
 - Boer-Mulders function (E866/COMPASS Experiment)
- **Generalized Parton Distribution (GPD)**
 - Exclusive Drell-Yan process (J-PARC Proposal)
- Summary
- References

Massive Dimuon Pairs in Hadron Collisions

J.H. Christenson et al., PRL 25 (1970) 1523



- Target: $p+U \rightarrow V+X$
- Found: $p+U \rightarrow \mu\mu + X$
- Observation:
 - Shoulder-like structure around 3 GeV.
 - Evidence of J/ψ was absent due to bad momentum resolution.
 - Rapid fall-off of cross section with the dimuon mass ($\sim 1/M^5$).

The Drell-Yan Process

S.D. Drell and T.M. Yan, PRL 25 (1970) 316



MASSIVE LEPTON-PAIR PRODUCTION IN HADRON-HADRON COLLISIONS AT HIGH ENERGIES*

Sidney D. Drell and Tung-Mow Yan

Stanford Linear Accelerator Center, Stanford University, Stanford, California 94305

(Received 25 May 1970)

On the basis of a parton model studied earlier we consider the production process of large-mass lepton pairs from hadron-hadron inelastic collisions in the limiting region, $s \rightarrow \infty$, Q^2/s finite, Q^2 and s being the squared invariant masses of the lepton pair and the two initial hadrons, respectively. General scaling properties and connections with deep inelastic electron scattering are discussed. In particular, a rapidly decreasing cross section as $Q^2/s \rightarrow 1$ is predicted as a consequence of the observed rapid falloff of the inelastic scattering structure function νW_2 near threshold.

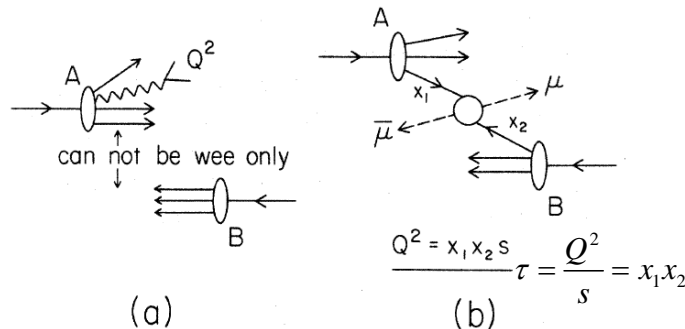


FIG. 1. (a) Production of a massive pair Q^2 from one of the hadrons in a high-energy collision. In this case it is kinematically impossible to exchange "wee" partons only. (b) Production of a massive pair by parton-antiparton annihilation.

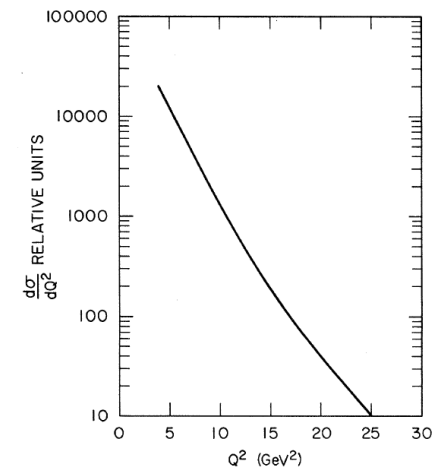


FIG. 2. $d\sigma/dQ^2$ computed from Eq. (10) assuming identical parton and antiparton momentum distributions and with relative normalization.

$$\frac{d\sigma}{dQ^2} = \left(\frac{4\pi\alpha^2}{3Q^2} \right) \left(\frac{1}{Q^2} \right) \mathcal{F}(\tau) = \left(\frac{4\pi\alpha^2}{3Q^2} \right) \left(\frac{1}{Q^2} \right) \int_0^1 dx_1 \int_0^1 dx_2 \delta(x_1 x_2 - \tau) \sum_a \lambda_a^{-2} F_{2a}(x_1) F_{2\bar{a}}'(x_2),$$

Drell-Yan “naïve” Parton Model

T.M. Yan, hep-ph/9810268

- Sid and I got interested in the process for two reasons:
 - (1) we were looking for application of the parton model outside deep inelastic lepton scatterings, and
 - (2) we wanted to understand if the rapid decrease of the cross section with the muon pair mass could be reconciled with the point-like cross sections observed in the deep inelastic electron scattering.

Drell-Yan “naïve” Parton Model

T.M. Yan, hep-ph/9810268

- The key idea in our approach was the **impulse approximation**.
- In infinite momentum frame,
 $\tau_{\text{probe}} \ll \tau_{\text{initial state}}$. The constituents could be treated as free.
- The cross section in the impulse approximation is a product of the probability to find the particular parton configuration and the cross section for the free parton(s).

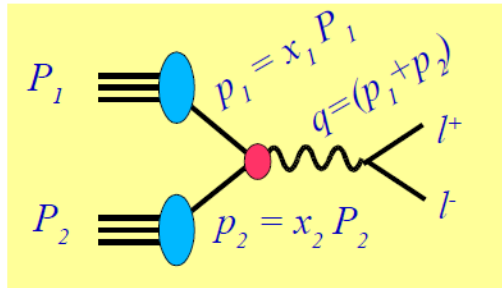
Drell-Yan “naïve” Parton Model

T.M. Yan, [hep-ph/9810268](#)

- It is interesting to note that our original crude fit did not even remotely resemble the data. Sid and I went ahead to publish our paper because of the model’s simplicity and our belief that future experiments would be able to definitively confirm or demolish the model.

Formalism (I)

Kinematics in the Hadronic Frame



$$P_1 = \frac{\sqrt{s}}{2} (1, 0, 0, +1) \quad P_1^2 = 0$$

$$P_2 = \frac{\sqrt{s}}{2} (1, 0, 0, -1) \quad P_2^2 = 0$$

$$s = (P_1 + P_2)^2 = \frac{\hat{s}}{x_1 x_2} = \frac{\hat{s}}{\tau}$$

Therefore

$$\tau = x_1 x_2 = \frac{\hat{s}}{s} \equiv \frac{Q^2}{s}$$

Fractional energy² between partonic and hadronic system

$$\frac{d\sigma}{dQ^2} = \sum_{q, \bar{q}} \int dx_1 \int dx_2 \{q(x_1)\bar{q}(x_2) + \bar{q}(x_1)q(x_2)\} \hat{\sigma}_0 \delta(Q^2 - \hat{s})$$

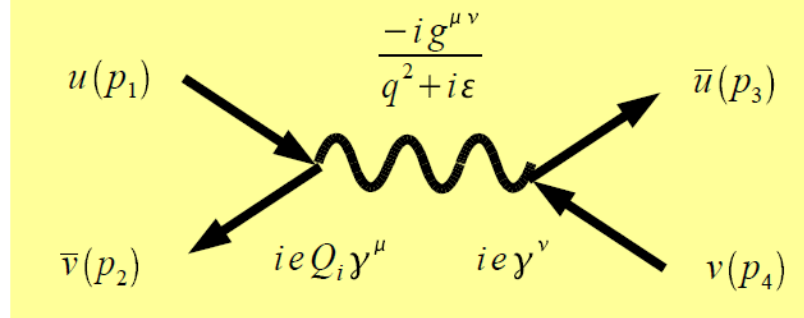
Hadronic cross section

Parton distribution functions

Partonic cross section

Formalism (2)

Let's compute the Born process: $q + \bar{q} \rightarrow e^+ + e^-$



Gathering factors and contracting $g^{\mu\nu}$, we obtain:

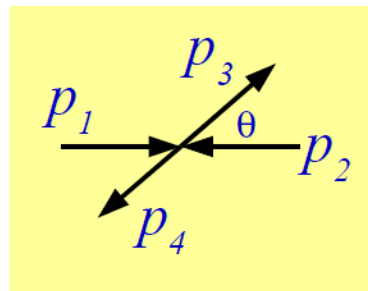
$$-iM = iQ_i \frac{e^2}{q^2} \{\bar{v}(p_2)\gamma^\mu u(p_1)\} \{\bar{u}(p_3)\gamma_\mu v(p_4)\}$$

Squaring, and averaging over spin and color, ...

$$|\overline{M}|^2 = \left(\frac{1}{2}\right)^2 3 \left(\frac{1}{3}\right)^2 Q_i^2 \frac{e^4}{q^4} \text{Tr}[\not{p}_2 \gamma^\mu \not{p}_1 \gamma^\nu] \text{Tr}[\not{p}_3 \gamma_\mu \not{p}_4 \gamma_\nu]$$

Formalism (3)

Let's work out some parton level kinematics



$$p_1^2 = p_2^2 = p_3^2 = p_4^2 = 0$$

$$p_1 = \frac{\sqrt{\hat{s}}}{2} (1, 0, 0, +1)$$

$$p_2 = \frac{\sqrt{\hat{s}}}{2} (1, 0, 0, -1)$$

$$p_3 = \frac{\sqrt{\hat{s}}}{2} (1, +\sin(\theta), 0, +\cos(\theta))$$

$$p_4 = \frac{\sqrt{\hat{s}}}{2} (1, -\sin(\theta), 0, -\cos(\theta))$$

Defining the Mandelstam variables ...

$$\hat{s} = (p_1 + p_2)^2 = (p_3 + p_4)^2$$

$$\hat{t} = (p_1 - p_3)^2 = (p_2 - p_4)^2$$

$$\hat{u} = (p_1 - p_4)^2 = (p_2 - p_3)^2$$

$$\hat{t} = -\frac{\hat{s}}{2} (1 - \cos(\theta))$$

$$\hat{u} = -\frac{\hat{s}}{2} (1 + \cos(\theta))$$

Formalism (4)

We'll now compute the matrix element M

Manipulating the traces, we find ...

$$\begin{aligned}
 & \text{Tr}[\not{p}_2 \not{\gamma}^\mu \not{p}_1 \not{\gamma}^\nu] \text{Tr}[\not{p}_3 \not{\gamma}_\mu \not{p}_4 \not{\gamma}_\nu] \\
 &= 4[p_1^\mu p_2^\nu + p_2^\mu p_1^\nu - g^{\mu\nu}(p_1 \cdot p_2)] \times 4[p_3^\mu p_4^\nu + p_4^\mu p_3^\nu - g^{\mu\nu}(p_3 \cdot p_4)] \\
 &= 2^5 [(p_1 \cdot p_3)(p_2 \cdot p_4) + (p_1 \cdot p_4)(p_2 \cdot p_3)] \\
 &= 2^3 [\hat{t}^2 + \hat{u}^2]
 \end{aligned}$$

Where we have used:

$$p_1^2 = p_2^2 = p_3^2 = p_4^2 = 0$$

$$\hat{s} = 2(p_1 \cdot p_2) = 2(p_3 \cdot p_4)$$

$$\hat{t} = 2(p_1 \cdot p_3) = 2(p_2 \cdot p_4)$$

$$\hat{u} = 2(p_1 \cdot p_4) = 2(p_2 \cdot p_3)$$

Putting all the pieces together, we have:

$$|\overline{M}|^2 = Q_i^2 \alpha^2 \frac{2^5 \pi^2}{3} \left(\frac{\hat{t}^2 + \hat{u}^2}{\hat{s}^2} \right) \quad \text{with}$$

$$q^2 = (p_1 + p_2)^2 = \hat{s}$$

$$\alpha = \frac{e^2}{4\pi}$$

Formalism (5)

... and put it together to find the cross section

$$d\hat{\sigma} \simeq \frac{1}{2\hat{s}} \overline{|M|^2} d\Gamma$$

In the partonic
CMS system

$$d\Gamma = \frac{d^3 p_3}{(2\pi)^3 2E_3} \frac{d^3 p_4}{(2\pi)^3 2E_4} (2\pi)^4 \delta(p_1 + p_2 - p_3 - p_4) = \frac{d\cos(\theta)}{16\pi}$$

Recall,

$$\hat{t} = \frac{-\hat{s}}{2} (1 - \cos(\theta)) \quad \text{and} \quad \hat{u} = \frac{-\hat{s}}{2} (1 + \cos(\theta))$$

so, the differential cross section is ...

$$\frac{d\hat{\sigma}}{d\cos(\theta)} = Q_i^2 \alpha^2 \frac{\pi}{6} \frac{1}{\hat{s}} (1 + \cos^2(\theta))$$

and the total cross section is ...

$$\hat{\sigma} = Q_i^2 \alpha^2 \frac{\pi}{6} \frac{1}{\hat{s}} \int_{-1}^1 d\cos(\theta) (1 + \cos^2(\theta)) = \frac{4\pi\alpha^2}{9\hat{s}} Q_i^2 \equiv \hat{\sigma}_0$$

Predictions for Drell-Yan Process

I.R. Kenyon, Rep. Prog. Phys. 45 (1982) 1261

- Scaling: cross sections scales with $\tau = Q^2/s$
- Decay angular distributions: $1 + \cos^2\theta$
- A-dependence of cross sections: $\sim A^1$
- Transverse momentum distributions: intrinsic parton p_T should be small (~ 300 - 500 MeV).

Drell-Yan Experiments

<http://hepdata.cedar.ac.uk/review/dy/>

[Home Page](#)
[Other Data Reviews](#)
[Reaction Database](#)

CONTENTS

HEPDATA
ON-LINE
DATA
REVIEW

Compilation of Data on Drell Yan Production Cross Sections .

EP publication:

[W J Stirling and M R Whalley 1993 J.Phys.G.Nucl.Part.Phys: 19 D1-D102](#)

HEPDATA
ON-LINE
DATA
REVIEW

Experiments

[CERN-NA3](#)
[CERN-NA10](#)
[CERN-WA11](#)
[CERN-WA39](#)
[CERN-R108](#)
[CERN-R209](#)
[CERN-R808](#)
[CERN-UA2](#)
[Fermilab-E288](#)
[Fermilab-E325](#)
[Fermilab-E326](#)
[Fermilab-E439](#)
[Fermilab-E444](#)
[Fermilab-E537](#)
[Fermilab-E605](#)
[Fermilab-F615](#)
[Fermilab-E740\(D0\)](#)
[Fermilab-E741\(CDF\)](#)
[Fermilab-E772](#)
[Fermilab-E866\(NUSEA\)](#)

Measurements of:-

[p p -> mu+ mu- X](#)
[p p -> e+ e- X](#)
[pbar p -> mu+ mu- X](#)
[pbar p -> e+ e- X](#)
[p Nucleus -> mu+ mu- X](#)
[pbar Nucleus -> mu+ mu- X](#)
[pi+ Nucleus -> mu+ mu- X](#)
[pi- Nucleus -> mu+ mu- X](#)

This is an archive of experimental data on Drell Yan production cross sections. Data are given in both tabular and graphical form for invariant cross sections and transverse momentum distributions from experiments at CERN and Fermilab.

Select data from a specific experimental collaboration:

CERN	Fermilab
NA3	E288
NA10	E325
WA11	E326
WA39	E439
R108	E444
R209	E537
R808	E605
UA2	E615
	E740(D0)
	E741(CDF)
	E772
	E866(NUSEA)

or select data for a specific measurement:

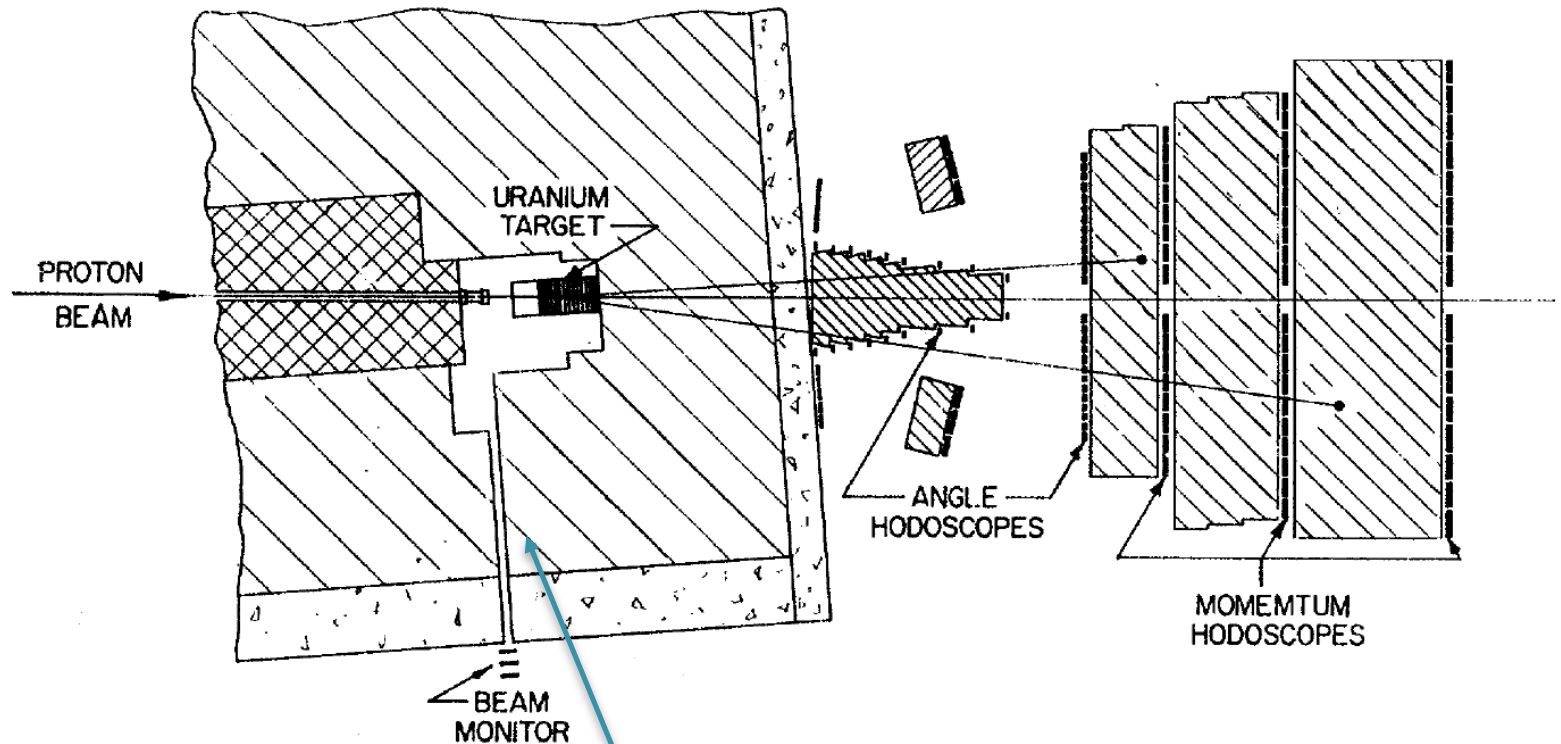
Measurement	Measurement
p p -> mu+ mu- X	p Nucleus -> mu+ mu- X
p p -> e+ e- X	pbar Nucleus -> mu+ mu- X
pbar p -> mu+ mu- X	pi+ Nucleus -> mu+ mu- X
pbar p -> e+ e- X	pi- Nucleus -> mu+ mu- X

Please send any comments on this service to hepdata@projects.hepforge.org

Massive Dimuon Pairs in Hadron Collisions

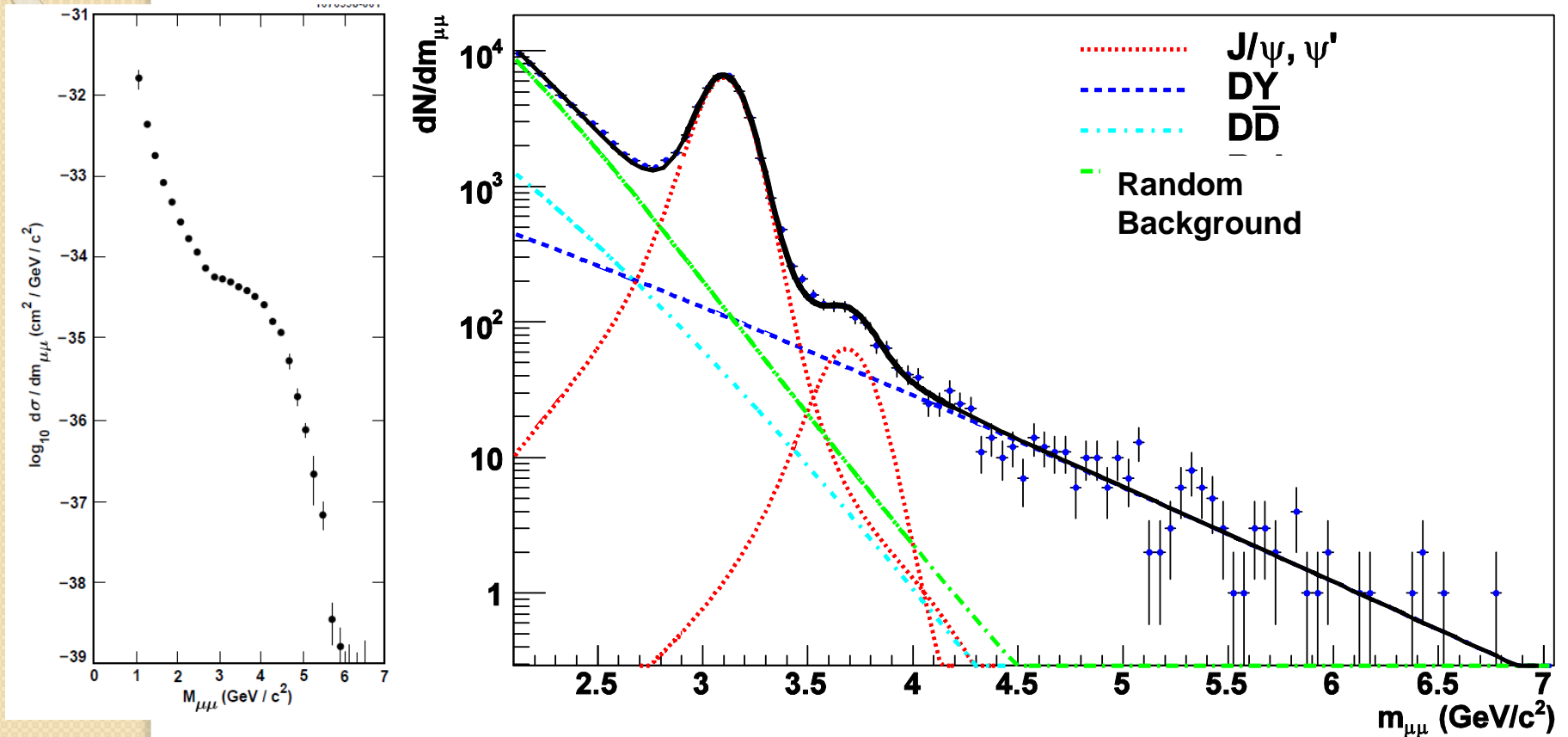
J.H. Christenson et al., PRL 25 (1970) 1523

$$(\vec{P}^{\mu^+}, \vec{P}^{\mu^-})|_{lab, S} \Rightarrow (M^{\gamma^*}, X_F^{\gamma^*}, X_1^q, X_2^{\bar{q}})|_{CMS}$$



Hadron absorber

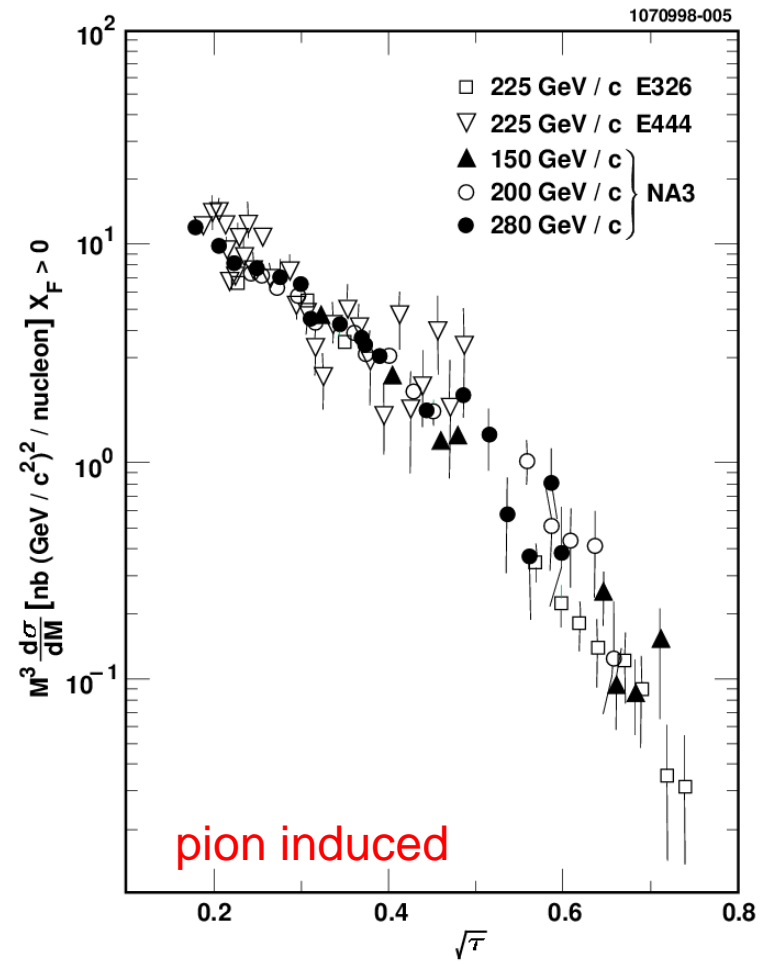
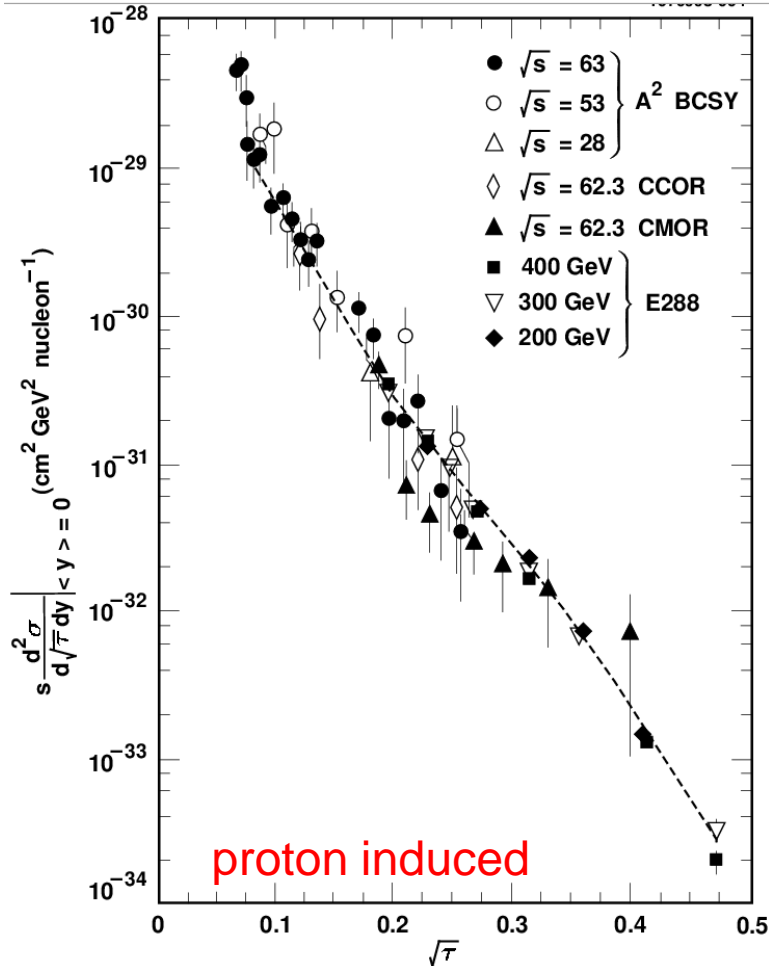
Dimuon Invariant Mass Spectrum



Indium-Indium collisions at 158 GeV/nucleon
NA60, PRL 99 (2007) 132302

Scaling

T.M. Yan, hep-ph/9810268



A-dependence of Cross Sections

CIP, PRL 42 (1979) 944

The quark-antiquark annihilation that produces dileptons is a point-like electromagnetic interaction; the cross section on a nucleus is the incoherent sum of the cross section on its component nucleons and will be proportional to **A**, the atomic number.

$$\sigma(A) \propto A^\alpha$$

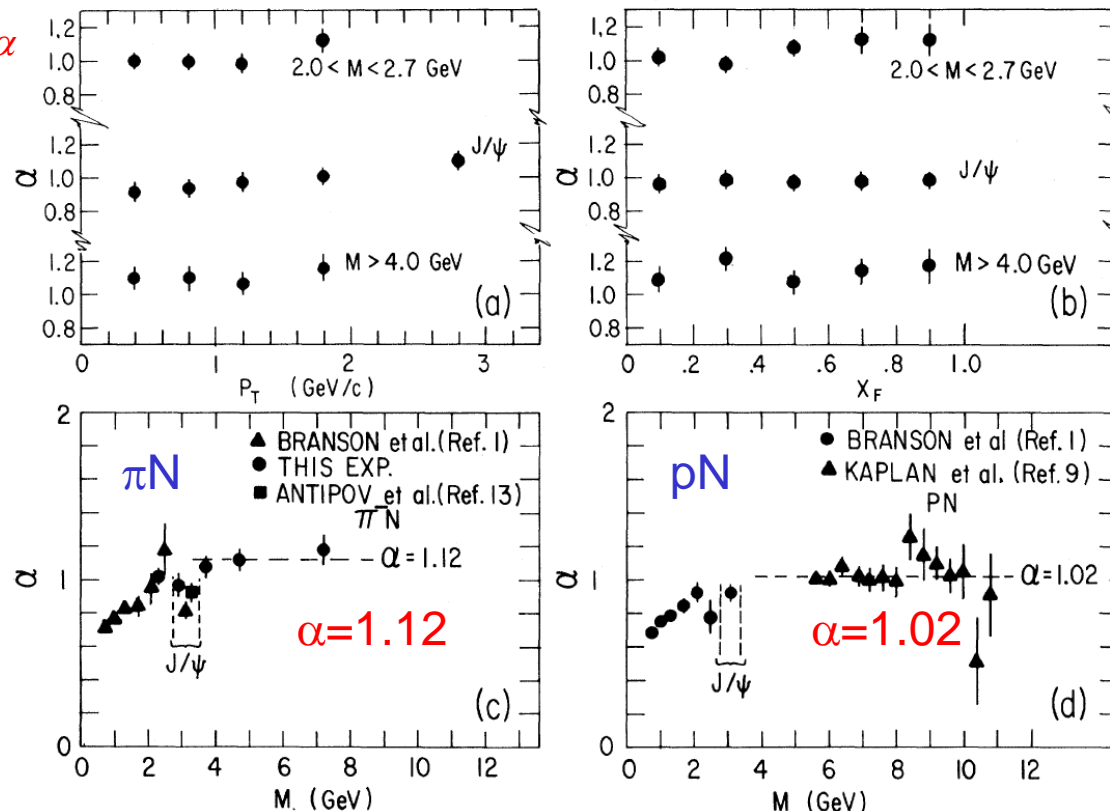


FIG. 4. The atomic mass number dependence A^α is displayed for $\pi^- N \rightarrow \mu^+ \mu^- X$. (a) α vs transverse momentum of the muon pair. (b) α vs x_F . (c) α vs M . (d) α vs M for $p N \rightarrow \mu^+ \mu^- X$.

Angular Distribution

I.R. Kenyon, Rep. Prog. Phys. 45 (1982) 1261

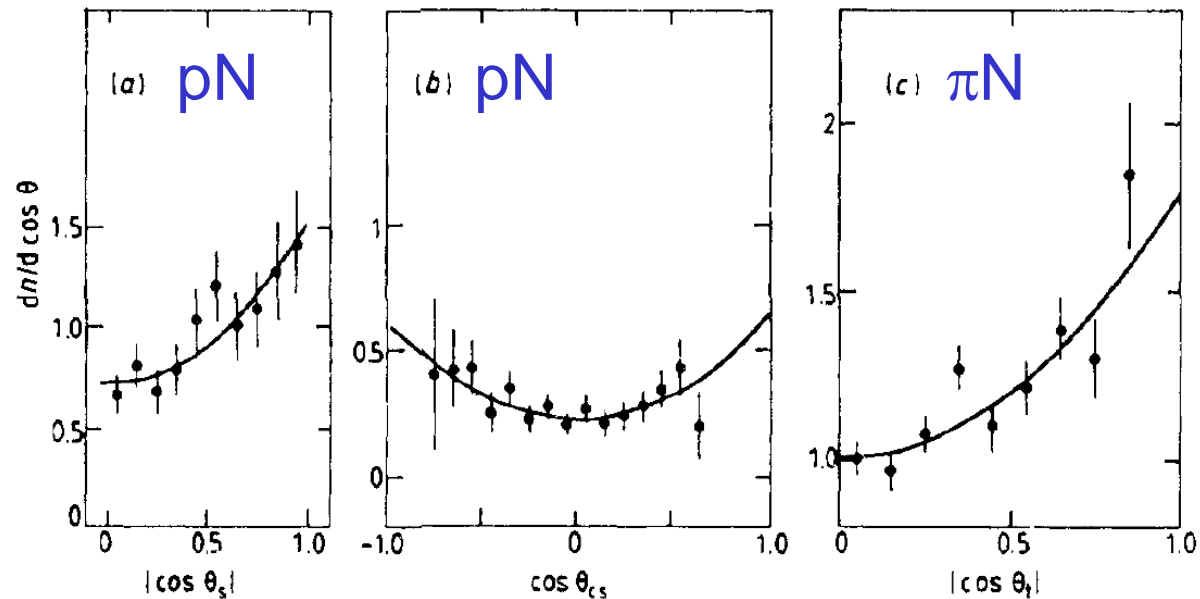


Figure 17. Measurements of the decay angular distribution of lepton pairs by Kourkouvelis *et al* (1980), Antreasyan *et al* (1980) and Badier *et al* (1980a). Fits to the form $1 + \alpha \cos^2 \theta$ are shown as full curves and are discussed in the text. (a) ISR ABCS, $4.5 < M < 8.7$ GeV, (b) ISR CHFMP, $6 < M < 8$ GeV, (c) NA3, π^- 200 GeV, $4 < M < 6$ GeV, $p_t < 1$ GeV.

$$d\sigma(\Omega) \propto (1 + \cos^2 \theta)$$

Angular Distributions

CIP, PRL 42 (1979) 948

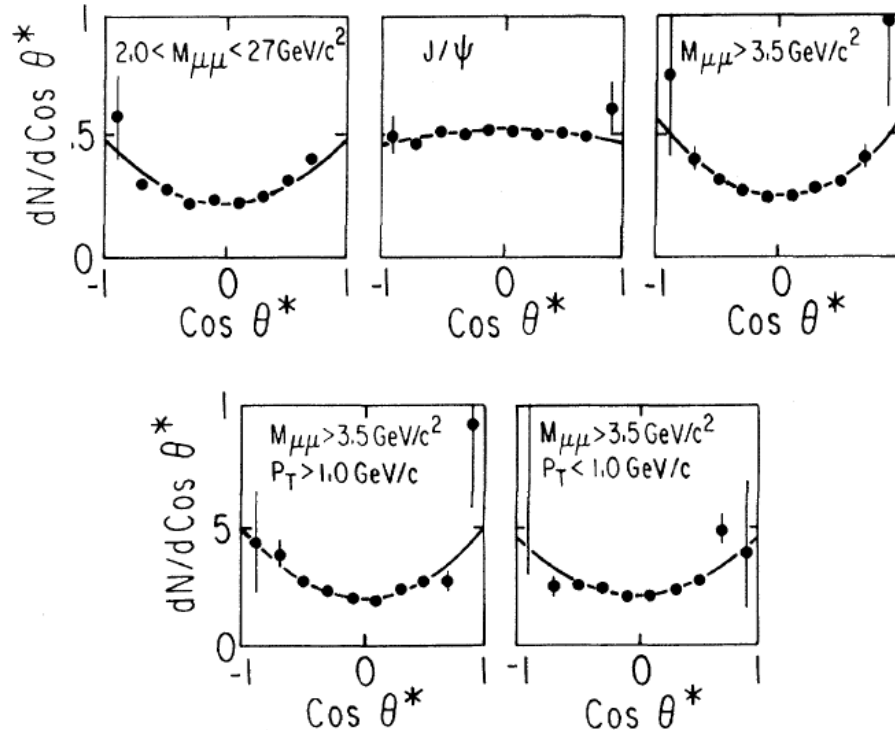
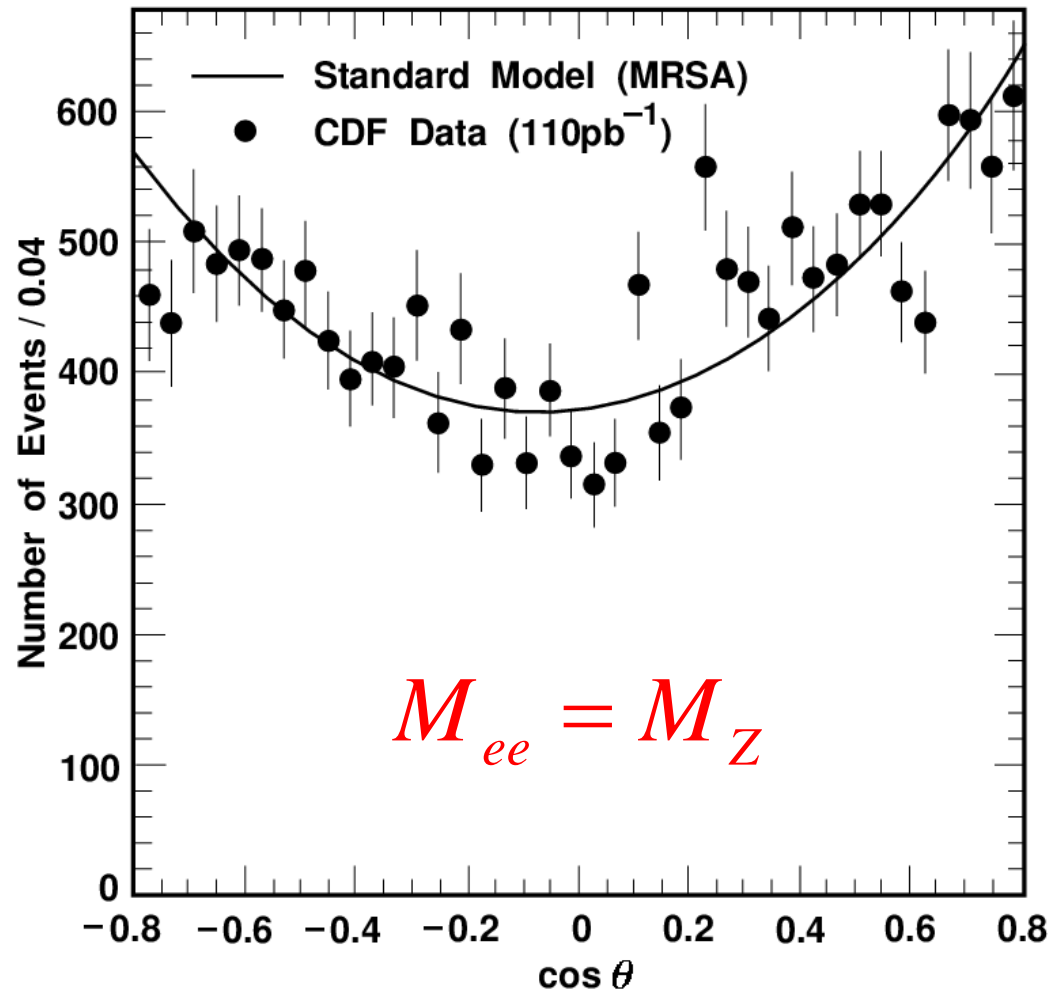


FIG. 3. Helicity angular distributions in three different mass intervals. The $M > 3.5 \text{ GeV}/c^2$ interval is also shown divided in two p_T intervals. The Collins-Soper angle (θ^*) is defined in the text.

$$d\sigma(\Omega) \propto (1 + \cos^2 \theta)$$

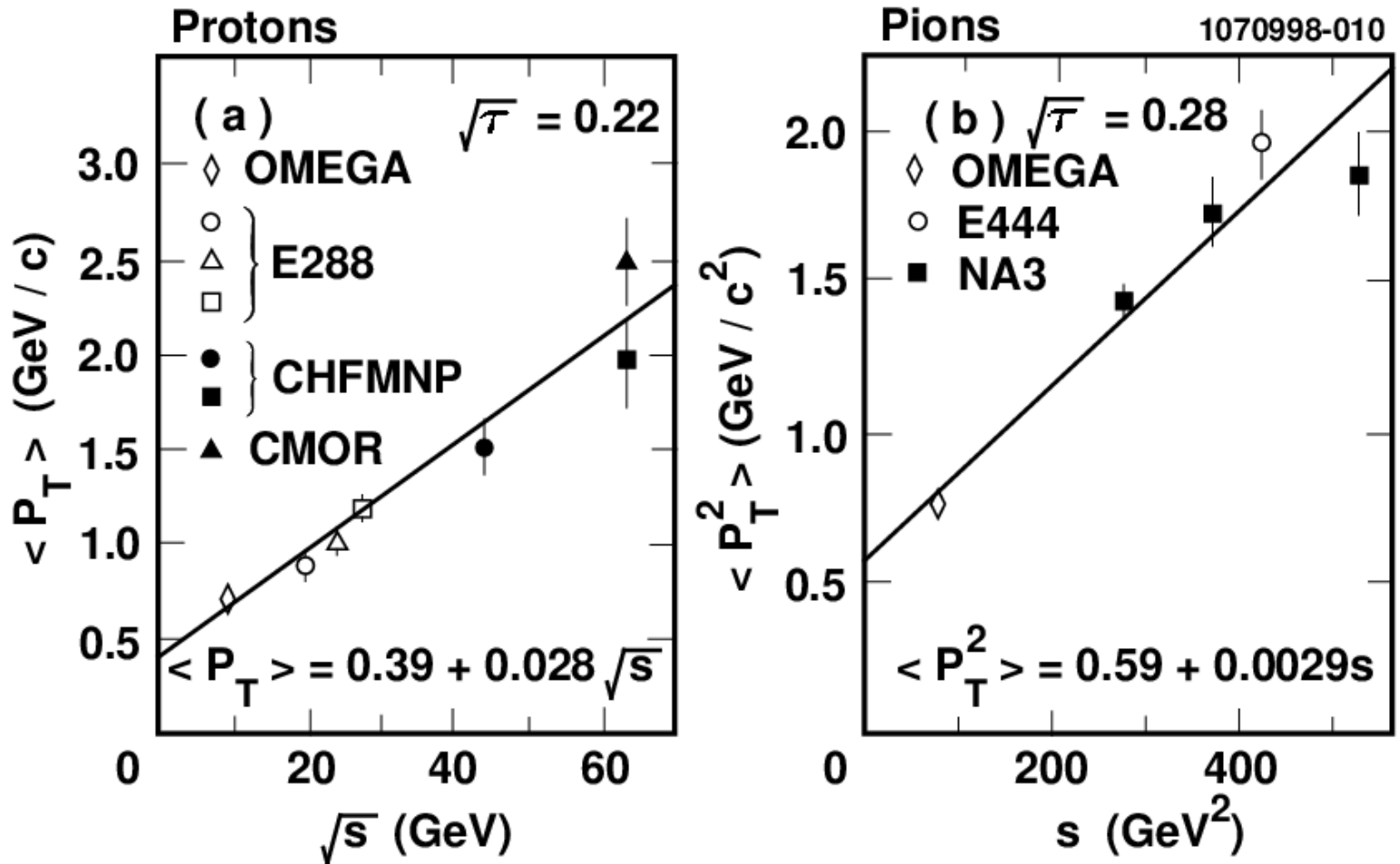
Angular Distribution

CDF, PRL 77 (1996) 2616



Transverse momentum distributions

T.M. Yan, hep-ph/9810268



A clear increase of p_T of lepton pairs with s .

Absolute Cross Sections

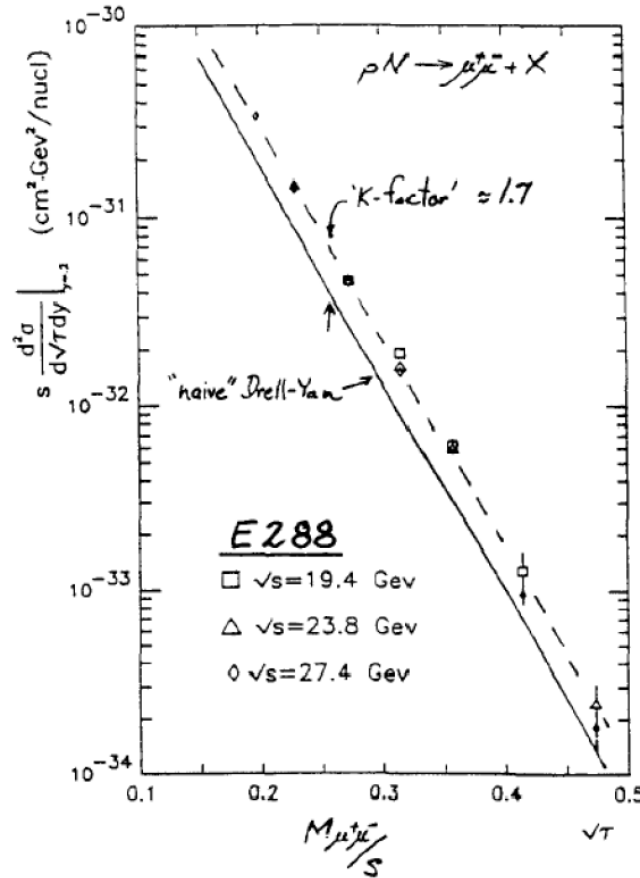


Table 1.2: Experimental K -factors.

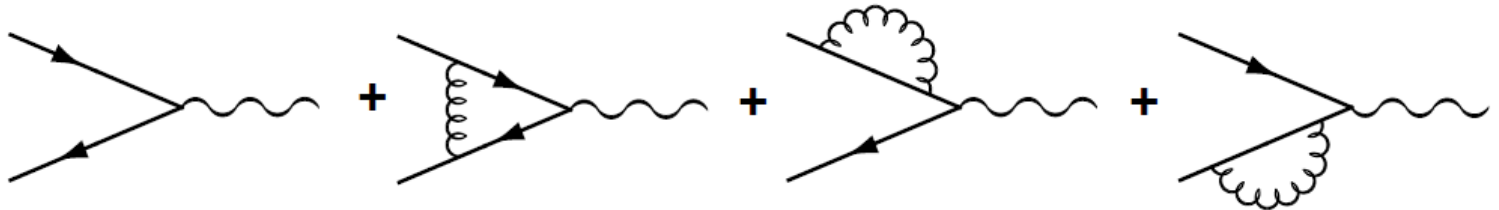
Experiment	Interaction	Beam Momentum	$K = \sigma_{\text{meas.}} / \sigma_{\text{DY}}$
E288 [Kap 78]	$p Pt$	300/400 GeV	~ 1.7
WA39 [Cor 80]	$\pi^\pm W$	39.5 GeV	~ 2.5
E439 [Smi 81]	$p W$	400 GeV	1.6 ± 0.3
NA3 [Bad 83]	$(\bar{p} - p)Pt$	150 GeV	2.3 ± 0.4
	$p Pt$	400 GeV	$3.1 \pm 0.5 \pm 0.3$
	$\pi^\pm Pt$	200 GeV	2.3 ± 0.5
	$\pi^- Pt$	150 GeV	2.49 ± 0.37
NA10 [Bet 85]	$\pi^- Pt$	280 GeV	2.22 ± 0.33
	$\pi^- W$	194 GeV	$\sim 2.77 \pm 0.12$
E326 [Gre 85]	$\pi^- W$	225 GeV	$2.70 \pm 0.08 \pm 0.40$
E537 [Ana 88]	$\bar{p} W$	125 GeV	$2.45 \pm 0.12 \pm 0.20$
E615 [Con 89]	$\pi^- W$	252 GeV	1.78 ± 0.06

J. C. Webb, Measurement of continuum dimuon production in 800-GeV/c proton nucleon collisions, arXiv:hep-ex/0301031.

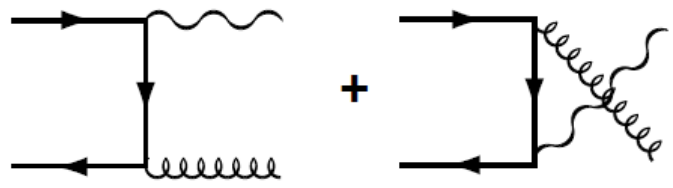
Success and Failure of the “naïve” Drell-Yan parton model

- **Success:**
 - Scaling of the cross sections (depends on x_1 and x_2 only)
 - Nuclear dependence (cross section depends linearly on the mass A)
 - Angular distributions ($1 + \cos^2\theta$ distributions)
- **Failure:**
 - Absolute cross sections (a factor of 2-3 larger than expected)
 - Transverse momentum distributions (much larger $\langle p_T \rangle$ than 200-300 MeV)

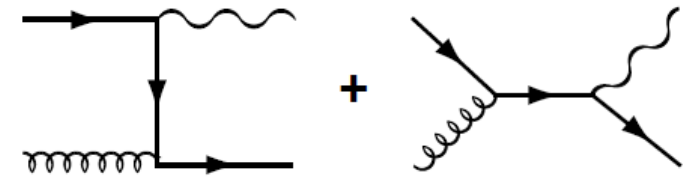
Drell-Yan Process with QCD



(a)



(b)



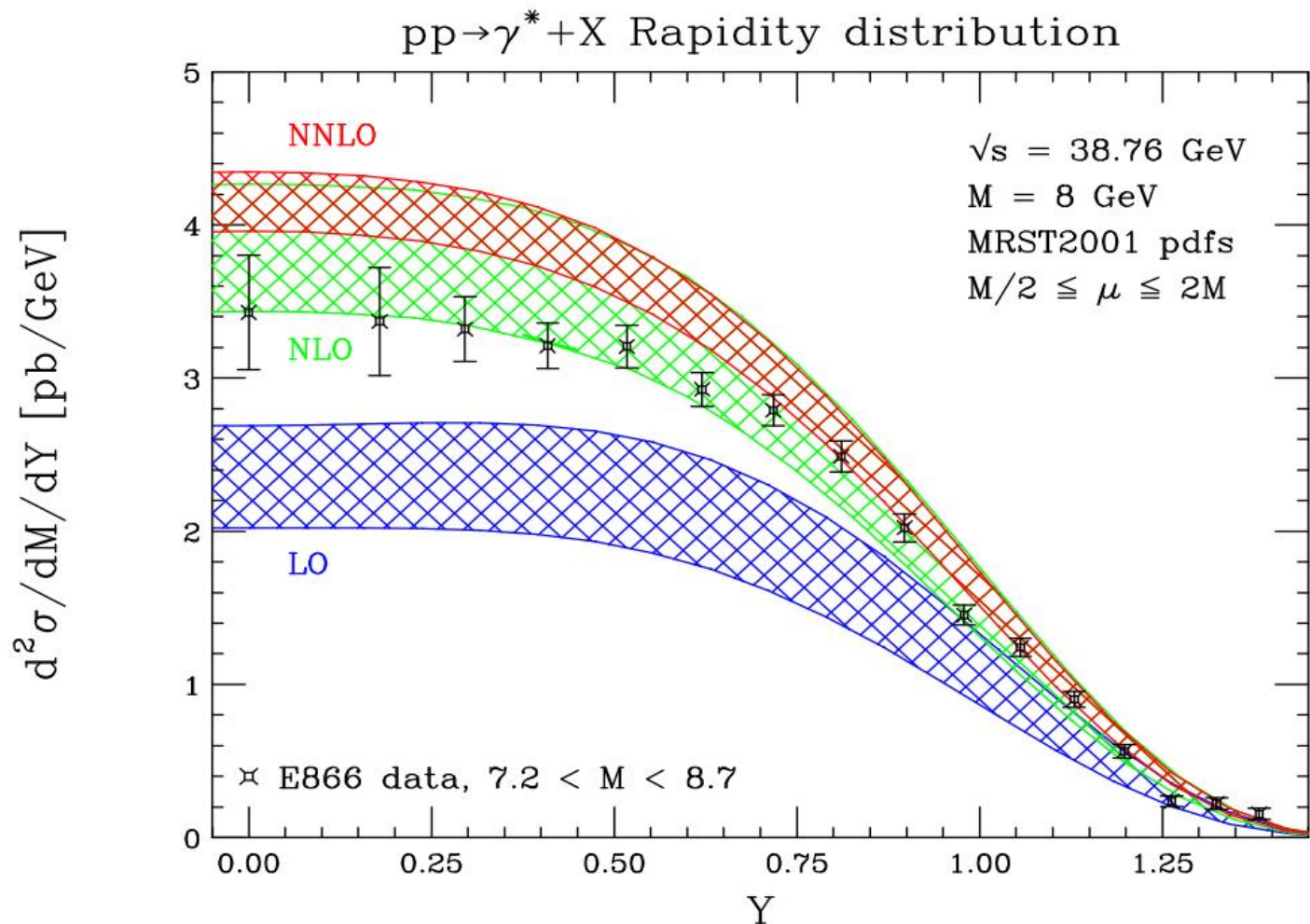
(c)

Drell-Yan Process with QCD

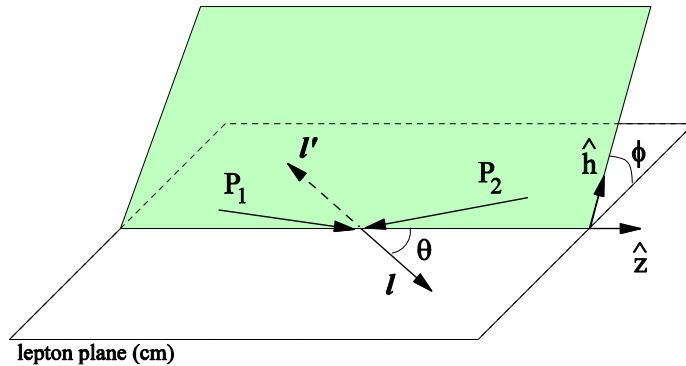
- **Scaling:** The logarithmic corrections in Q^2 can be absorbed by Q^2 -dependent quark and antiquark distribution functions of the hadrons. Scaling is violated but only logarithmically
- **Absolute cross section:** LO, NLO.
- **Angular distribution:** Lam-Tung relation.
- **Transverse momentum distribution:** A large transverse momentum of the lepton pair can be produced by recoil of quarks or gluons.

Absolute Cross Sections

C. Anastasiou et al., PRL 91 (2003) 182002



Drell-Yan decay angular distributions



θ and ϕ are the decay polar and azimuthal angles of the μ^+ in the dilepton rest-frame

Collins-Soper frame

$$\frac{d\sigma}{d\Omega} \propto (1 + \lambda \cos^2 \theta + \mu \sin 2\theta \cos \phi + \frac{\nu}{2} \sin^2 \theta \cos 2\phi)$$

$$\propto (W_T (1 + \cos^2 \theta) + W_L (1 - \cos^2 \theta) + W_\Delta \sin 2\theta \cos \phi + W_{\Delta\Delta} \sin^2 \theta \cos 2\phi)$$

$q\bar{q}$ annihilation parton model:

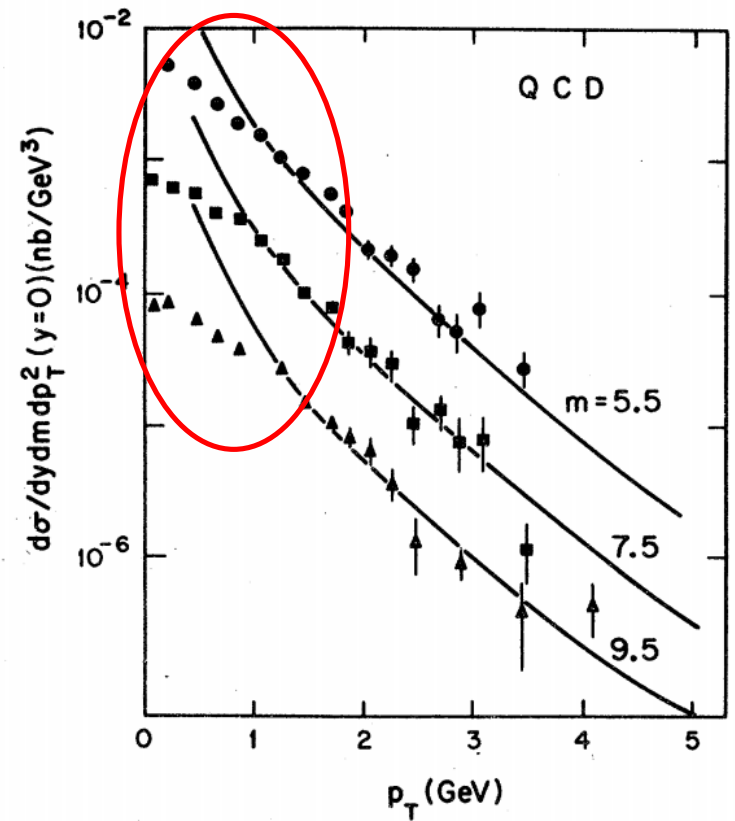
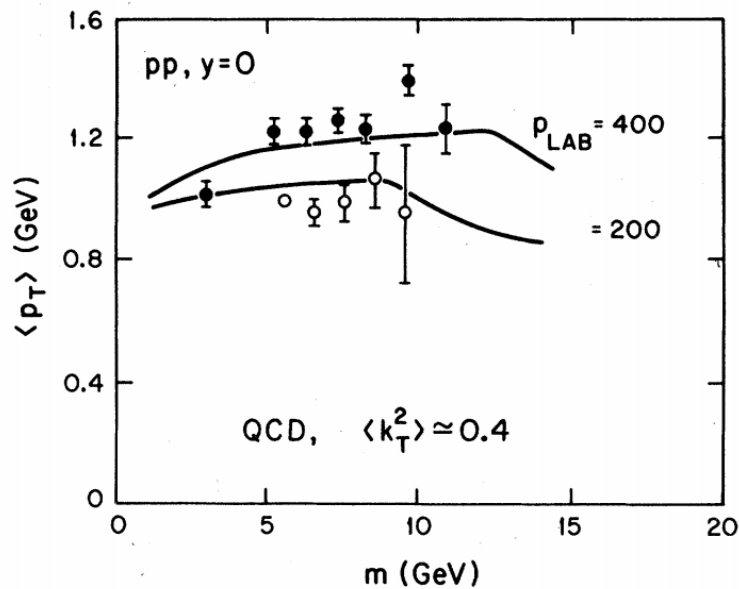
$$O(\alpha_s^0) \quad \lambda=1, \mu=\nu=0; \quad W_T = 1, W_L = 0$$

Lam-Tung relation (1978)

$$\text{pQCD: } O(\alpha_s^1), \quad W_L = 2W_{\Delta\Delta}; \quad 1 - \lambda - 2\nu = 0$$

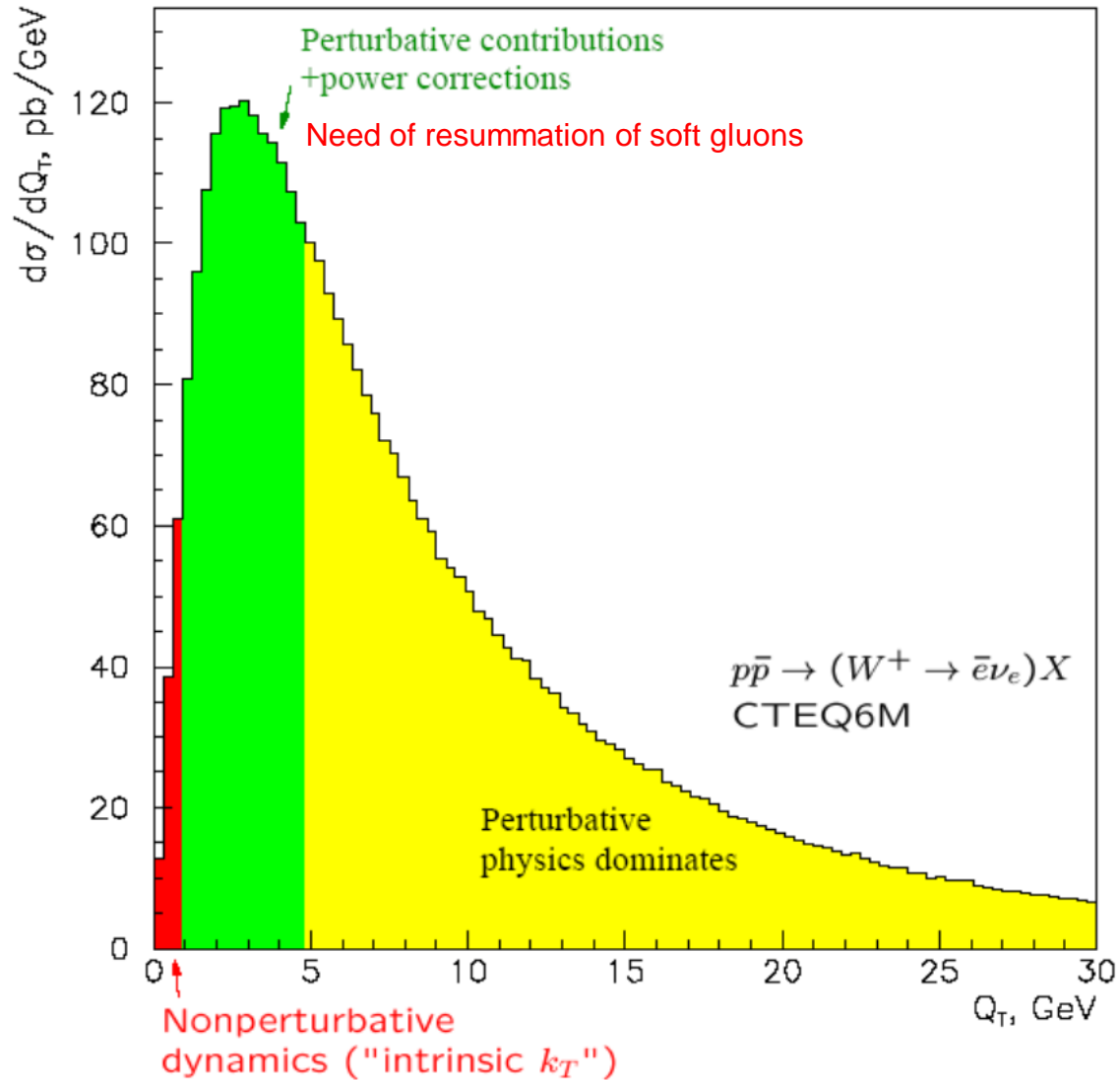
Transverse Momentum Distribution of Lepton Pairs with Gluon Effects

F. Halzen and D.M. Scott, PRD 18 (1978) 3378



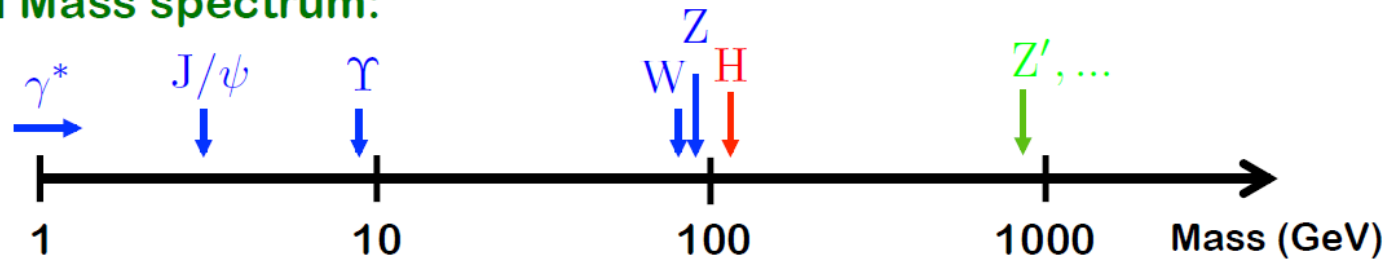
$$\langle p_T \rangle \propto s$$

Transverse Momentum Distribution of Lepton Pairs with Gluon Effects

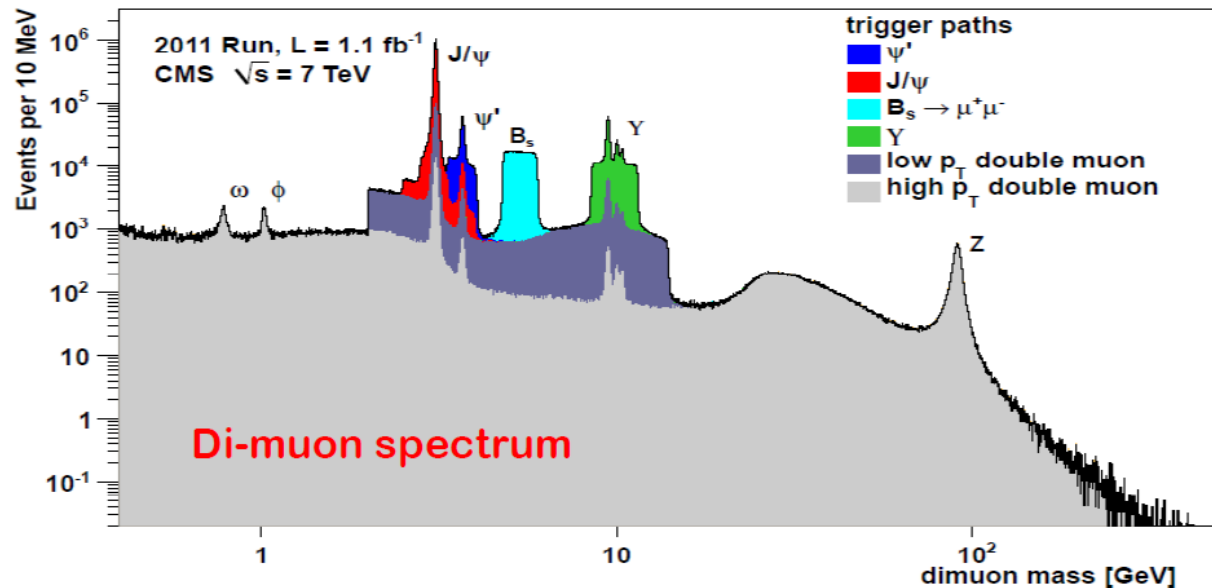


Vector Bosons

□ Mass spectrum:



□ Real data:



Basics of vector bosons

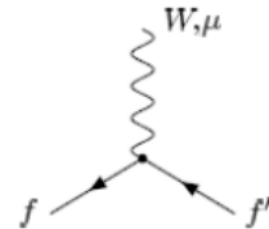
□ Electro-weak gauge bosons (physical states):

W^\pm boson:

$$M_W = 80.4 \text{ GeV}$$

$g_2 = g_w$ – weak coupling

$V_{ff'}$ – CKM matrix for quarks
 couples only to left-handed fermions

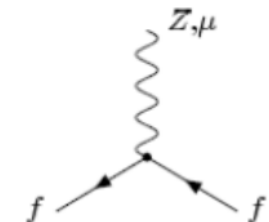


$$= \frac{-ig_2}{2\sqrt{2}} \gamma^\mu (1 - \gamma_5) V_{ff'}$$

Z^0 boson:

$$M_Z = 91.2 \text{ GeV}$$

$\cos \theta_w$ – weak mixing angle
 couples to both left- and right-hand fermions



$$= \frac{-ig_2}{\cos \theta_w} \gamma^\mu (g_V^f + g_A^f \gamma_5)$$

$$g_A^f = -\frac{1}{2} T_3^f$$

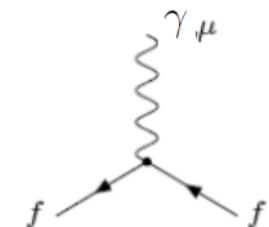
$$g_V^f = \frac{1}{2} T_3^f - \sin^2 \theta_w Q_f$$

γ – photon:

$$M_\gamma = 0$$

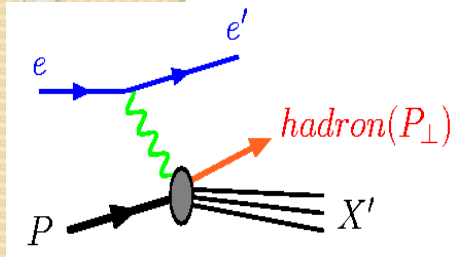
e – electro-charge

Q_f – fraction in electro-charge



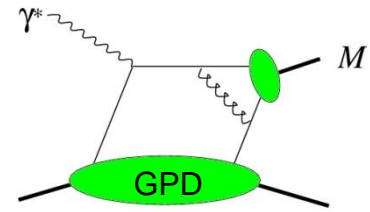
$$= -ie Q_f \gamma^\mu$$

Parton Distributions in Protons



Wigner Distribution
 $W(\vec{r}, x, \vec{k}_T)$

Ji, PRL91,062001(2003)



$\int d\vec{r}$

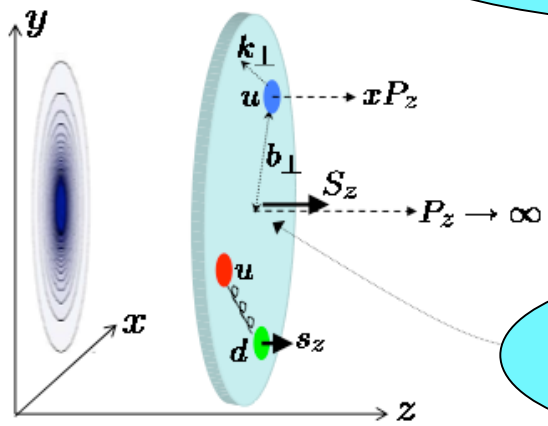
$\int e^{i\vec{q}\cdot\vec{r}} d\vec{r} d\vec{k}_T$
 $\xi = q^z / 2E_q, t = -\vec{q}^2$

Transverse Momentum
 Dependent PDF $f(x, \vec{k}_T)$

Generalized Parton Distr.
 $F(x, \xi, t)$

$\int d\vec{k}_T$

PDF
 $f(x)$



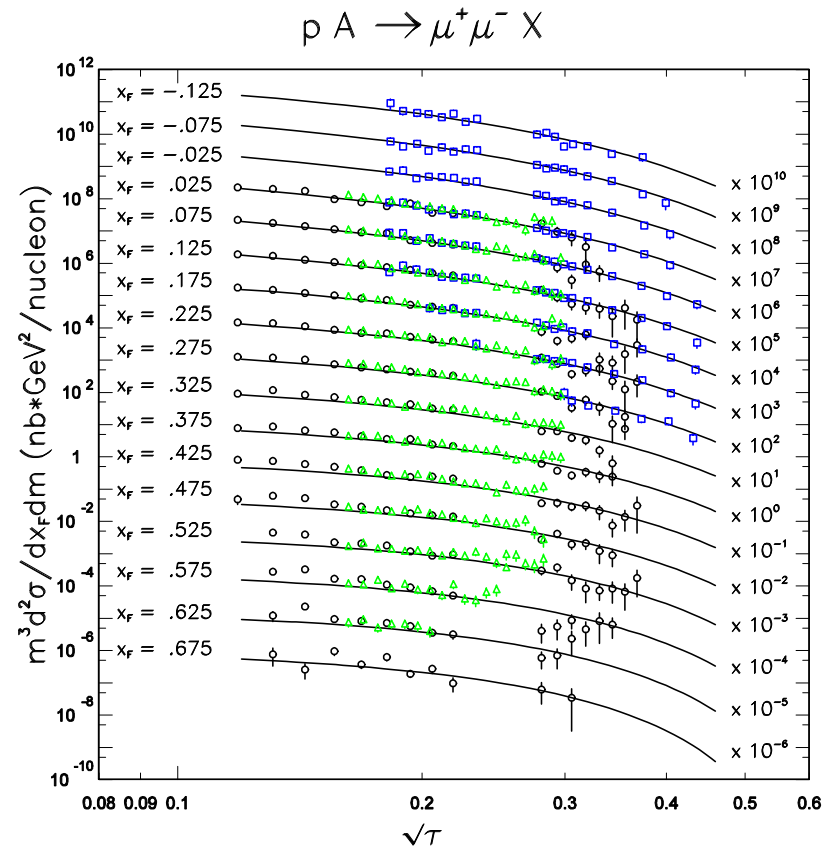
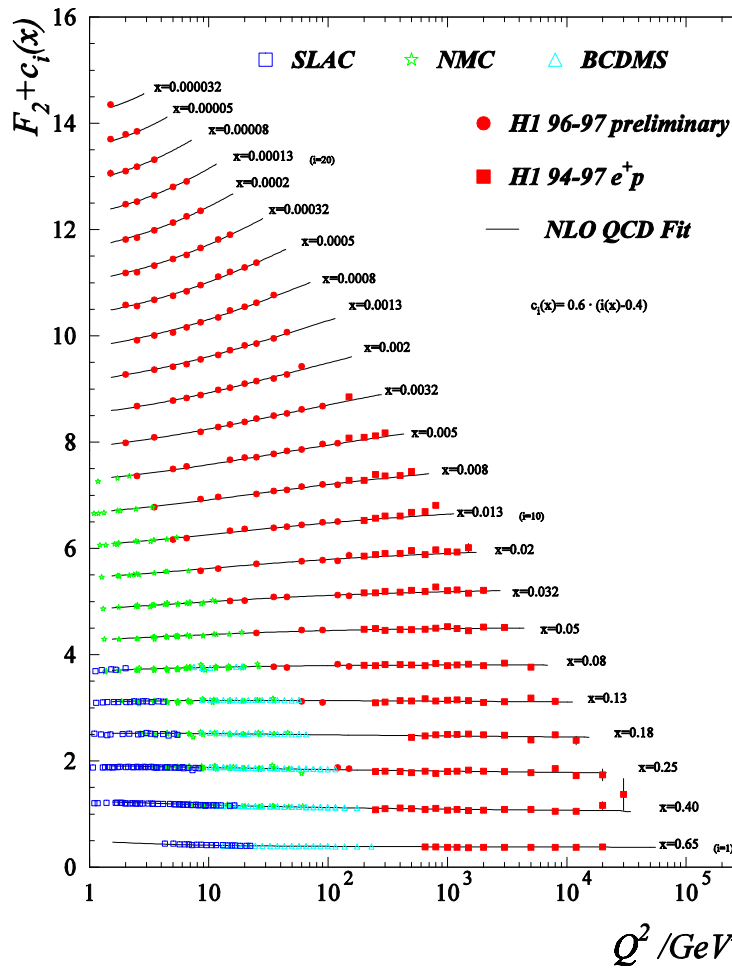
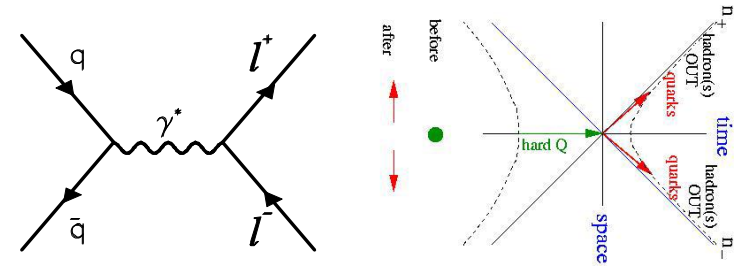
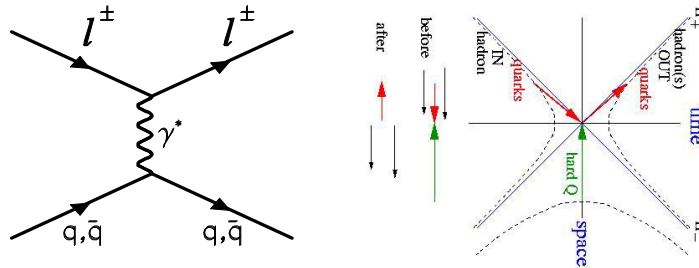
$\int dx$
 Form Factors
 $F_1(t), F_2(t)$

Main Processes in Global PDF Analysis

Eur. Phys. J. C (2009) 63: 189–285

Process	Subprocess	Partons	x range
$\ell^\pm\{p, n\} \rightarrow \ell^\pm X$	$\gamma^* q \rightarrow q$	q, \bar{q}, g	$x \gtrsim 0.01$
$\ell^\pm n/p \rightarrow \ell^\pm X$	$\gamma^* d/u \rightarrow d/u$	d/u	$x \gtrsim 0.01$
$pp \rightarrow \mu^+ \mu^- X$	$u\bar{u}, d\bar{d} \rightarrow \gamma^*$	\bar{q}	$0.015 \lesssim x \lesssim 0.35$
$pn/pp \rightarrow \mu^+ \mu^- X$	$(u\bar{d})/(u\bar{u}) \rightarrow \gamma^*$	\bar{d}/\bar{u}	$0.015 \lesssim x \lesssim 0.35$
$\nu(\bar{\nu})N \rightarrow \mu^-(\mu^+)X$	$W^* q \rightarrow q'$	q, \bar{q}	$0.01 \lesssim x \lesssim 0.5$
$\nu N \rightarrow \mu^- \mu^+ X$	$W^* s \rightarrow c$	s	$0.01 \lesssim x \lesssim 0.2$
$\bar{\nu} N \rightarrow \mu^+ \mu^- X$	$W^* \bar{s} \rightarrow \bar{c}$	\bar{s}	$0.01 \lesssim x \lesssim 0.2$
$e^\pm p \rightarrow e^\pm X$	$\gamma^* q \rightarrow q$	g, q, \bar{q}	$0.0001 \lesssim x \lesssim 0.1$
$e^+ p \rightarrow \bar{\nu} X$	$W^+ \{d, s\} \rightarrow \{u, c\}$	d, s	$x \gtrsim 0.01$
$e^\pm p \rightarrow e^\pm c\bar{c} X$	$\gamma^* c \rightarrow c, \gamma^* g \rightarrow c\bar{c}$	c, g	$0.0001 \lesssim x \lesssim 0.01$
$e^\pm p \rightarrow \text{jet} + X$	$\gamma^* g \rightarrow q\bar{q}$	g	$0.01 \lesssim x \lesssim 0.1$
$p\bar{p} \rightarrow \text{jet} + X$	$gg, qg, qq \rightarrow 2j$	g, q	$0.01 \lesssim x \lesssim 0.5$
$p\bar{p} \rightarrow (W^\pm \rightarrow \ell^\pm \nu) X$	$ud \rightarrow W, \bar{u}\bar{d} \rightarrow W$	u, d, \bar{u}, \bar{d}	$x \gtrsim 0.05$
$p\bar{p} \rightarrow (Z \rightarrow \ell^+ \ell^-) X$	$uu, dd \rightarrow Z$	d	$x \gtrsim 0.05$

Complementarity between DIS and Drell-Yan



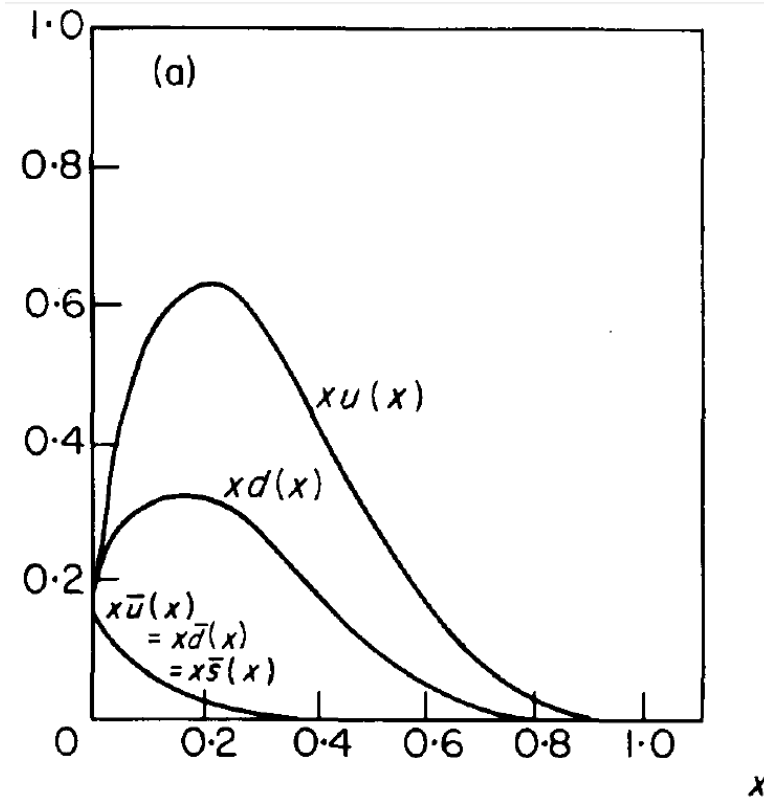
Naïve Expectation of Nucleon Sea: SU(3) Symmetric

$$q(x) = q_V(x) + q_S(x)$$

$$u_V(x) = 2d_V(x)$$

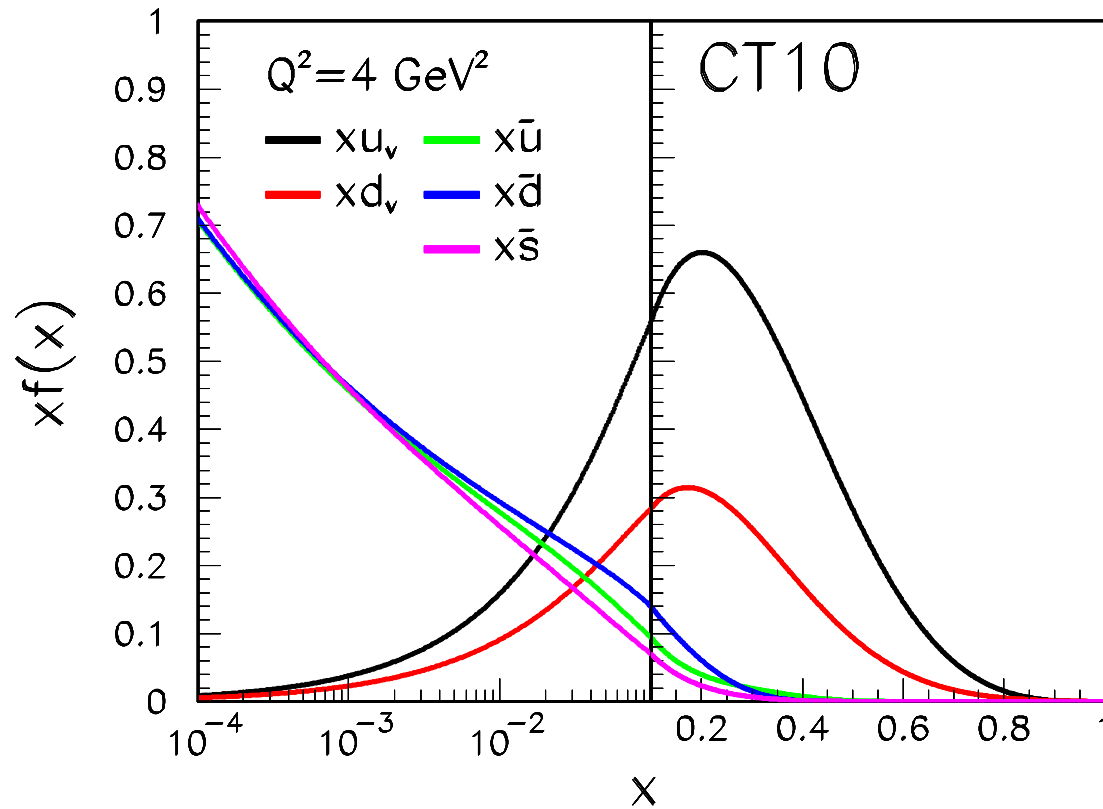
$$s_V(x) = \bar{u}_V(x) = \bar{d}_V(x) = \bar{s}_V(x) = 0$$

$$u_S(x) = \bar{u}_S(x) = d_S(x) = \bar{d}_S(x) = s_S(x) = \bar{s}_S(x)$$

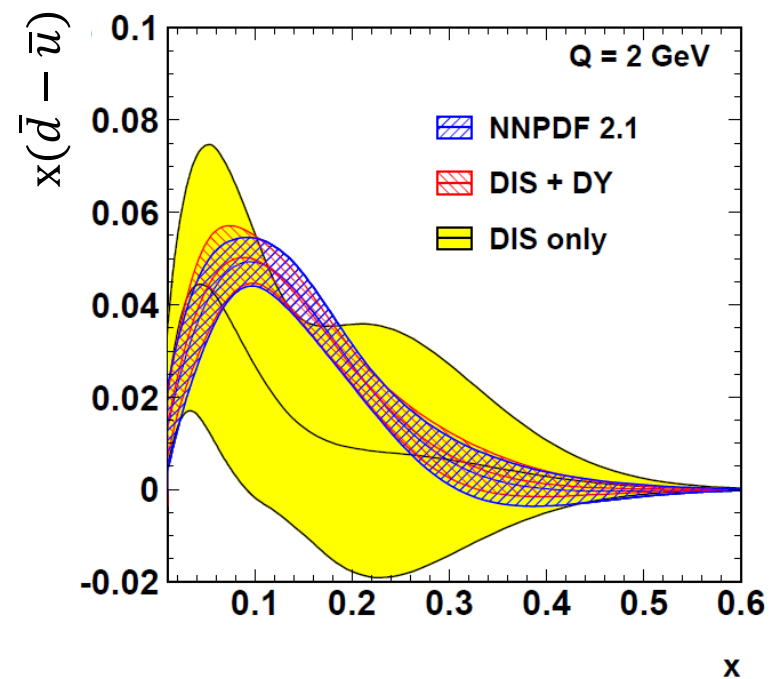
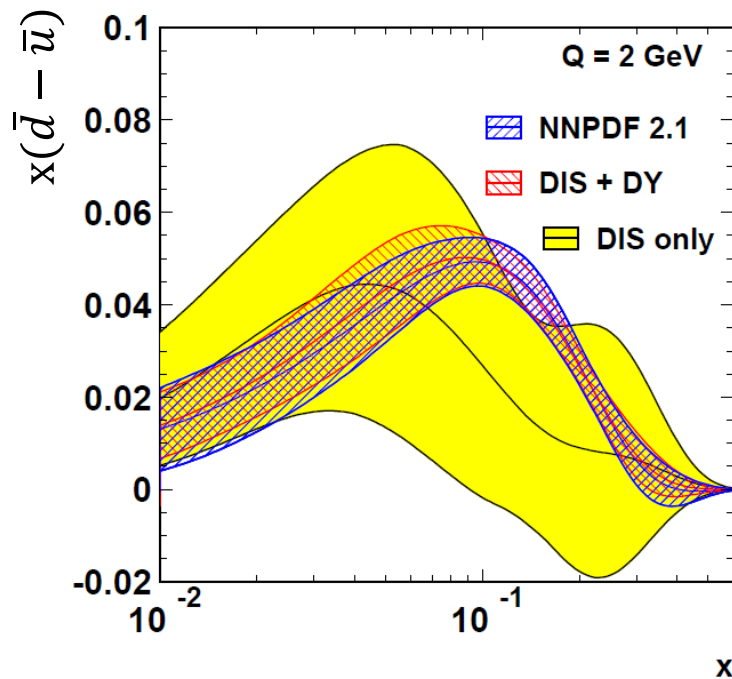


F.E. Close, "An Introduction to Quarks and Partons"

Parton Distribution Functions (PDF) of Protons



Constraint of $x(\bar{d} - \bar{u})$ in Global Analysis



E. Pereza and E. Rizvib, arXiv:1208.1178

Is $\bar{u} = \bar{d}$ in the Proton?

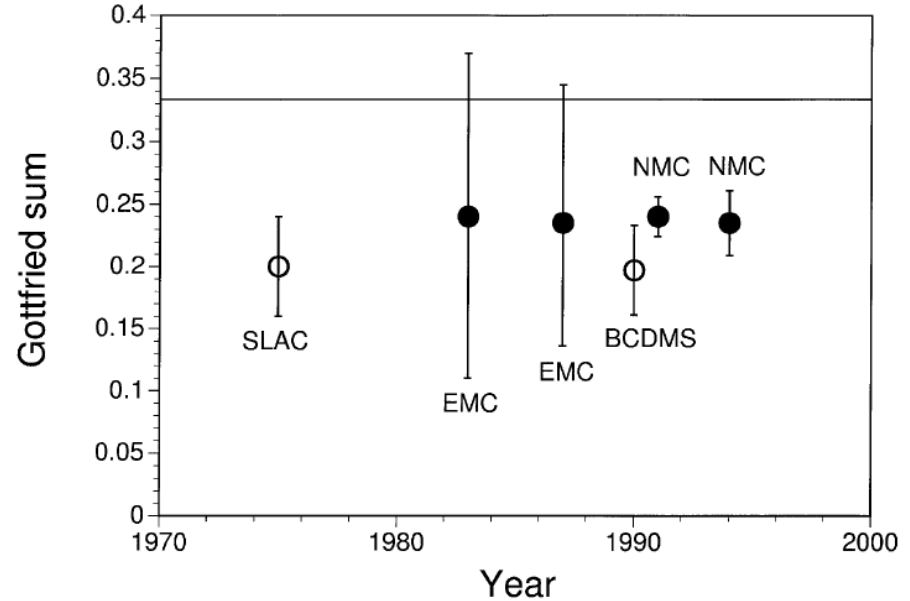
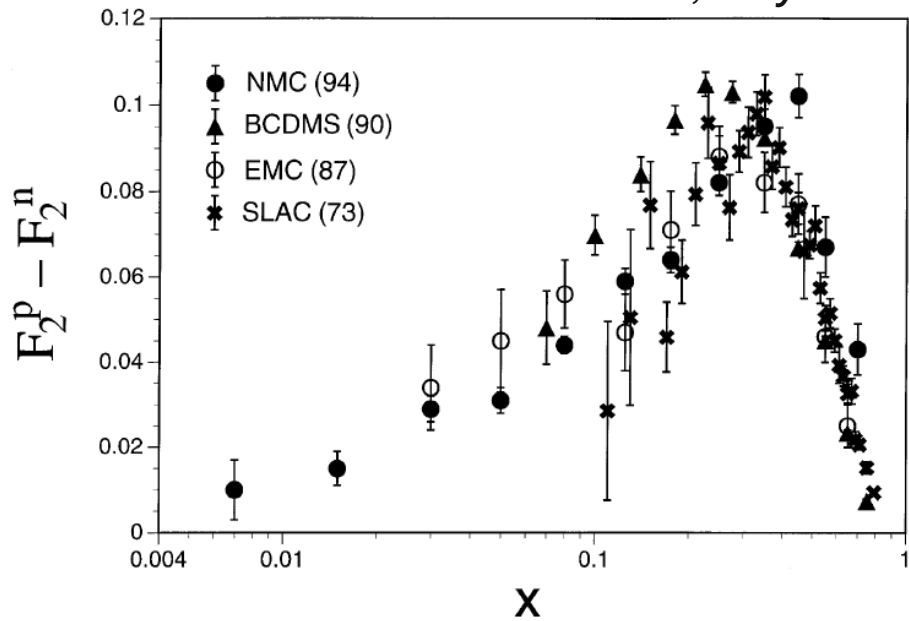


Gottfried Sum Rule

$$\begin{aligned} S_G &= \int_0^1 [(F_2^p(x) - F_2^n(x)) / x] dx \\ &= \frac{1}{3} \int_0^1 (u_v(x) - d_v(x)) dx + \frac{2}{3} \int_0^1 (\bar{u}(x) - \bar{d}(x)) dx \\ &= \frac{1}{3} \quad (\text{if } \bar{u}(x) = \bar{d}(x)) \end{aligned}$$

Experimental Measurement of Gottfried Sum

S. Kumano, Physics Reports, 303 (1998) 183



New Muon Collaboration (NMC), Phys. Rev. D50 (1994) R1

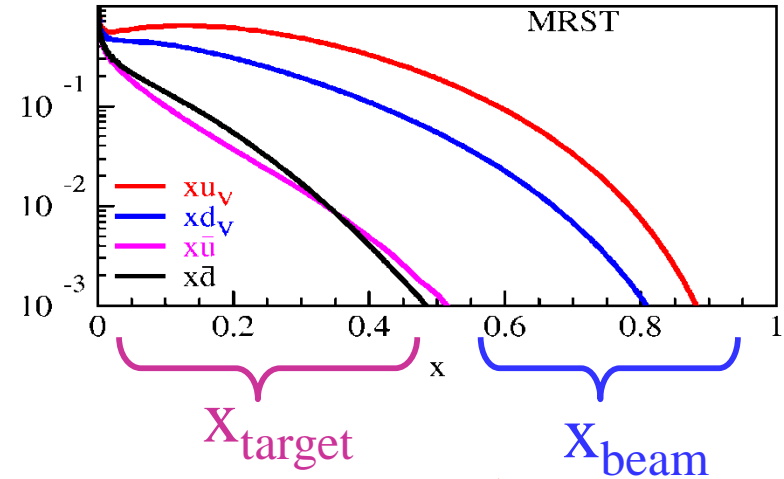
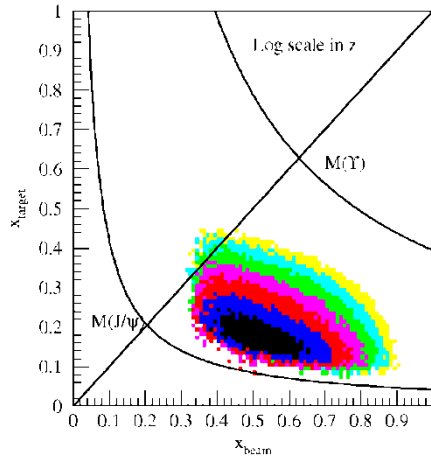
$$S_G = 0.235 \pm 0.026$$

(Significantly lower than 1/3 !)

x-dependence of Sea Quarks

Acceptance for fixed-target experiment:

$$x_{\text{beam}} \gg x_{\text{target}}$$



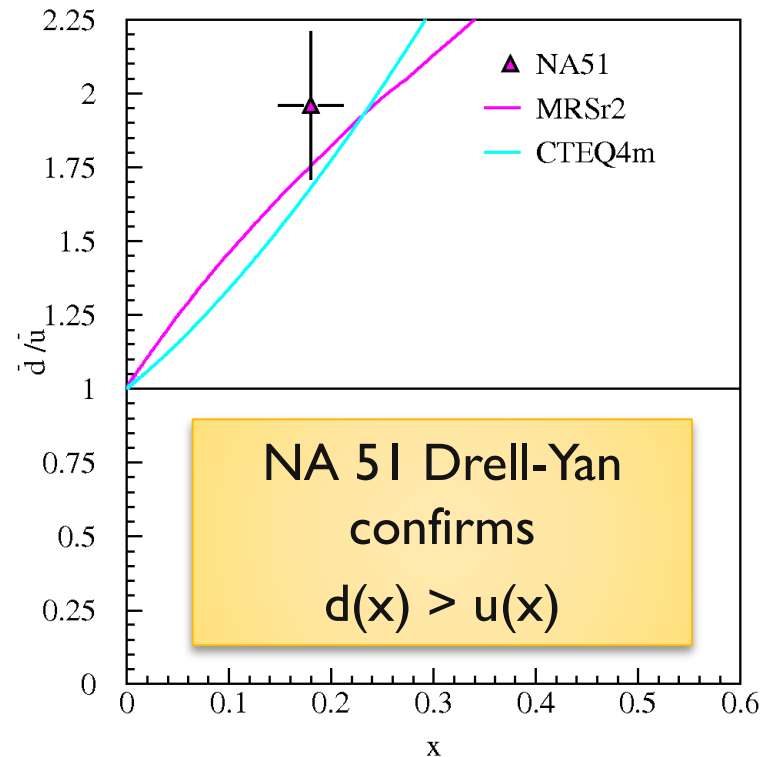
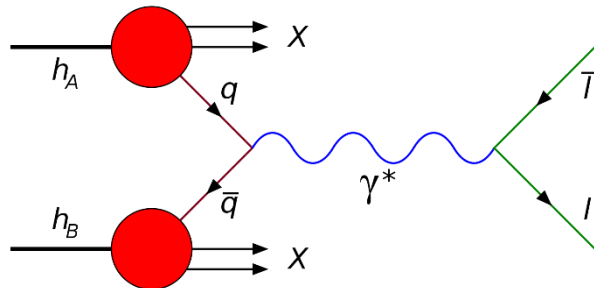
$$\frac{d^2\sigma}{dx_{\text{beam}} dx_{\text{target}}} = \frac{4\pi\alpha^2}{9x_{\text{beam}}x_{\text{target}}} \frac{1}{s} \sum_i e_i^2 [q_i(x_{\text{beam}})\bar{q}_i(x_{\text{target}}) + \bar{q}_i(x_{\text{beam}})q_i(x_{\text{target}})]$$

$$\frac{\sigma^{pd}}{2\sigma^{pp}} \Big|_{x_{\text{beam}} \gg x_{\text{target}}} \approx \frac{1}{2} \left[1 + \frac{\bar{d}(x_{\text{target}})}{u(x_{\text{target}})} \right]$$

Light Antiquark Flavor Asymmetry: Drell-Yan Experiments

- Naïve Assumption: $\bar{d}(x) = \bar{u}(x)$
- NMC (Gottfried Sum Rule):

$$\int_0^1 [\bar{d}(x) - \bar{u}(x)] dx \neq 0$$
- NA51 (Drell-Yan, 1994):
 $\bar{d} > \bar{u}$ at $x = 0.18$



$$\frac{\sigma^{pd}}{2\sigma^{pp}} \Big|_{x_b \gg x_t} \approx \frac{1}{2} \left[1 + \frac{\bar{d}(x_t)}{\bar{u}(x_t)} \right]$$

Light Antiquark Flavor Asymmetry: Drell-Yan Experiments

- Naïve Assumption: $\bar{d}(x) = \bar{u}(x)$

- NMC (Gottfried Sum Rule):

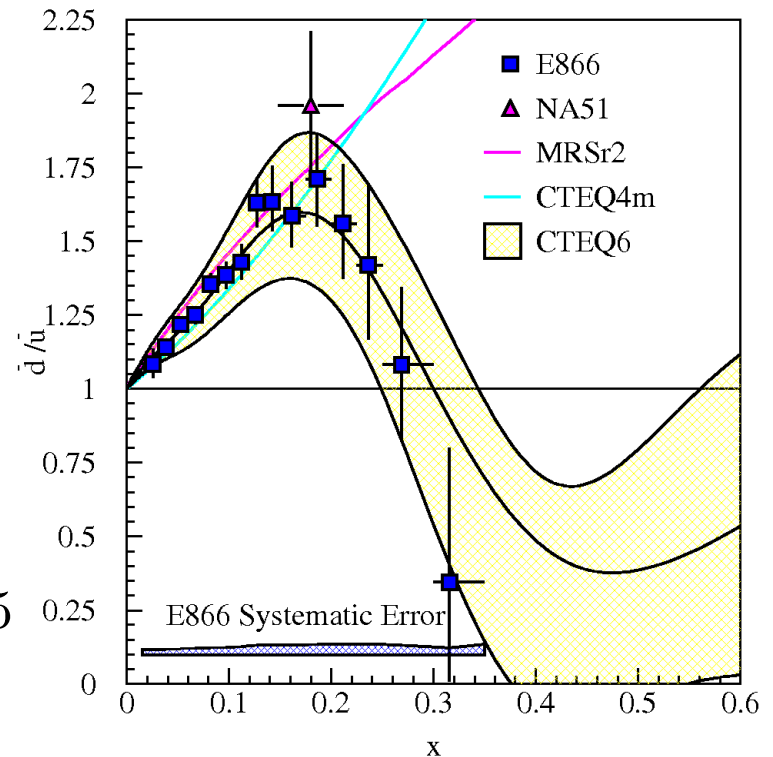
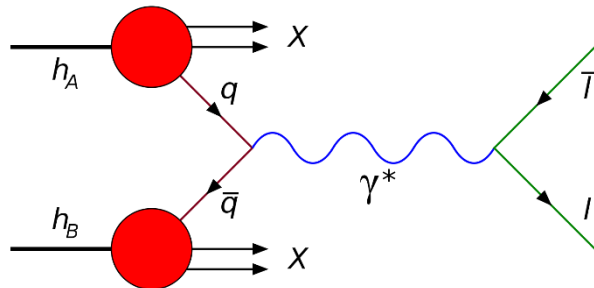
$$\int_0^1 [\bar{d}(x) - \bar{u}(x)] dx \neq 0$$

- NA51 (Drell-Yan, 1994):

$$\bar{d} > \bar{u} \text{ at } x = 0.18$$

- E866/NuSea (Drell-Yan, 1998):

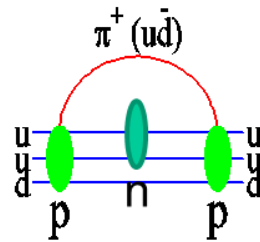
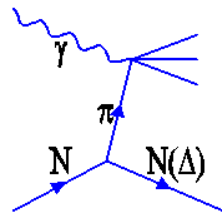
$$\bar{d}(x)/\bar{u}(x) \text{ for } 0.015 \leq x \leq 0.35$$



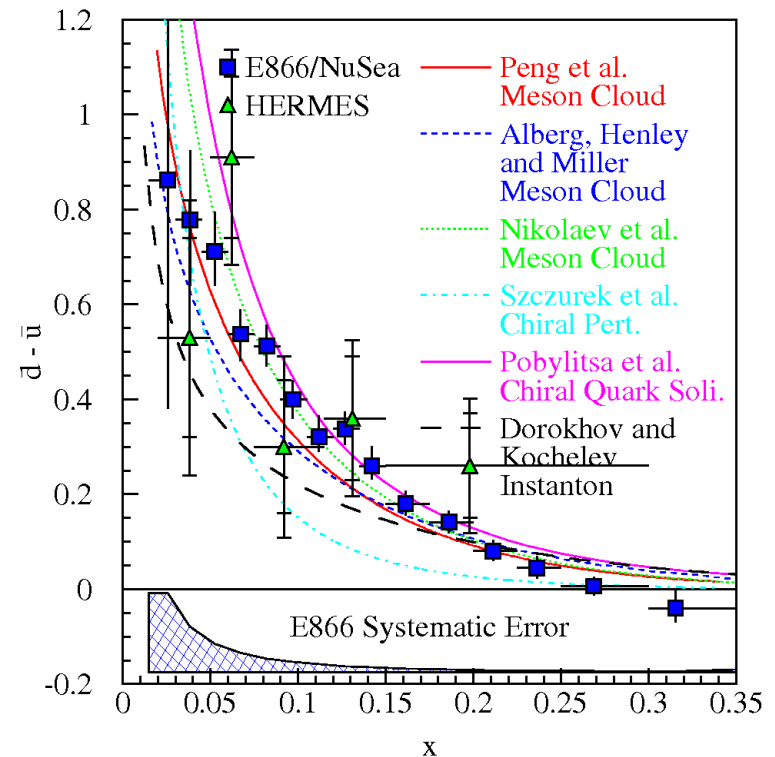
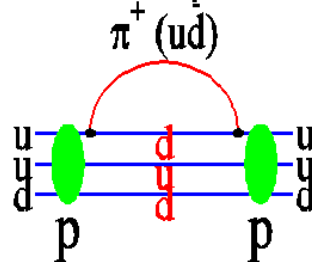
$$\frac{\sigma^{pd}}{2\sigma^{pp}} \Big|_{x_b \gg x_t} \approx \frac{1}{2} \left[1 + \frac{\bar{d}(x_t)}{\bar{u}(x_t)} \right]$$

Origin of $\bar{u}(x) \neq \bar{d}(x)$?

- Pauli blocking of valance quarks
- Meson cloud in the nucleons (Thomas 1983, Kumano 1991): Sullivan process in DIS.



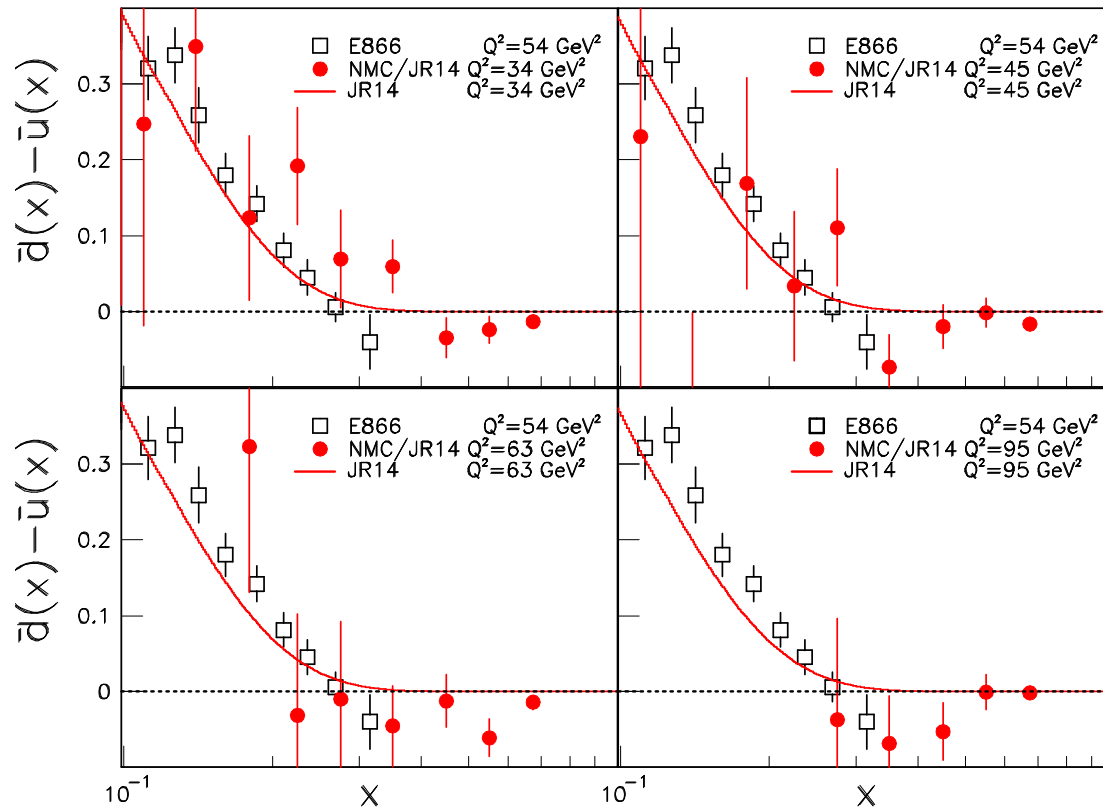
- Chiral quark model (Eichten et al. 1992; Wakamatsu 1992): Goldstone bosons couple to valance quarks.



Momentum Dependence of the Flavor Structure of the Nucleon Sea: NMC vs E866

J.C. Peng et al., PLB 736 (2014) 411

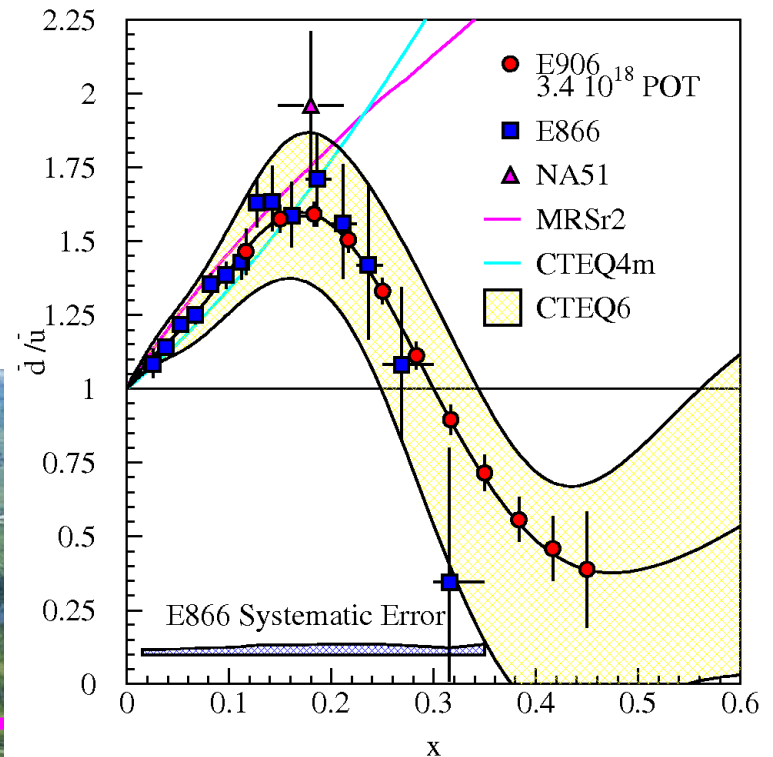
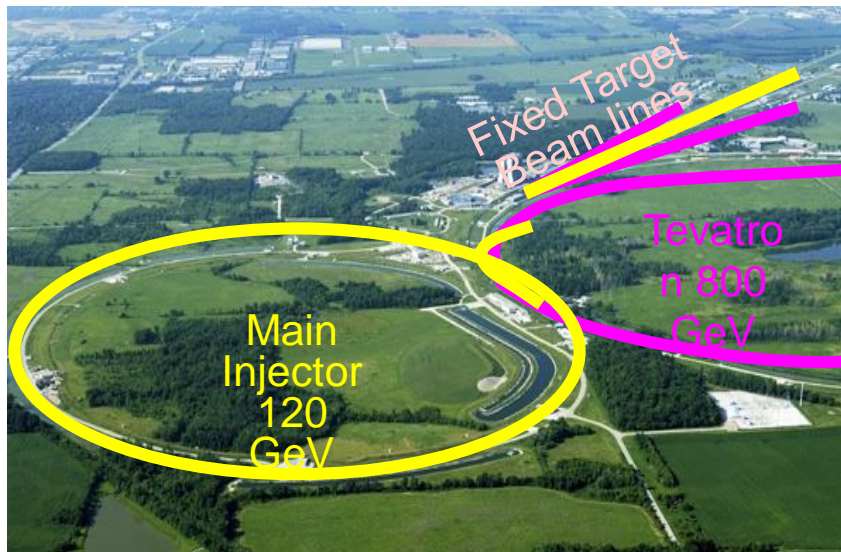
$$\bar{d}(x) - \bar{u}(x) = \frac{1}{2} \overset{\text{JR14}}{[u_v(x) - d_v(x)]} - \frac{3}{2x} \overset{\text{NMC}}{[F_2^p(x) - F_2^n(x)]}.$$



E906/SeaQuest Experiment

Fermilab E906

- First round of data taking:
Nov, 2013 – July, 2015.
- ^1H , ^2H , and nuclear targets
- **Unpolarized Drell-Yan using
120 GeV proton beam**



$(\bar{d}(x) / \bar{u}(x))$ up to $x \sim 0.45$

特集：ナノ医療

クォークの世界

支配者グルーオンの謎
エキゾチック粒子を発見

慢性疼痛を鎮める
新アプローチ
気候を揺さぶる
北極海の大波
石黒教授のアンドロイド
急速に進化する魚
シクリッド
好評連載
illusions 知覚は幻
From nature ダイジェスト
セルフコントロールの
心理学
http://www.nikkei-science.com/

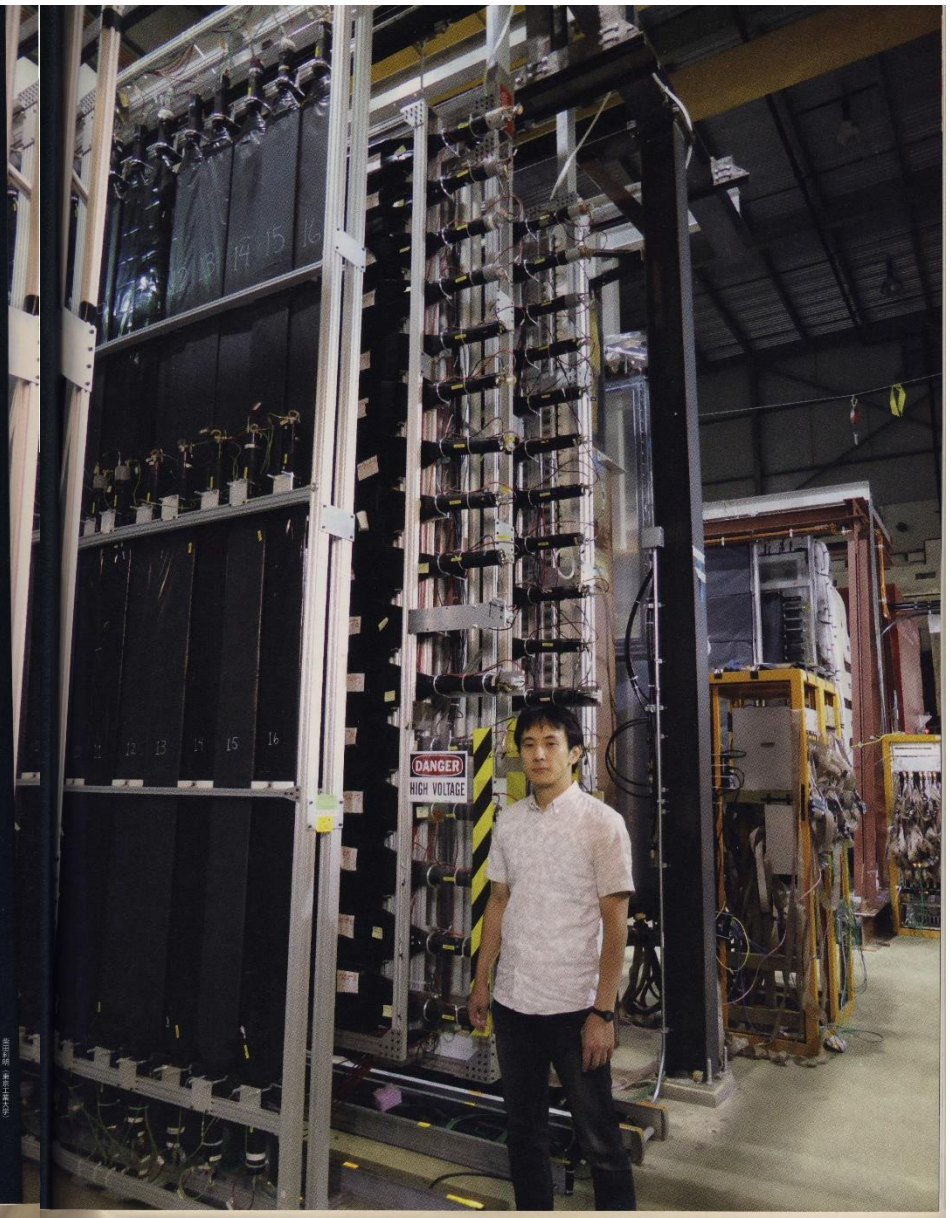
の世界

これらクォークと反クォークは激しく動き回っているが、それは私たちになじみがある重力や電磁気力の作用ではなく、それらをはるかにしのぐ別種の強大な力、その名も「強い力」によっている。強い力は超強力な引力になったり、ほとんど作用しないこともある。この奇妙な力はクォークや反クォークの間でグルーオンという素粒子がキャッチボールされることによって伝わる。グルーオンは物理的な力を及ぼすだけではない。クォークは三原色になぞらえられるカラーを、反クォークは三原色の補色になぞらえられる反カラーを持つが、グルーオンをやり取りすると、そのカラーや反カラーの種類が変わる、いわば“変色”する場合がある。力の作用で粒子や反粒子のタイプがころころと変化するわけだ。さらに強い力はクォークと反クォークに質量ももたらす。先に話題になったヒッグス粒子は万物に質量を与える素粒子だが、クォークについてはヒッグス粒子に関連する質量よりも、強い力の作用で生じる質量の方がはるかに大きい。

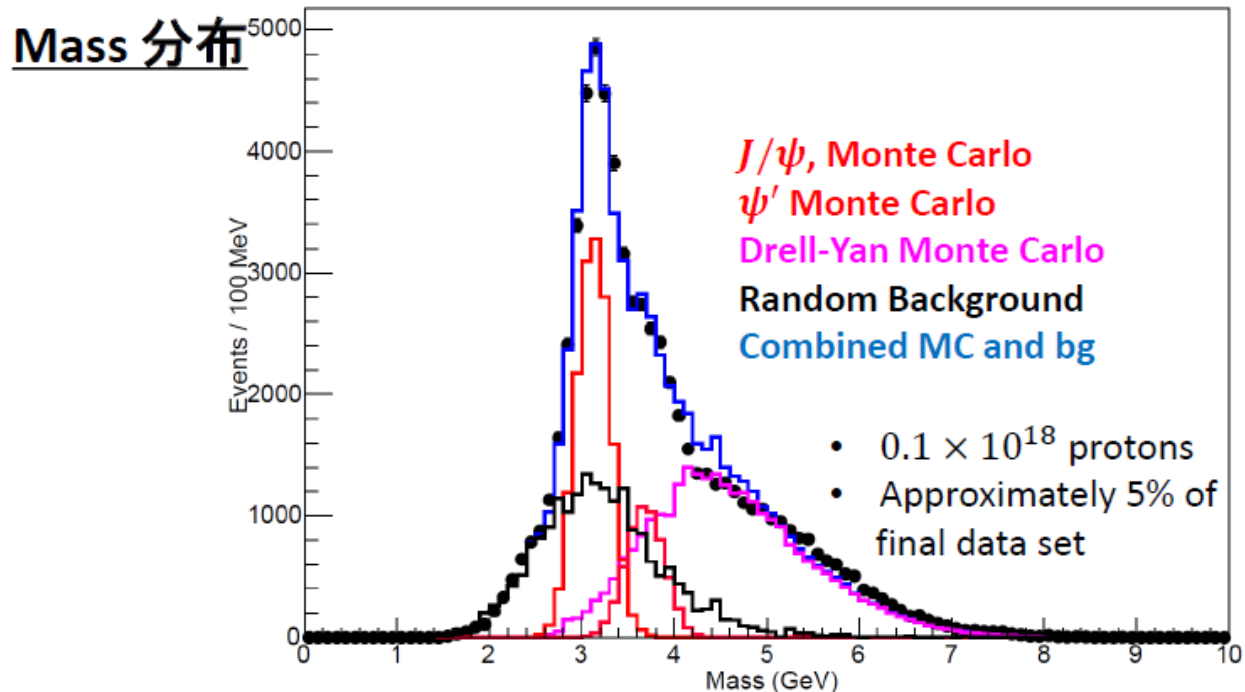
クォークと反クォークに満ちた核子内部は、一人役も果たす「強い力」が支配する別世界だ。私たちは強い力の振る舞いが量子色力学（QCD）によって記述されることは知っているが、QCDがいったいどんな物質世界を構築しているのか、わからないことが多い。日本を含む世界の研究機関が様々な実験によって、この世界を探っている。（編集部）

陽子の内部を覗く 陽子内部はクォークや反クォークに満ちている。左はそのイメージ。全体を包む球殻が陽子、球殻内の色つきの球はクォーク、球の色はクォークが持つカラー（色荷）を表す。クォークをつなぐスプリング状のものは、強い力を持つグルーオンを表す。クォークやグルーオンなどは自転角運動量になぞらえられるスピンという物理量を持ち、その総体が陽子を持つスピン（図中の矢印）になるとされるが、陽子スピンの由来はそのかなりの部分が謎のまま。陽子など核子の内部世界を探るため、国際協力で大がかりな実験が進んでいる。右ページは米国立フェルミ加速器研究所で進んでいるSeaQuest実験の施設。日本からは東京工業大学を中心とするグループが参加している。写真中の人物は研究グループの中心メンバーである中野健一東京工業大学助教。

反粒子の反クォークと混ざっている。ただし、クォークと反クォークの数の比は1対1からほんの少しだけずれていて、クォークから反クォークを引くと、3つだけクォークが多い。粒子と反粒子の間にわずかな不均衡が生じている。



E906/SeaQuest Experiment



- Run2 の極一部のデータを用いた（最終的なデータ総量の約 5%）
- 検出器は想定通りに働いている
- イベント再構成に成功
- 良い Mass 分解能を持つ（ ~ 180 MeV）、MC の予想と一致

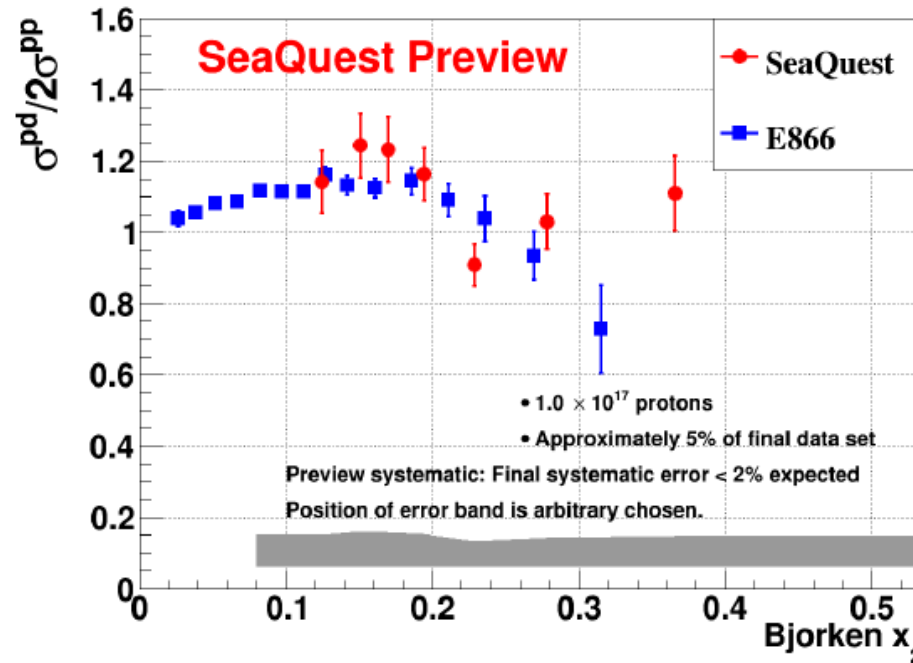
2015/3/24

JPS meeting 2015 Spring @Waseda Univ.

Shou Miyasaka (Tokyo Tech)

E906/SeaQuest Experiment

Cross section ratio, $\sigma^{pd} / 2\sigma^{pp}$ vs Bjorken x_2



- Run2 の極一部のデータを用いた（最終的なデータ総量の約 5%）
- Systematic error は study 中。最終的には 2% 以下になる見積もり
- 妥当なデータを取得している
- 現在は Run3 の QA を行っている

2015/3/24

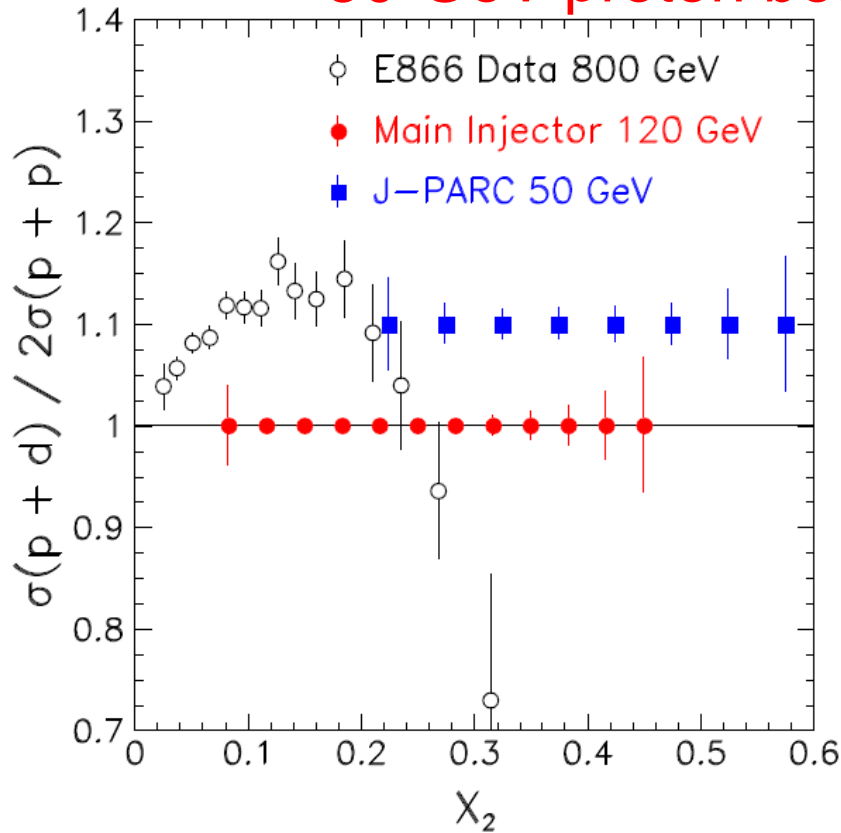
JPS meeting 2015 Spring @Waseda Univ.

Shou Miyasaka (Tokyo Tech)

\bar{d} / \bar{u} at large x

Advange of relatively low beam energy

J-PARC Proposal P-04 (Peng and Sawada)
50-GeV proton beam



10^{12} protons per spill (3 s)

50-cm long LH_2 / LD_2 targets

60-day runs for each targets

assuming 50% efficiency

6

W⁺ and W⁻ Production at Colliders

$$\begin{aligned} \frac{d\sigma}{dY}(pp \rightarrow W^+ X) = K_W \frac{2\pi G_F}{3\sqrt{2}} x_1 x_2 & \left\{ |V_{ud}|^2 [u(x_1)\bar{d}(x_2) + \bar{d}(x_1)u(x_2)] + |V_{us}|^2 [u(x_1)\bar{s}(x_2) + \bar{s}(x_1)u(x_2)] \right. \\ & + |V_{cs}|^2 [c(x_1)\bar{s}(x_2) + \bar{s}(x_1)c(x_2)] + |V_{cd}|^2 [c(x_1)\bar{d}(x_2) + \bar{d}(x_1)c(x_2)] \\ & \left. + |V_{ub}|^2 [u(x_1)\bar{b}(x_2) + \bar{b}(x_1)u(x_2)] + |V_{cb}|^2 [c(x_1)\bar{b}(x_2) + \bar{b}(x_1)c(x_2)] \right\} \end{aligned}$$

$$\begin{aligned} \frac{d\sigma}{dY}(pp \rightarrow W^- X) = K_W \frac{2\pi G_F}{3\sqrt{2}} x_1 x_2 & \left\{ |V_{ud}|^2 [\bar{u}(x_1)d(x_2) + d(x_1)\bar{u}(x_2)] + |V_{us}|^2 [\bar{u}(x_1)s(x_2) + s(x_1)\bar{u}(x_2)] \right. \\ & + |V_{cs}|^2 [\bar{c}(x_1)s(x_2) + s(x_1)\bar{c}(x_2)] + |V_{cd}|^2 [\bar{c}(x_1)d(x_2) + d(x_1)\bar{c}(x_2)] \\ & \left. + |V_{ub}|^2 [\bar{u}(x_1)b(x_2) + b(x_1)\bar{u}(x_2)] + |V_{cb}|^2 [\bar{c}(x_1)b(x_2) + b(x_1)\bar{c}(x_2)] \right\} \end{aligned}$$

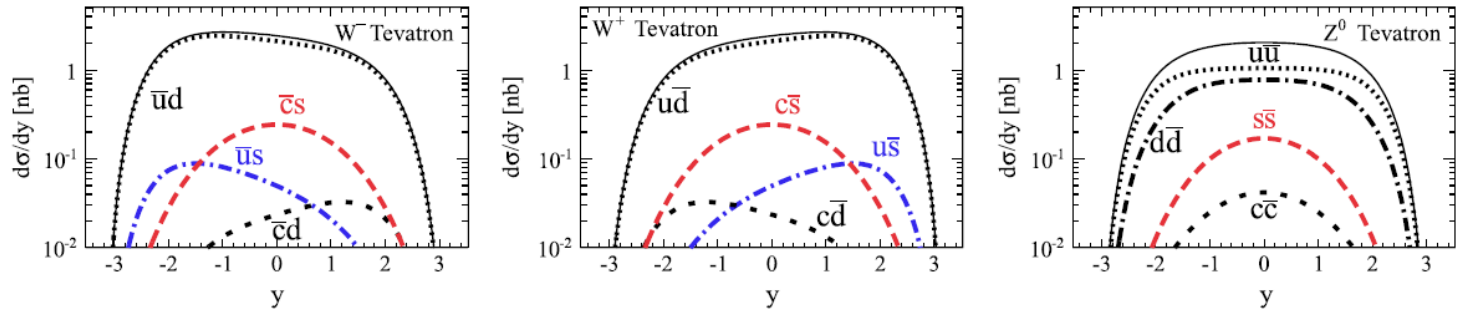
- $V_{ud}^2 = V_{cs}^2 \sim 0.95$, $V_{us}^2 = V_{cd}^2 \sim 0.05$, $V_{ub}^2 \sim 10^{-5}$, $V_{cb}^2 \sim 10^{-3}$

- $s(x) = \bar{s}(x)$, $c(x) = \bar{c}(x)$, $b(x) = \bar{b}(x)$

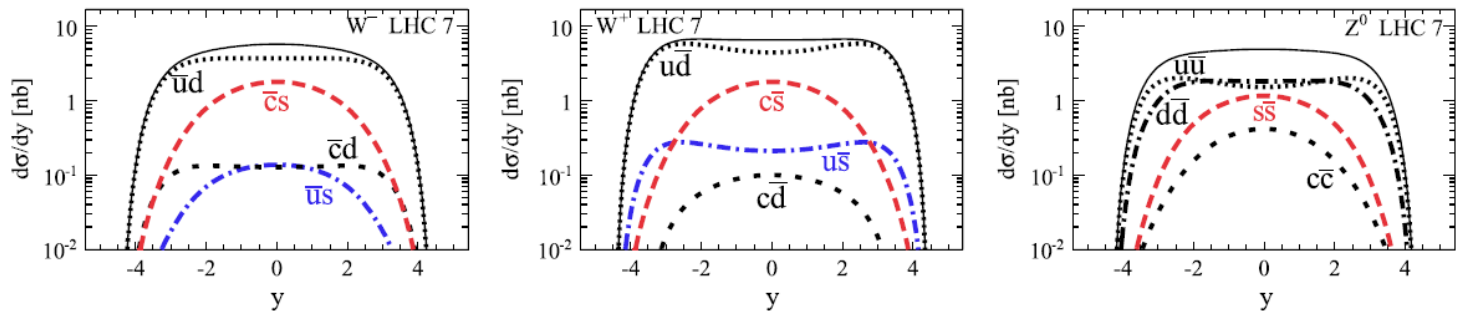
⇒ The W charge asymmetry is mainly from u-d quark interactions.

W^+, W^-, Z Production at Colliders

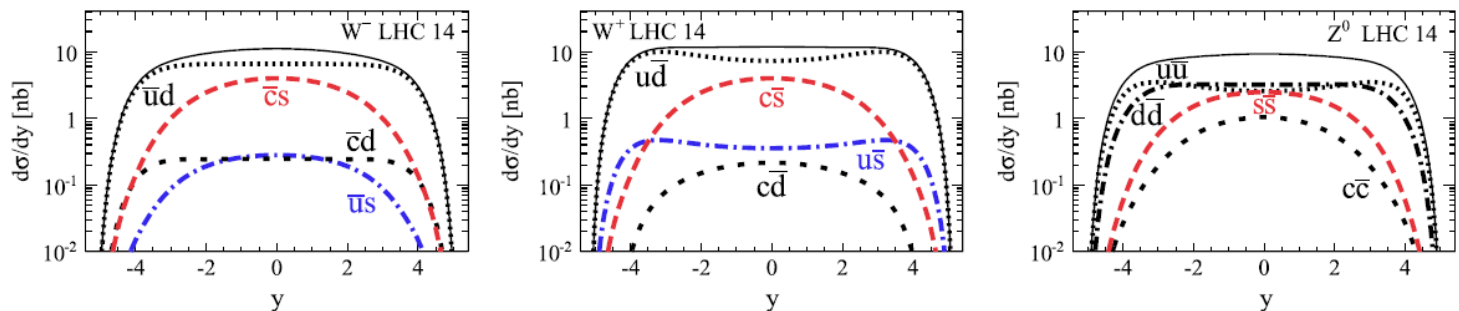
A. Kusina et al., PRD 85 (2012) 094028



(a) $d\sigma/dy$ for W^- (left), W^+ (middle), Z^0 (right) boson production at the Tevatron.



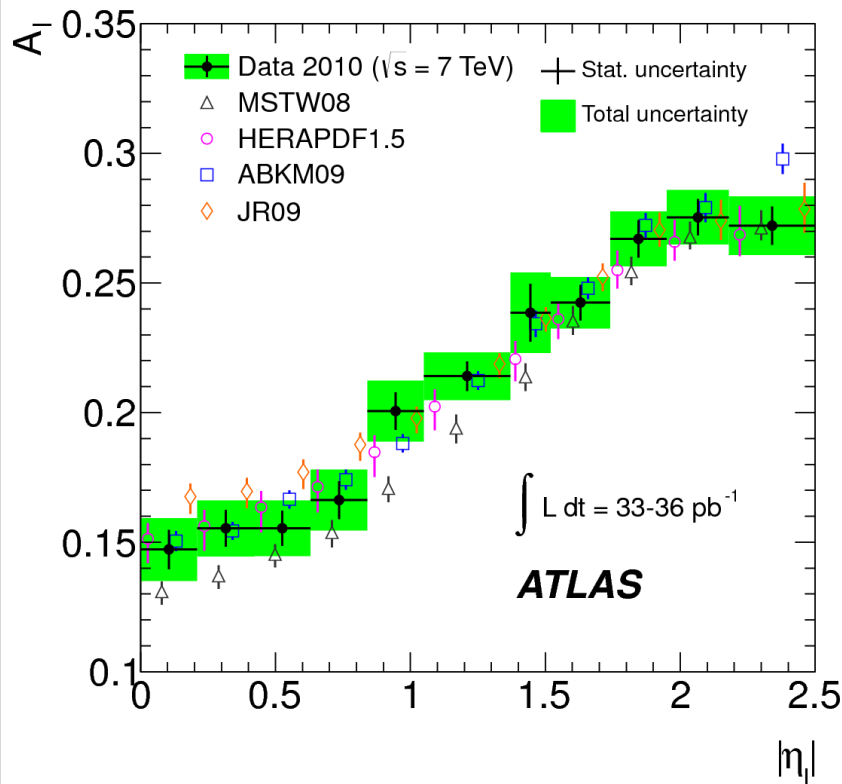
(b) $d\sigma/dy$ for W^- (left), W^+ (middle), Z^0 (right) boson production at the LHC with $\sqrt{S} = 7$ TeV.



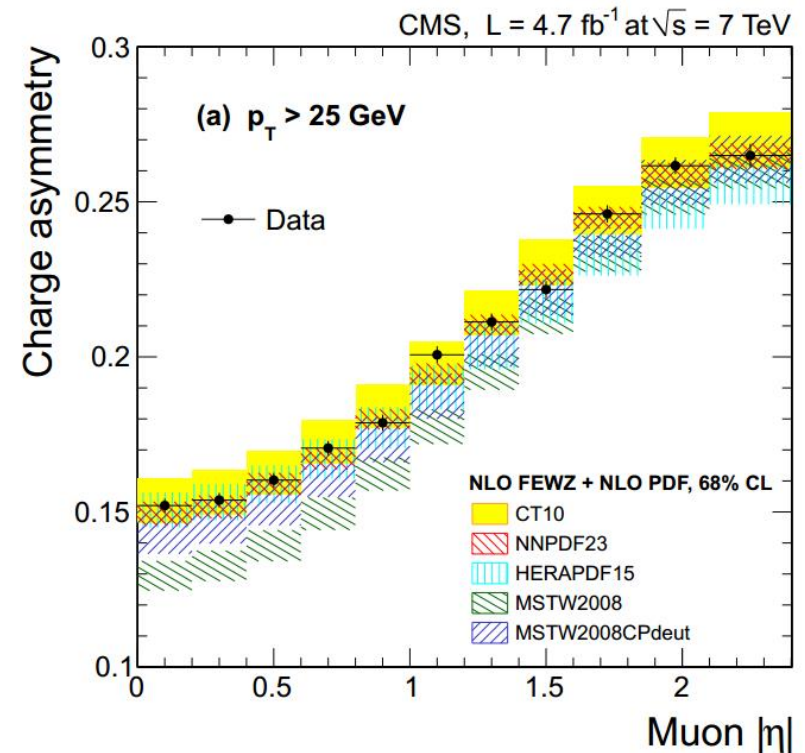
(c) $d\sigma/dy$ for W^- (left), W^+ (middle), Z^0 (right) boson production at the LHC with $\sqrt{S} = 14$ TeV.

Lepton Charge Asymmetry at LHC

ATLAS, PRD 85 (2012) 072004



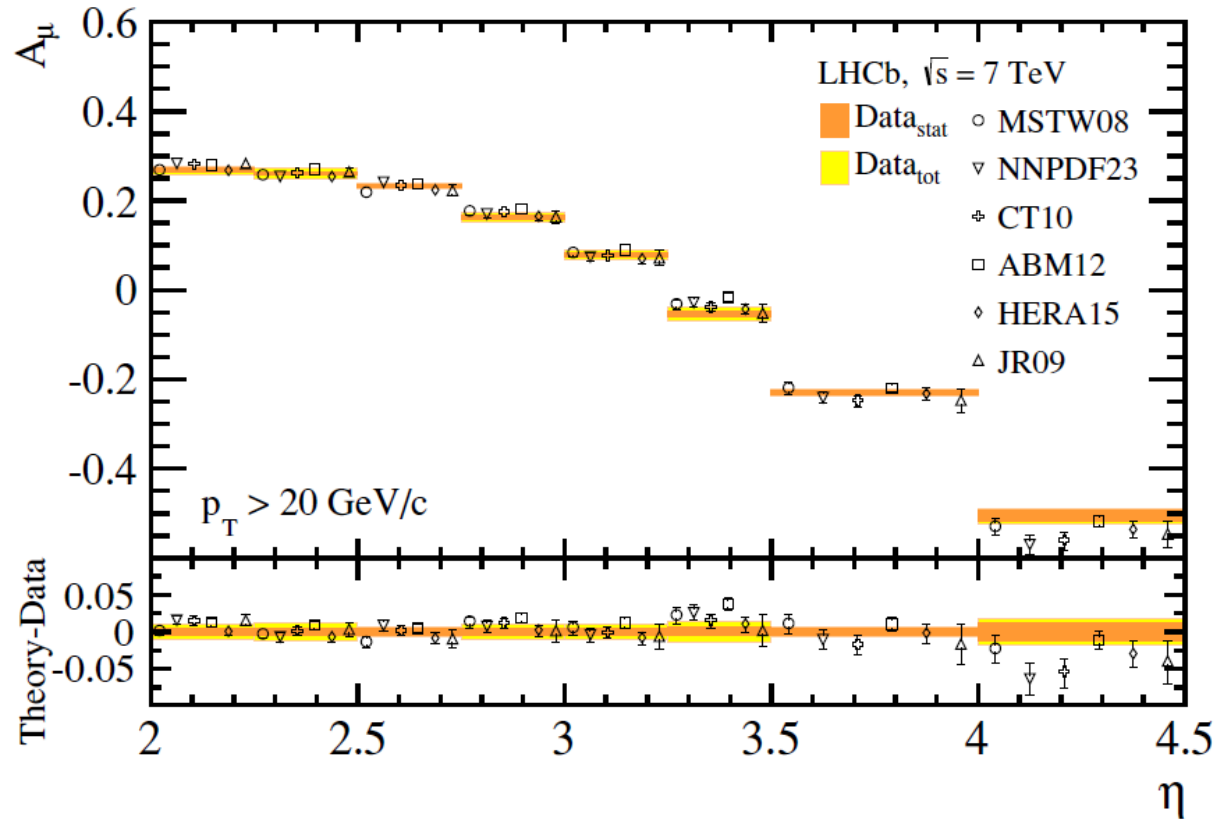
CMS, PRD 90 (2014) 032004



$$A = \frac{W^+ - W^-}{W^+ + W^-}$$

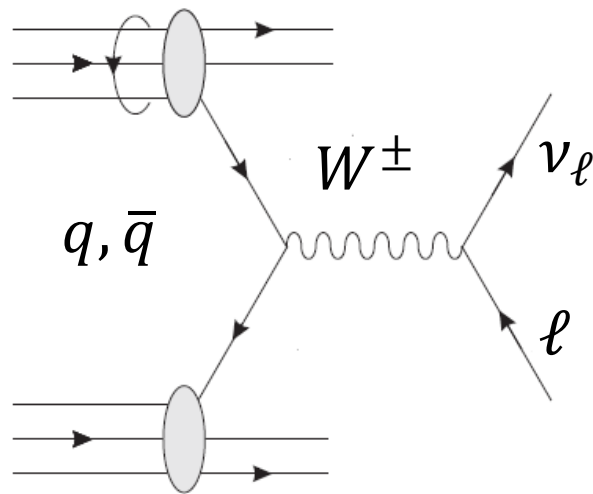
Lepton Charge Asymmetry at LHC

LHCb, JHEP 12 (2014) 079



$$A = \frac{W^+ - W^-}{W^+ + W^-}$$

Sea-quark polarization from W production in polarized pp collision



Parity-violating asymmetry

$$A_L^{W^\pm} \equiv \frac{d\sigma^{++} + d\sigma^{+-} - (d\sigma^{-+} + d\sigma^{--})}{d\sigma^{++} + d\sigma^{+-} + d\sigma^{-+} + d\sigma^{--}}$$

$$A_L^{W^+} = \frac{-\Delta u(x_1)\bar{d}(x_2) + \Delta\bar{d}(x_1)u(x_2)}{u(x_1)\bar{d}(x_2) + \bar{d}(x_1)u(x_2)}$$

$$A_L^{W^-} = \frac{-\Delta d(x_1)\bar{u}(x_2) + \Delta\bar{u}(x_1)d(x_2)}{d(x_1)\bar{u}(x_2) + \bar{u}(x_1)d(x_2)}$$

• $x_1 \gg x_2$

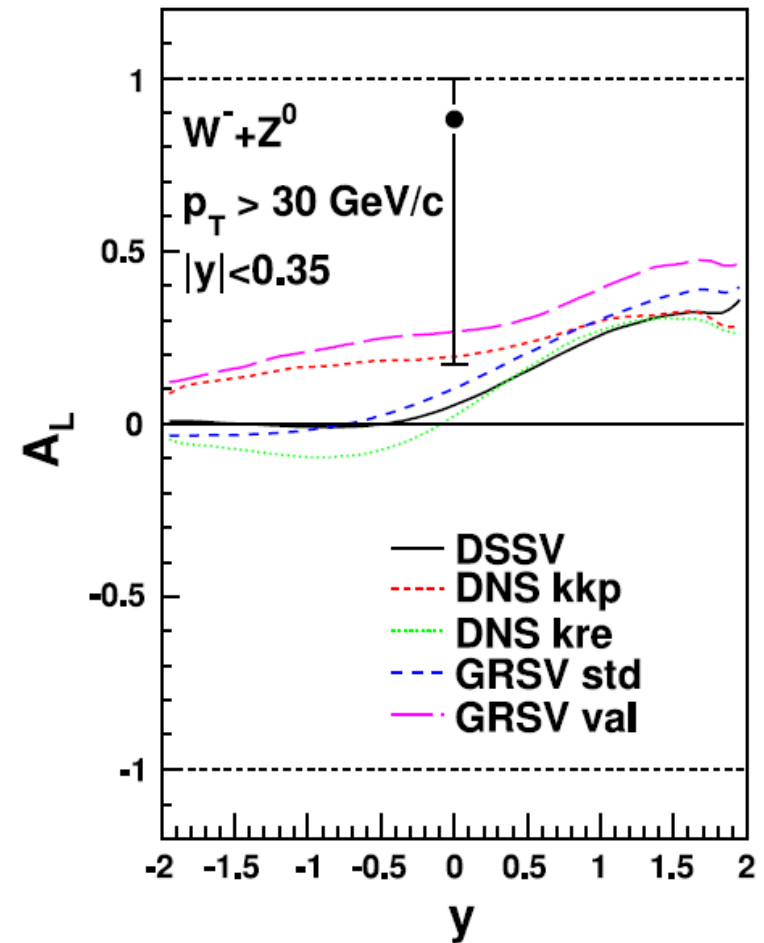
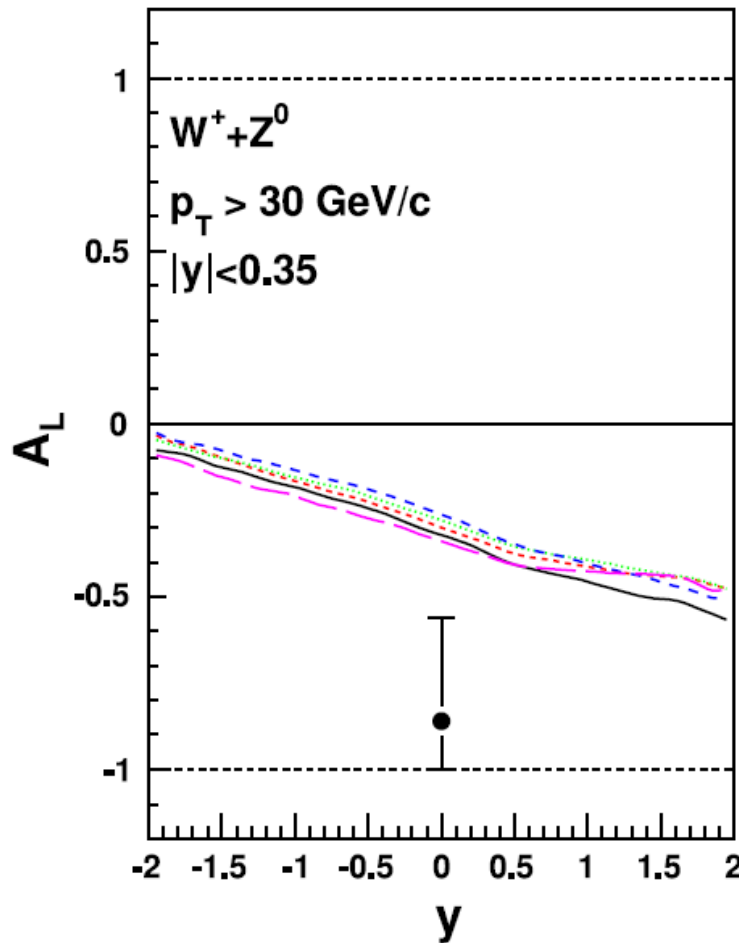
$$A_L^{W^+} \approx -\frac{\Delta u(x_1)}{u(x_1)}, A_L^{W^-} \approx -\frac{\Delta d(x_1)}{d(x_1)}$$

• $x_2 \gg x_1$

$$A_L^{W^+} \approx \frac{\Delta\bar{d}(x_1)}{\bar{d}(x_1)}, A_L^{W^-} \approx \frac{\Delta\bar{u}(x_1)}{\bar{u}(x_1)}$$

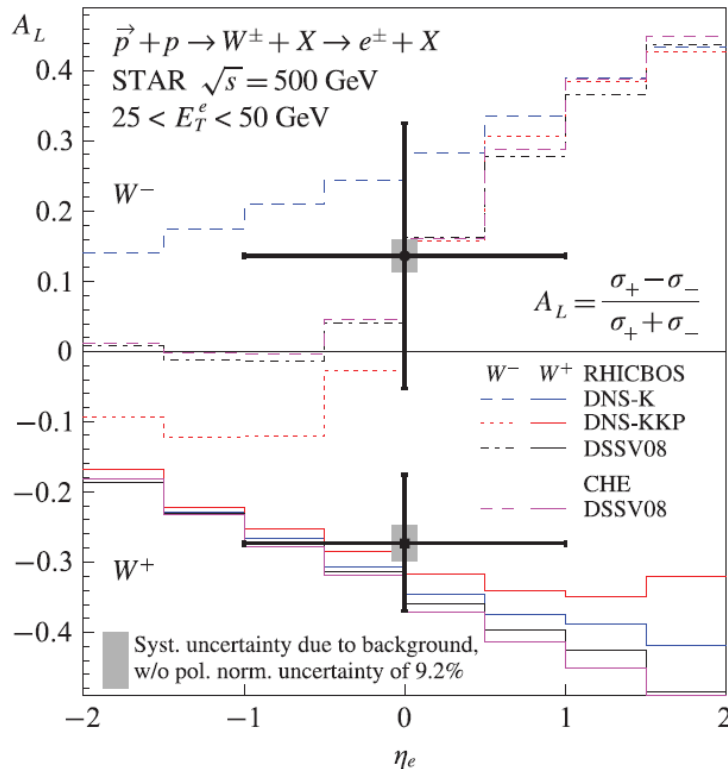
Parity-violating spin asymmetries in W production

PHENIX, PRL 106, 062001 (2011)

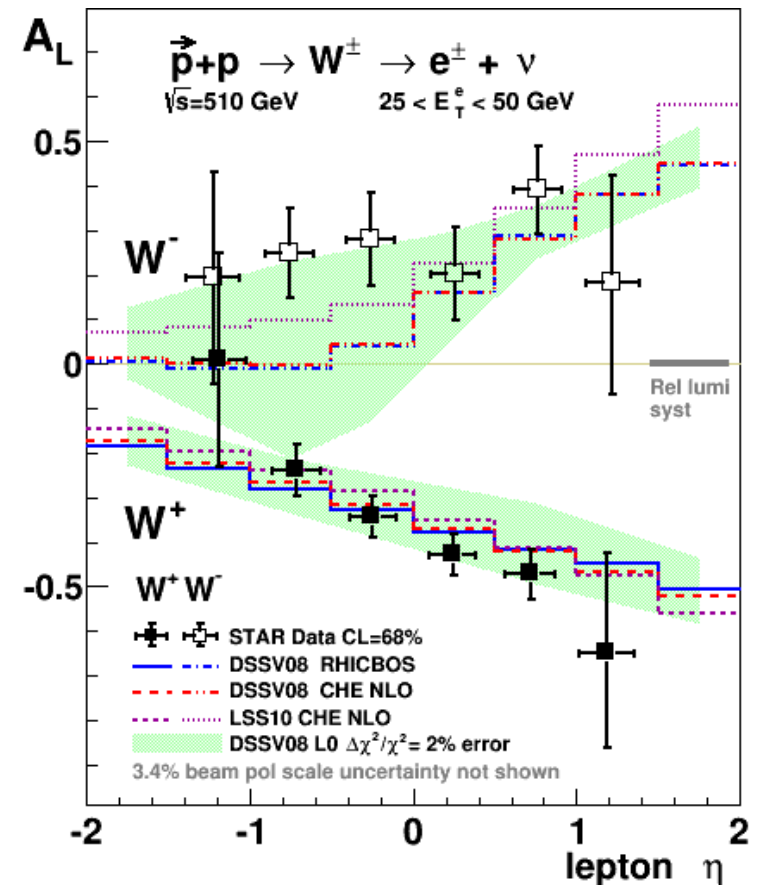


Parity-violating spin asymmetries in W production

STAR, PRL 106, 062002 (2011)

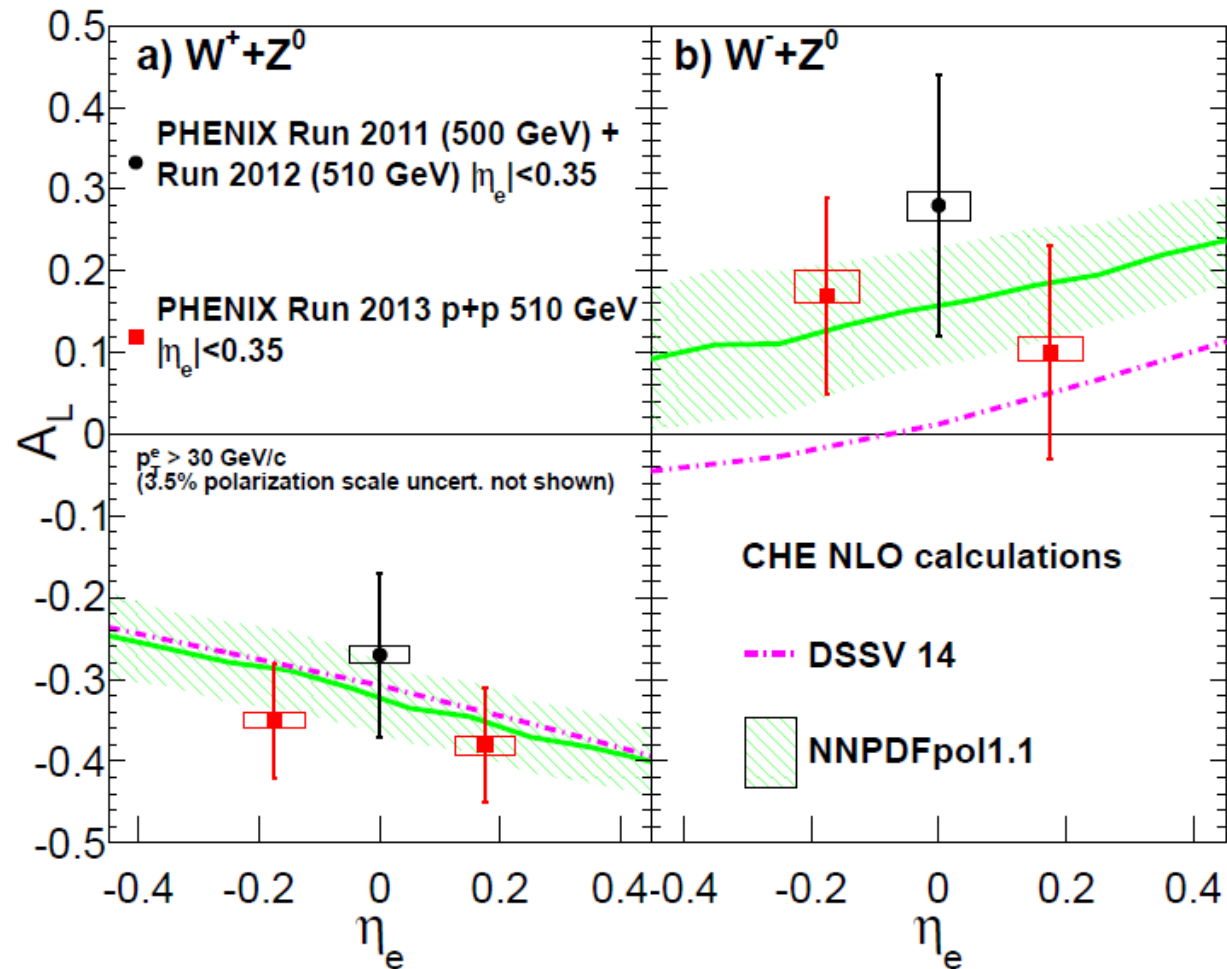


STAR, PRL 113, 072301 (2014)



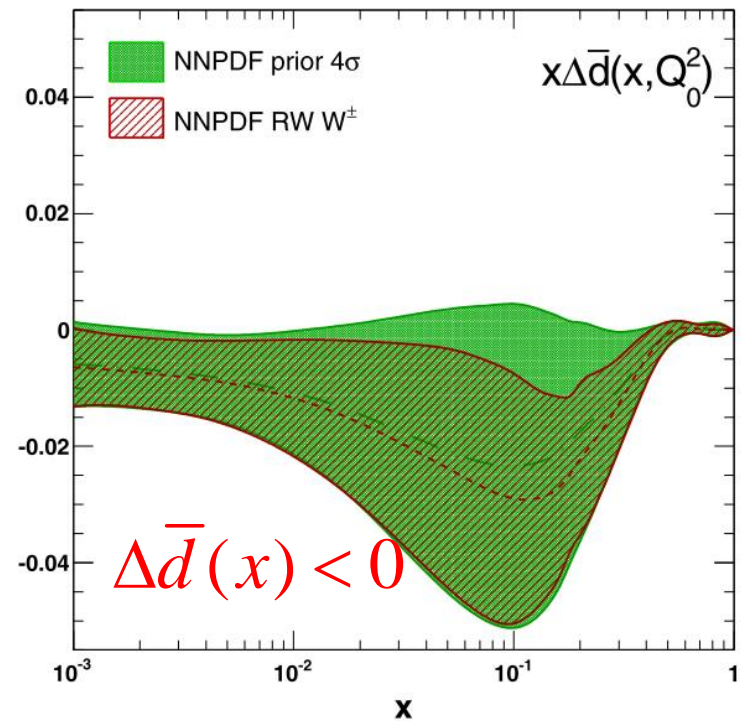
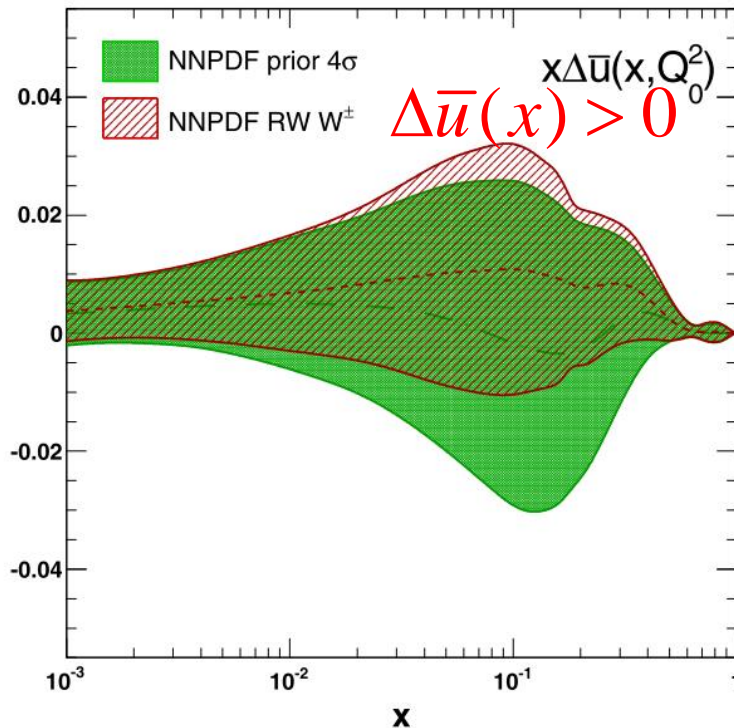
Parity-violating spin asymmetries in W production

PHENIX, arXiv:1504.07451

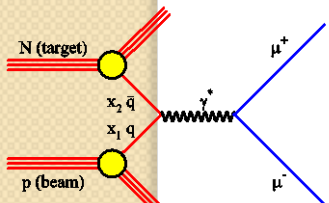
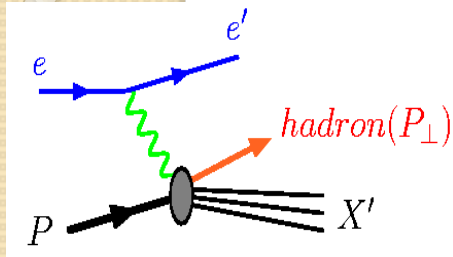


Longitudinal Polarization of Sea-Quarks in NNPDFpol1.1

NPB 877 (2014) 276

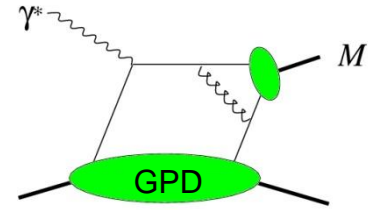


Parton Distributions in Protons



Wigner Distribution
 $W(\vec{r}, x, \vec{k}_T)$

Ji, PRL91,062001(2003)



$$\int d\vec{r}$$

$$\int e^{i\vec{q}\cdot\vec{r}} d\vec{r} d\vec{k}_T$$

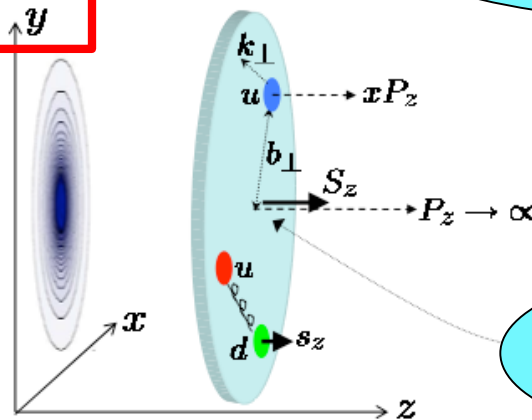
$$\xi = q^z / 2E_q, t = -\vec{q}^2$$

Transverse Momentum
 Dependent PDF $f(x, \vec{k}_T)$

Generalized Parton Distr.
 $F(x, \xi, t)$

$$\int d\vec{k}_T$$

PDF
 $f(x)$



Form Factors
 $F_1(t), F_2(t)$

Quark Distribution Functions

At leading twist

$$q(x) = \text{[Diagram: A circle with a black dot in the center]} \quad \text{Quark Momentum Distribution}$$

$$\Delta q(x) = \text{[Diagram: Two circles connected by a horizontal line. The left circle has a black dot and a red arrow pointing right. The right circle has a black dot and a red arrow pointing left. Green arrows point right from the red arrows. A black line connects the two circles.]}$$

Quark Helicity Distribution

$$\delta q(x) = \text{[Diagram: Two circles connected by a horizontal line. The left circle has a black dot and a red arrow pointing up. The right circle has a black dot and a red arrow pointing down. Green arrows point up from the red arrows. A black line connects the two circles.]}$$

Quark Transversity Distribution

$\delta q(x)$:

Positivity Bound $|\delta q(x)| \leq q(x)$

Soffer Bound $|\delta q(x)| \leq \frac{1}{2} [q(x) + \Delta q(x)]$

Prehistory of Transverse Spin Effect

- 1966 Christ and Lee: transverse **single-spin asymmetry (SSA)**, a chiral-odd quantity, is prohibited by time-reversal invariance in DIS.
- 1975 Large **SSA** in $p \uparrow p \rightarrow \pi X$
- 1976 Large transverse polarization of Λ in $pp \rightarrow \Lambda X$
- 1978 Kane, Pumplin and Repko: **SSAs** shall vanish in the massless limit.

History of Transverse Spin Effect

- **1990 Sivers: $SSAs$** originating from the intrinsic motion of quarks in a transversely polarized hadron.
- **1993 Collins:** a spin asymmetry in the fragmentation of transversely polarized quarks, correlating with p_t , into an unpolarized hadron, which enables the measurement of $SSAs$ in SIDIS.
- **1993 Collins:** Sivers function should vanish due to parity and time reversal invariance.

History of Transverse Spin Effect

- **2002 Brodsky, Hwang and Schmidt:** SSAs in SIDIS might be finite taking account of orbital motion of quarks and multiple gluon scattering.
- **2002 Collins:** Sivers function could be non-zero due to the **gauge link**. The Sivers functions for SIDIS and Drell-Yan processes are of opposite sign.

Transverse momentum dependent (TMD) PDF

Leading Twist TMDs



Nucleon Spin



Quark Spin

		Quark Polarization		
		Un-Polarized (U)	Longitudinally Polarized (L)	Transversely Polarized (T)
Nucleon Polarization	U	$f_1 = \text{circle with red dot}$		$h_1^\perp = \text{circle with red dot and arrow} - \text{circle with red dot and arrow}$ Boer-Mulders
	L		$g_{1L} = \text{circle with red arrow} - \text{circle with red arrow}$ Helicity	$h_{1L}^\perp = \text{circle with red arrow and arrow} - \text{circle with red arrow and arrow}$
	T	$f_{1T}^\perp = \text{circle with red dot and arrow} - \text{circle with red dot and arrow}$ Sivers	$g_{1T}^\perp = \text{circle with red arrow and arrow} - \text{circle with red arrow and arrow}$	$h_1 = \text{circle with red dot and arrow} - \text{circle with red dot and arrow}$ Transversity $h_{1T}^\perp = \text{circle with red arrow and arrow} - \text{circle with red arrow and arrow}$

Boer-Mulders $h_1^\perp(x, k_T)$ function

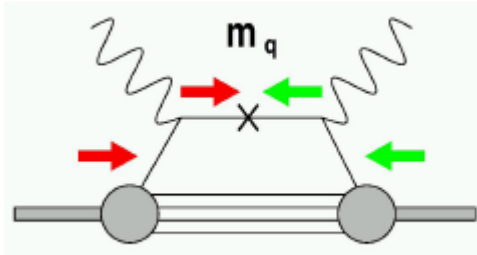
correlation between the transverse spin and the transverse momentum of the quark in unpolarized nucleons

Sivers function $f_{1T}^\perp(x, k_T)$

correlation between the transverse spin of the nucleon and the transverse momentum of the quark.

sensitive to orbital angular momentum

How to measure SSAs?



Chiral-odd \rightarrow not accessible in DIS

Require another chiral-odd object

- **Semi-Inclusive DIS:** ambiguity associated with fragmentation process
 - Single-hadron (Collins fragmentation function, Sivers function)
 - Two hadrons (Interference fragmentation function)
 - Vector meson polarization
 - Λ – polarization
- **Drell-Yan:** small cross sections but free from fragmentation
- **Proton-proton collision:** inclusive single-hadron, prompt jet, prompt photon production

High energy spin experiments

C.A. Aidala, S.D. Bass, D. Hasch, G.K. Mallot, Rev. Mod. Phys. 85, 655–691 (2013)

Experiment	Year	Beam	Target	Energy (GeV)	Q^2 (GeV ²)	x
Completed experiments						
SLAC – E80, E130	1976–1983	e^-	H-butanol	$\lesssim 23$	1–10	0.1–0.6
SLAC – E142/3	1992–1993	e^-	NH ₃ , ND ₃	$\lesssim 30$	1–10	0.03–0.8
SLAC – E154/5	1995–1999	e^-	NH ₃ , ⁶ LiD, ³ He	$\lesssim 50$	1–35	0.01–0.8
CERN – EMC	1985	μ^+	NH ₃	100, 190	1–30	0.01–0.5
CERN – SMC	1992–1996	μ^+	H/D-butanol, NH ₃	100, 190	1–60	0.004–0.5
FNAL E581/E704	1988–1997	p	p	200	~ 1	$0.1 < x_F < 0.8$
Analyzing and/or Running						
DESY – HERMES	1995–2007	e^+, e^-	H, D, ³ He	~ 30	1–15	0.02–0.7
CERN – COMPASS	2002–2012	μ^+	NH ₃ , ⁶ LiD	160, 200	1–70	0.003–0.6
JLab6 – Hall A	1999–2012	e^-	³ He	$\lesssim 6$	1–2.5	0.1–0.6
JLab6 – Hall B	1999–2012	e^-	NH ₃ , ND ₃	$\lesssim 6$	1–5	0.05–0.6
RHIC – BRAHMS	2002–2006	p	p (beam)	$2 \times (31–100)$	$\sim 1–6$	$-0.6 < x_F < 0.6$
RHIC – PHENIX, STAR	2002+	p	p (beam)	$2 \times (31–250)$	$\sim 1–400$	$\sim 0.02–0.4$
Approved future experiments (in preparation)						
CERN – COMPASS-II	2014+	μ^+, μ^-	unpolarized H ₂	160	$\sim 1–15$	$\sim 0.005–0.2$
		π^-	NH ₃	190		$-0.2 < x_F < 0.8$
JLab12 – HallA/B/C	2014+	e^-	HD, NH ₃ , ND ₃ , ³ He	$\lesssim 12$	$\sim 1–10$	$\sim 0.05–0.8$

Semi-Inclusive DIS (SIDIS)

$$q^2 = (l - l')^2 = -Q^2$$

Bjorken scaling variable

$$x = Q^2 / (2P \cdot q)$$

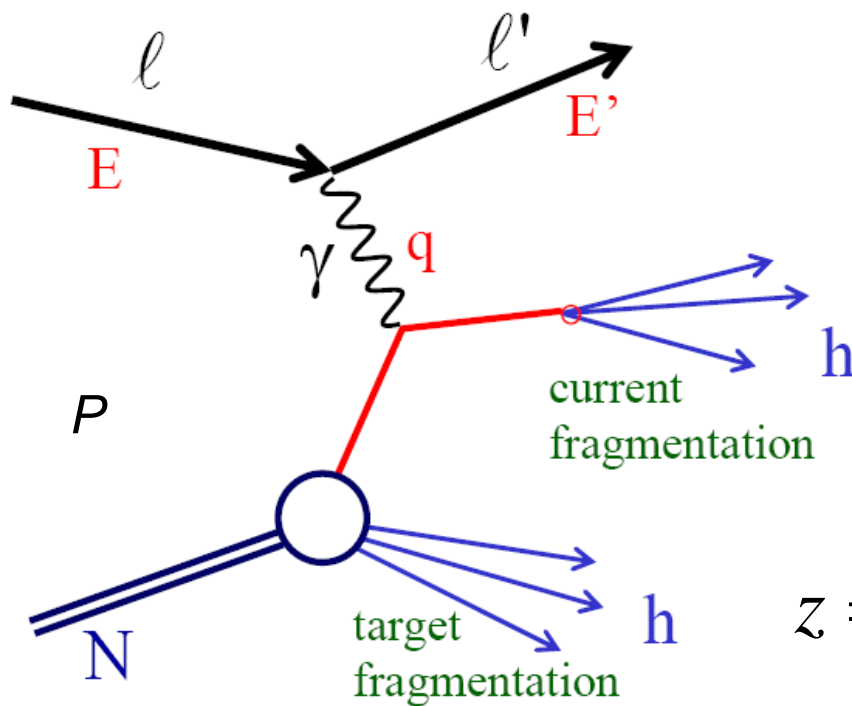
Energy fraction carried by γ

$$y = (P \cdot q) / (P \cdot l) = (E - E') / E$$

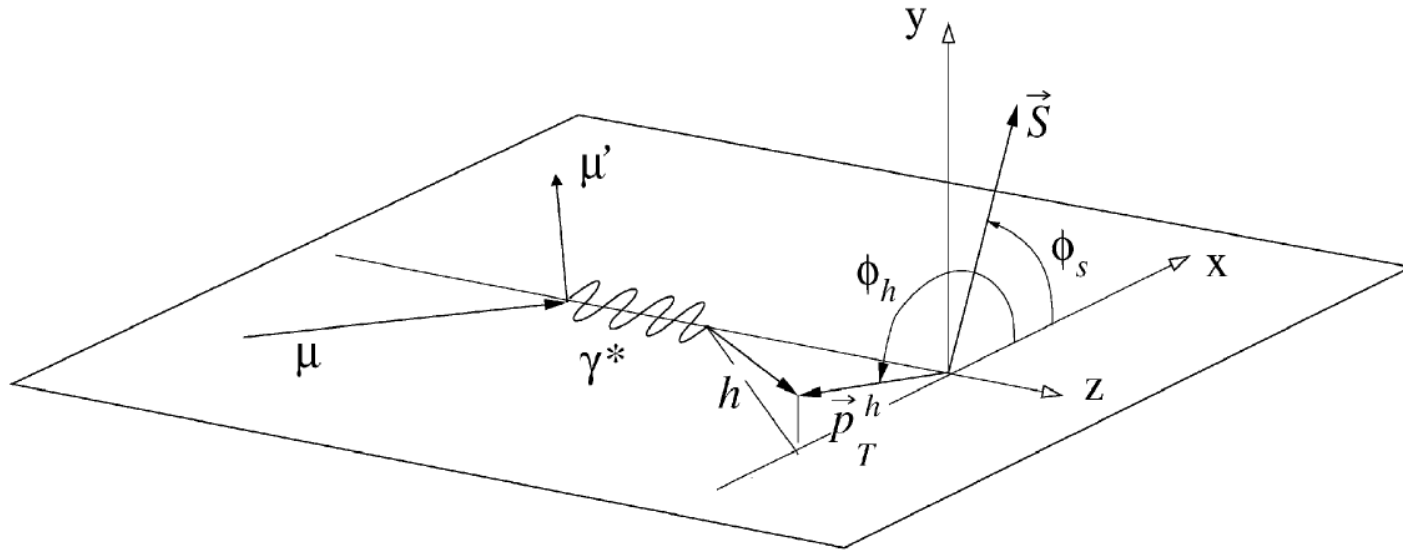
Energy fraction carried by h

$$z = (P \cdot P_h) / (P \cdot q) = E_h / (E - E')$$

$$W^2 = (P + q)^2$$



Collins and Sivers Asymmetries in SIDIS



$$A_T^h \equiv \frac{d\sigma(\vec{S}_\perp) - d\sigma(-\vec{S}_\perp)}{d\sigma(\vec{S}_\perp) + d\sigma(-\vec{S}_\perp)} = |\vec{S}_\perp| \cdot [D_{NN} \cdot A_{Coll} \cdot \sin(\phi_h + \phi_S - \pi) + A_{Siv} \cdot \sin(\phi_h - \phi_S)]$$

Collins asymmetry

$$A_{Coll} = \frac{\sum_q [e_q^2 \cdot \Delta_{Tq}(x) \cdot \Delta_T^0 D_q^h(z, p_T^h)]}{\sum_q [e_q^2 \cdot q(x) \cdot D_q^h(z, p_T^h)]}$$

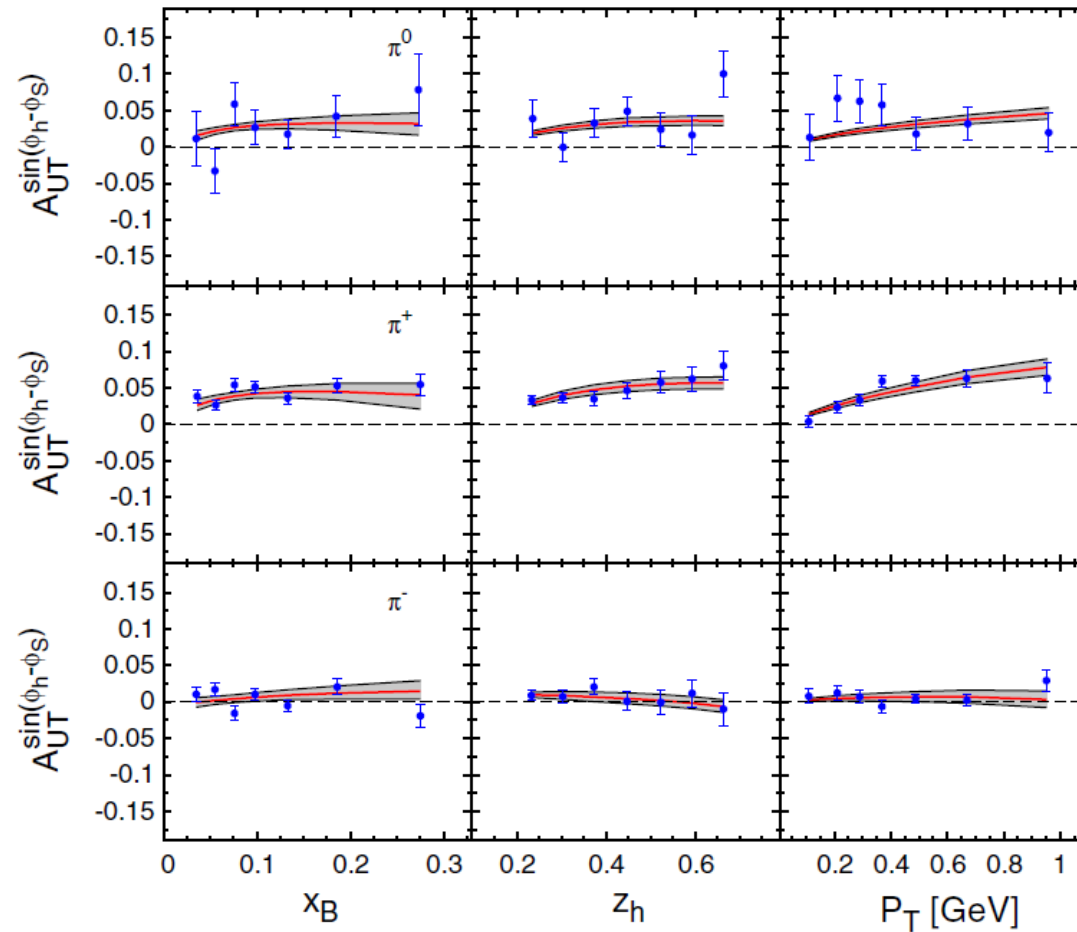
Sivers asymmetry

$$A_{Siv} = \frac{\sum_q [e_q^2 \cdot \Delta_{Tq}^0(x, p_T^h / z) \cdot D_q^h(z, p_T^h)]}{\sum_q [e_q^2 \cdot q(x, p_T^h / z) \cdot D_q^h(z)]}$$

Global Analysis of Sivers Functions from SIDIS

M. Anselmino et al., PRD 86 (2012) 014028

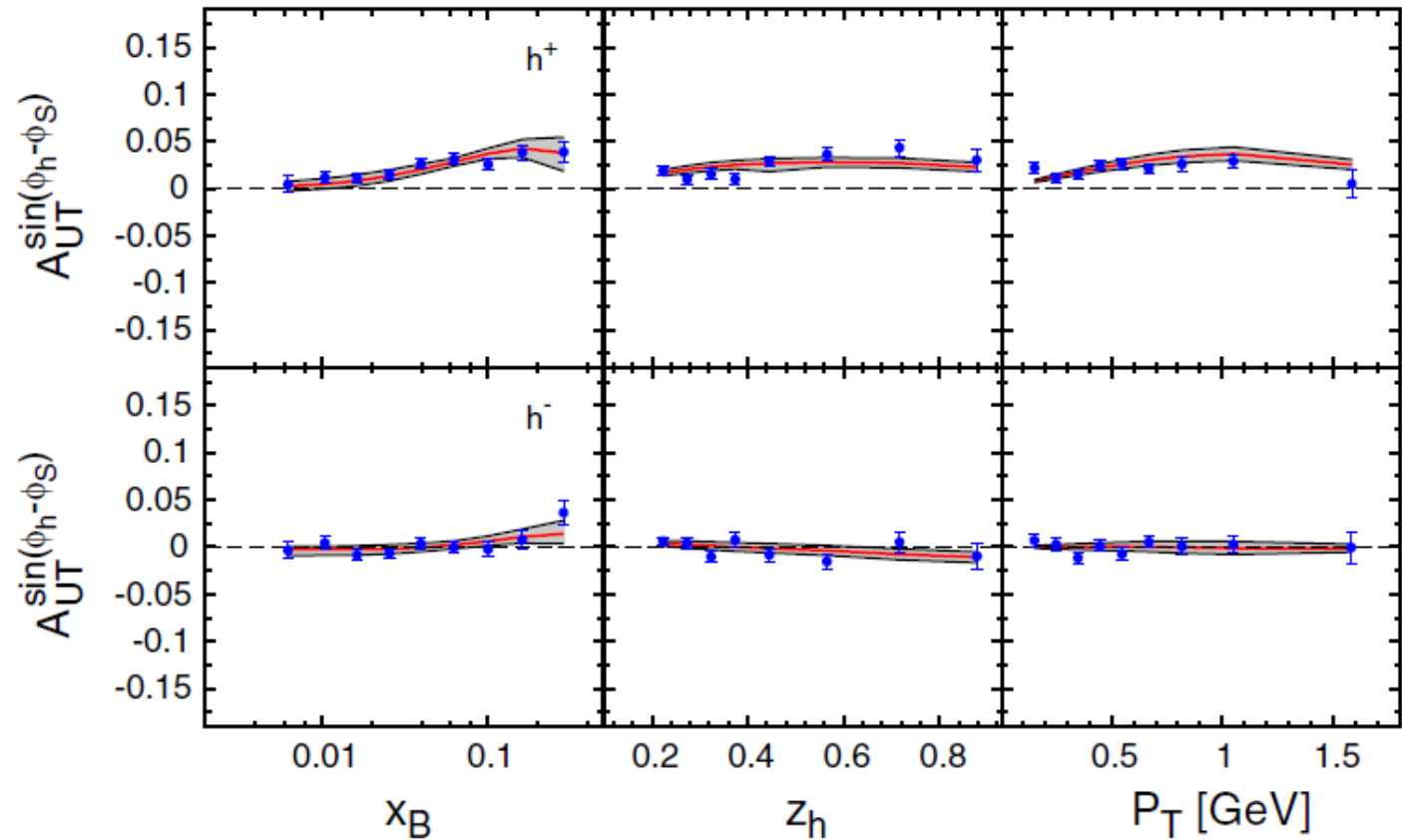
HERMES PROTON - TMD



Global Analysis of Sivers Functions from SIDIS

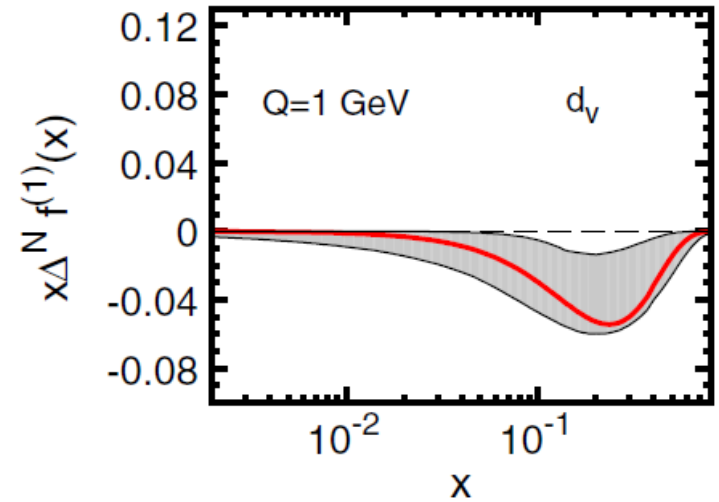
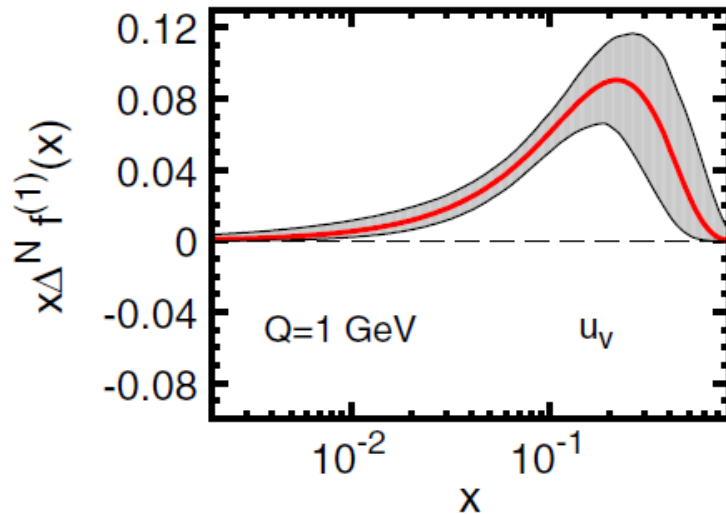
M. Anselmino et al., PRD 86 (2012) 014028

COMPASS PROTON - TMD



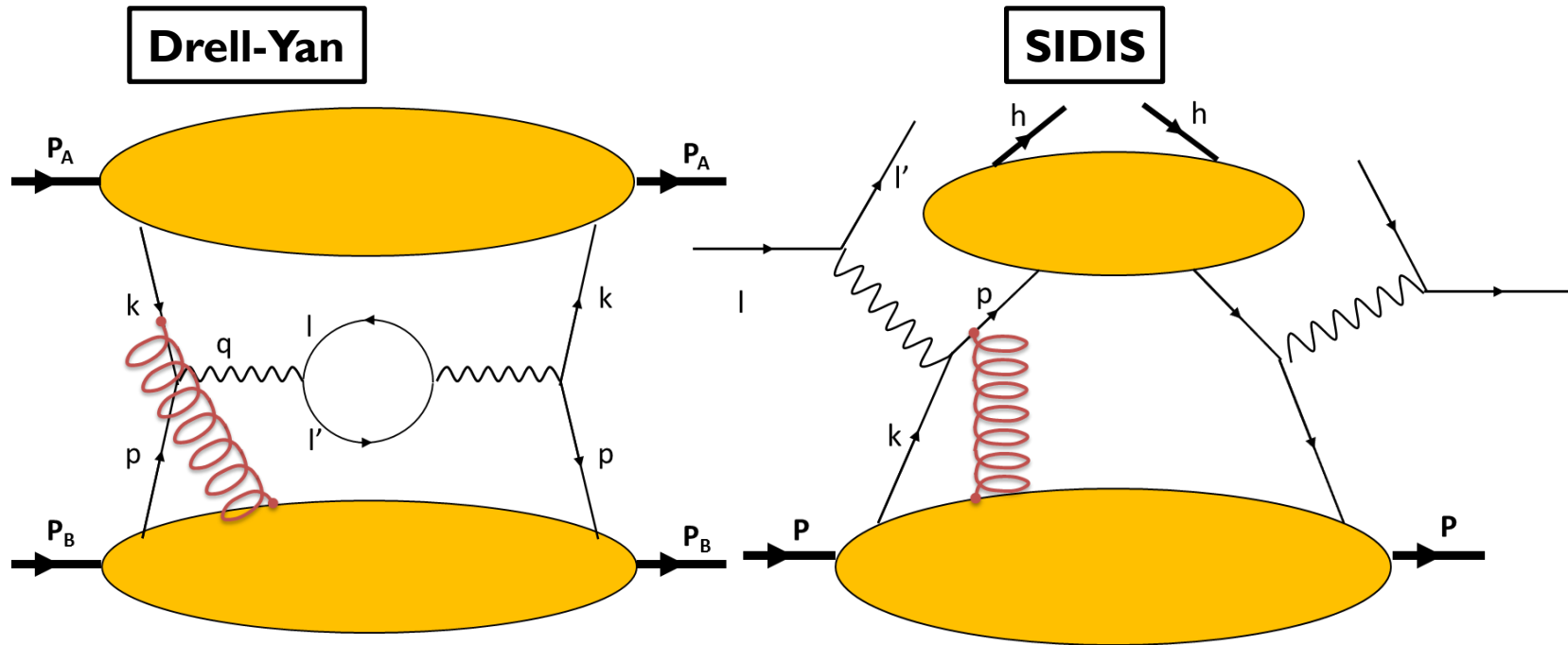
Global Analysis of Sivers Functions from SIDIS

M. Anselmino et al., PRD 86 (2012) 014028



Non-Universality of Sivers Functions

J.C. Collins, Phys. Lett. B 536 (2002) 43; A.V. Belitsky, X. Ji, F.Yuan, Nucl. Phys. B 656 (2003) 165;
 D. Boer, P.J. Mulders, F. Pijlman, Nucl. Phys. B 667 (2003) 201; Z.B. Kang, J.W. Qiu, Phys. Rev. Lett. 103
 (2009) 172001

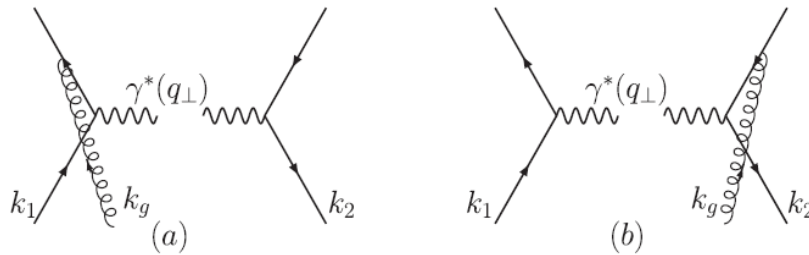


$$\text{Sivers} |_{DY} = -1 * \text{Sivers} |_{SIDIS}$$

- QCD gluon gauge link (Wilson line) in the initial state (DY) vs. final state interactions (SIDIS).
- **Experimental confirmation of the sign change will be a crucial test of perturbative QCD and TMD physics.**

“Opposite Sign of SSA for SIDIS and DY” NLO QCD

Z-B Kang, B-W Xiao and F.Yuan, PRL 107, 152002 (2011)



- Ji-Ma-Yuan factorization
- Collins-Soper-Sterman resummation

$$\Delta C_q^T \Big|_{DY} = - \Delta C_q^T \Big|_{SIDIS}$$

FIG. 2. Leading order Born diagram calculation of $\tilde{W}_{UT}(Q, b)$.

$$\frac{d\Delta\sigma(S_\perp)}{dvdO^2 d^2a_\perp} = \sigma_0 \epsilon^{\alpha\beta} S_\perp^\alpha W_{UT}^\beta(Q; q_\perp), \quad (2)$$

$$W_{UT}^\alpha(Q; q_\perp) = \int \frac{d^2b}{(2\pi)^2} e^{i\vec{q}_\perp \cdot \vec{b}} \tilde{W}_{UT}^\alpha(Q; b) + Y_{UT}^\alpha(Q; q_\perp),$$

$$q_\perp \ll Q$$

$$\begin{aligned} \tilde{W}_{UT}^\alpha(Q; b) &= e^{-S_{UT}(Q^2, b)} \tilde{W}_{UT}^\alpha(C_1/b, b) \\ &= (-ib_\perp^\alpha / 2) e^{-S_{UT}(Q^2, b)} \sum_{i,j} \\ &\times \Delta C_{qi}^T \otimes f_{i/A}^{(3)}(z_1', z_1'') C_{\bar{q}j} \otimes f_{j/B}(z_2'), \end{aligned} \quad (9)$$

Single transversely-polarized Drell-Yan cross-section in LO QCD Parton Model

S. Arnold, et al., Phys. Rev. D79 (2009) 034005

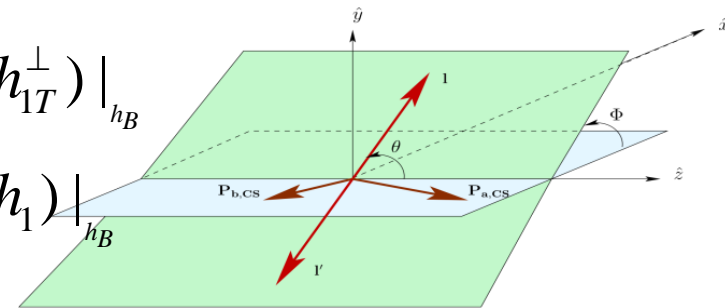
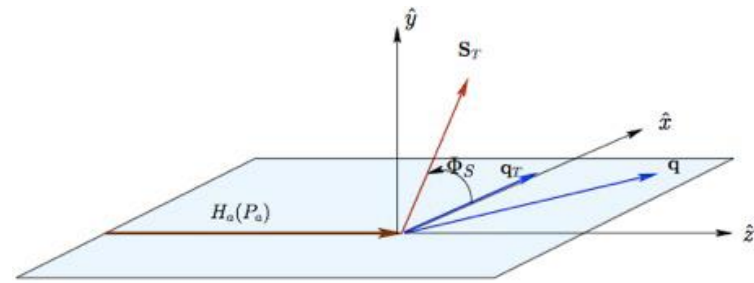
$$\begin{aligned} & \frac{d\sigma^{LO}}{d^4q d\Omega} \\ &= \frac{\alpha_{em}^2}{Fq^2} \widehat{\sigma}_U^{LO} \left\{ \left(1 + D_{[\sin^2 \theta]}^{LO} A_U^{\cos 2\varphi} \cos 2\varphi \right) \right. \\ &+ \left. |\vec{S}_T| \left[A_T^{\sin \varphi_s} \sin \varphi_s \right. \right. \end{aligned}$$

$$A_U^{\cos 2\varphi} \propto \text{BM}(h_1^\perp) |_{h_A} \otimes \text{BM}(h_1^\perp) |_{h_B}$$

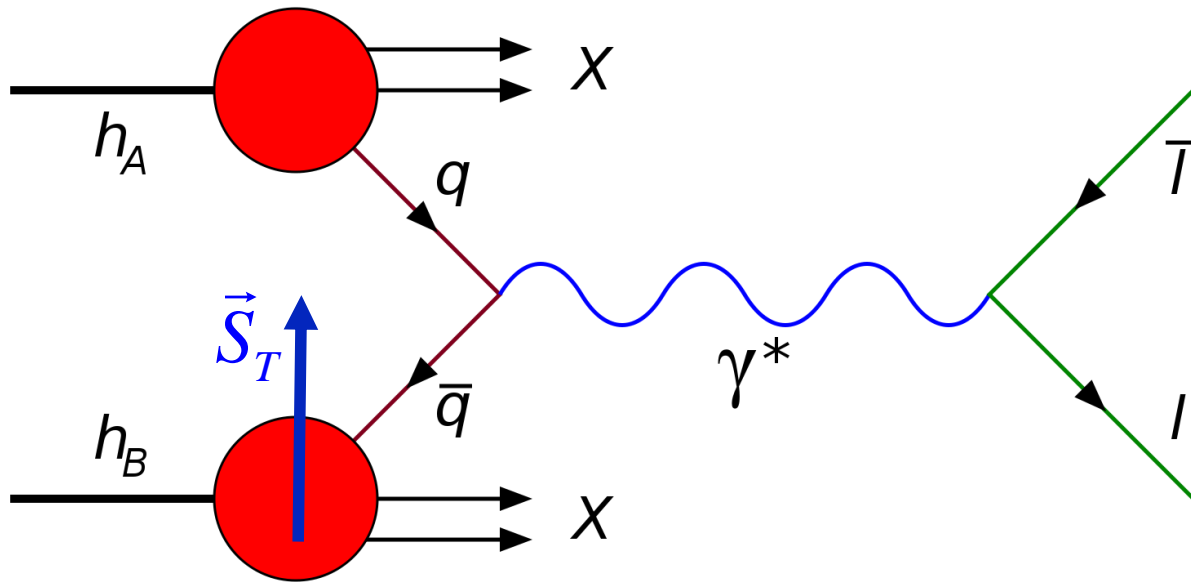
$$A_T^{\sin \varphi_s} \propto \text{Density}(f_1) |_{h_A} \otimes \text{Sivers}(f_{1T}^\perp) |_{h_B}$$

$$A_T^{\sin(2\varphi+\varphi_s)} \propto \text{BM}(h_1^\perp) |_{h_A} \otimes \text{pretzelosity}(h_{1T}^\perp) |_{h_B}$$

$$A_T^{\sin(2\varphi-\varphi_s)} \propto \text{BM}(h_1^\perp) |_{h_A} \otimes \text{transversity}(h_1) |_{h_B}$$



Transversely-polarized Drell-Yan experiments !!!



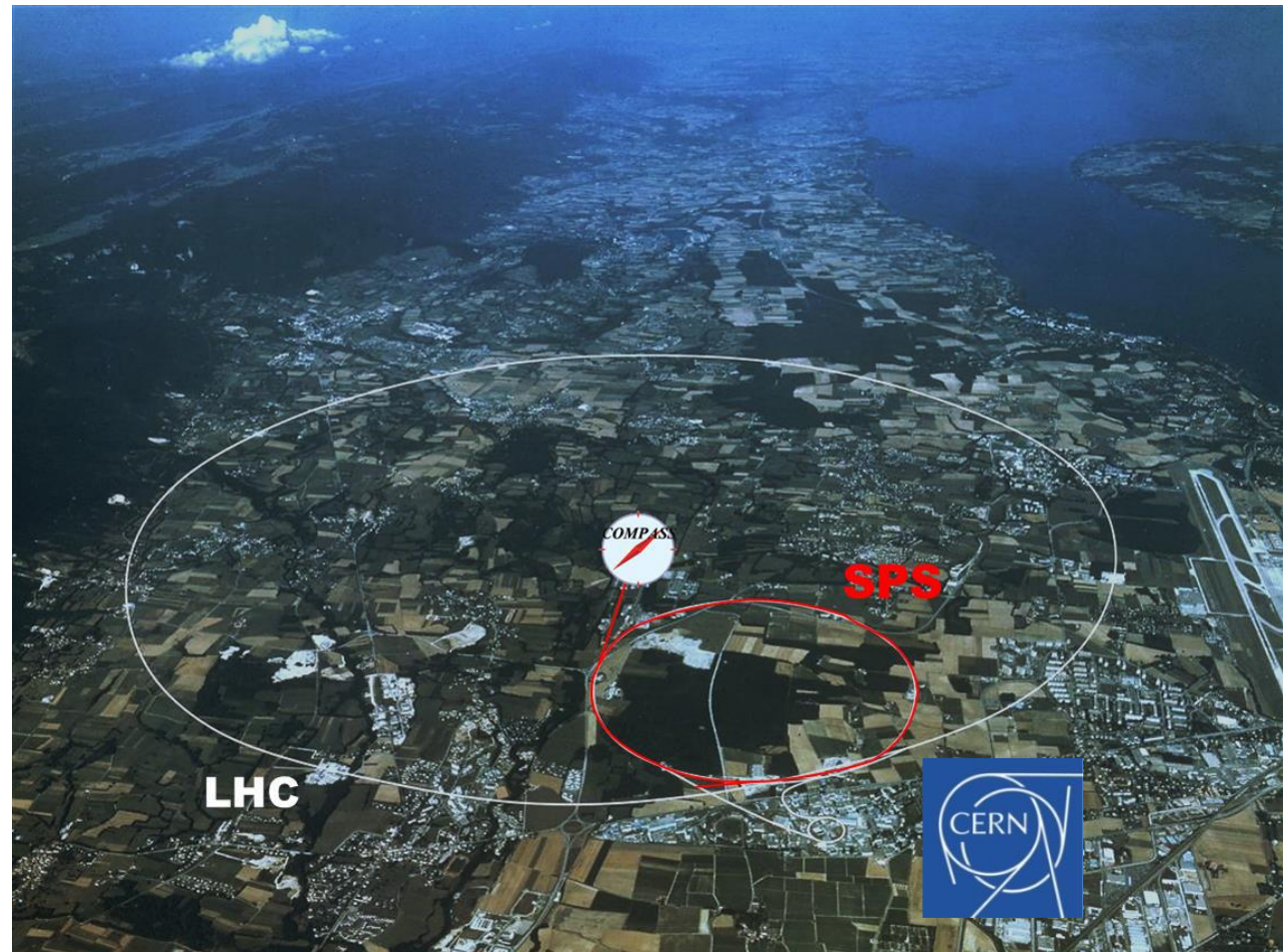
Planned Polarized Drell-Yan Experiments

experiment	particles	energy	x_1 or x_2	luminosity	timeline
COMPASS (CERN)	$\pi^\pm + p^\uparrow$	160 GeV $\sqrt{s} = 17.4$ GeV	$x_t = 0.2 - 0.3$	$2 \times 10^{33} \text{ cm}^{-2} \text{ s}^{-1}$	2014, 2018
PAX (GSI)	$p^\uparrow + p_{\text{bar}}$	collider $\sqrt{s} = 14$ GeV	$x_b = 0.1 - 0.9$	$2 \times 10^{30} \text{ cm}^{-2} \text{ s}^{-1}$	>2017
PANDA (GSI)	$p_{\text{bar}} + p^\uparrow$	15 GeV $\sqrt{s} = 5.5$ GeV	$x_t = 0.2 - 0.4$	$2 \times 10^{32} \text{ cm}^{-2} \text{ s}^{-1}$	>2016
NICA (JINR)	$p^\uparrow + p$	collider $\sqrt{s} = 20$ GeV	$x_b = 0.1 - 0.8$	$1 \times 10^{30} \text{ cm}^{-2} \text{ s}^{-1}$	>2018
PHENIX (RHIC)	$p^\uparrow + p$	collider $\sqrt{s} = 500$ GeV	$x_b = 0.05 - 0.1$	$2 \times 10^{32} \text{ cm}^{-2} \text{ s}^{-1}$	>2018
RHIC internal target phase-1	$p^\uparrow + p$	250 GeV $\sqrt{s} = 22$ GeV	$x_b = 0.25 - 0.4$	$2 \times 10^{33} \text{ cm}^{-2} \text{ s}^{-1}$	>2018
RHIC internal target phase-1	$p^\uparrow + p$	250 GeV $\sqrt{s} = 22$ GeV	$x_b = 0.25 - 0.4$	$6 \times 10^{34} \text{ cm}^{-2} \text{ s}^{-1}$	>2018
FNAL Pol tgt (E1039)	$p + p^\uparrow$	120 GeV $\sqrt{s} = 15$ GeV	$x_t = 0.1 - 0.45$	$3.4 \times 10^{35} \text{ cm}^{-2} \text{ s}^{-1}$	2016
FNAL Pol beam (E1027)	$p^\uparrow + p$	120 GeV $\sqrt{s} = 15$ GeV	$x_b = 0.35 - 0.85$	$2 \times 10^{35} \text{ cm}^{-2} \text{ s}^{-1}$	2018

COMPASS Collaboration

(Common Muon and Proton Apparatus for Structure and Spectroscopy)

- 24 institutions from 13 countries – nearly 250 physicists
- Fixed-target experiment at SPS north area
- Physics programs:
 - Nucleon spin and partonic structures
 - Hadron spectroscopy



ECAL2

ECAL1

ECAL0

CAMERA recoil proton detector
surrounding the 2.5m long
LH2 target



18-10-2012

COMPASS Setup (Drell-Yan Runs)

Beam:

Polarized lepton beam : μ^+ , μ^- 50-280 GeV/c

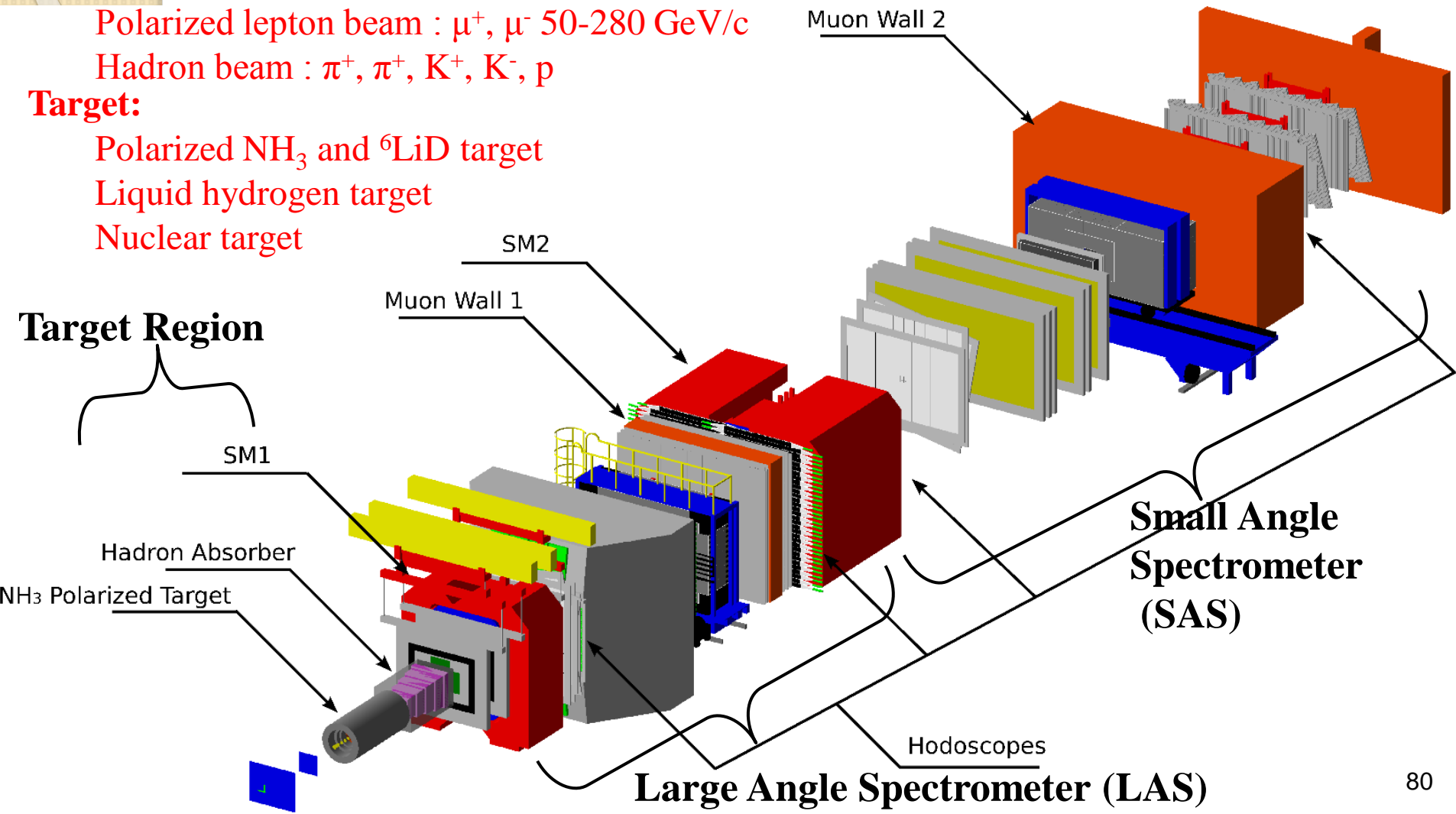
Hadron beam : π^+ , π^+ , K^+ , K^- , p

Target:

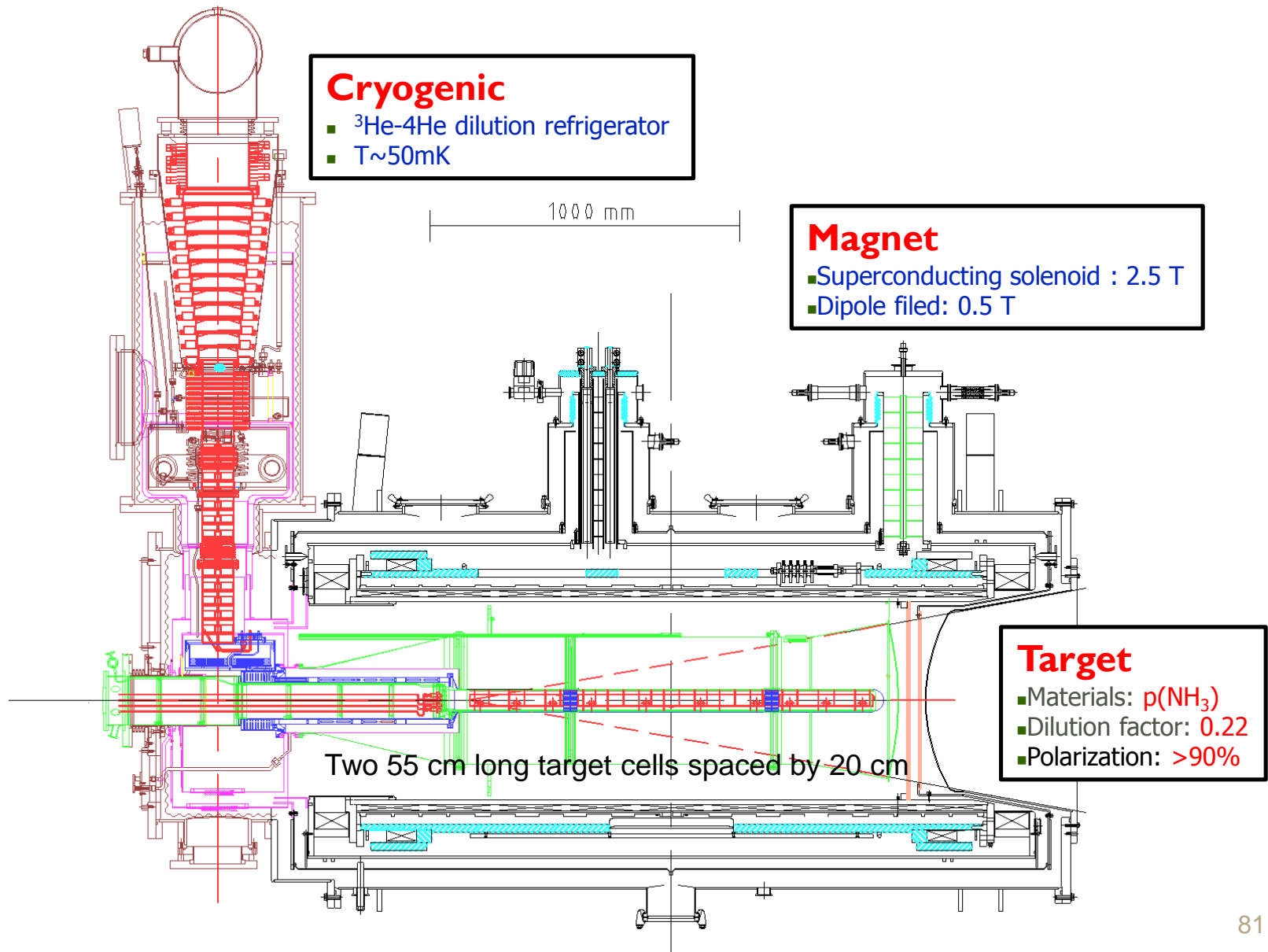
Polarized NH_3 and ${}^6\text{LiD}$ target

Liquid hydrogen target

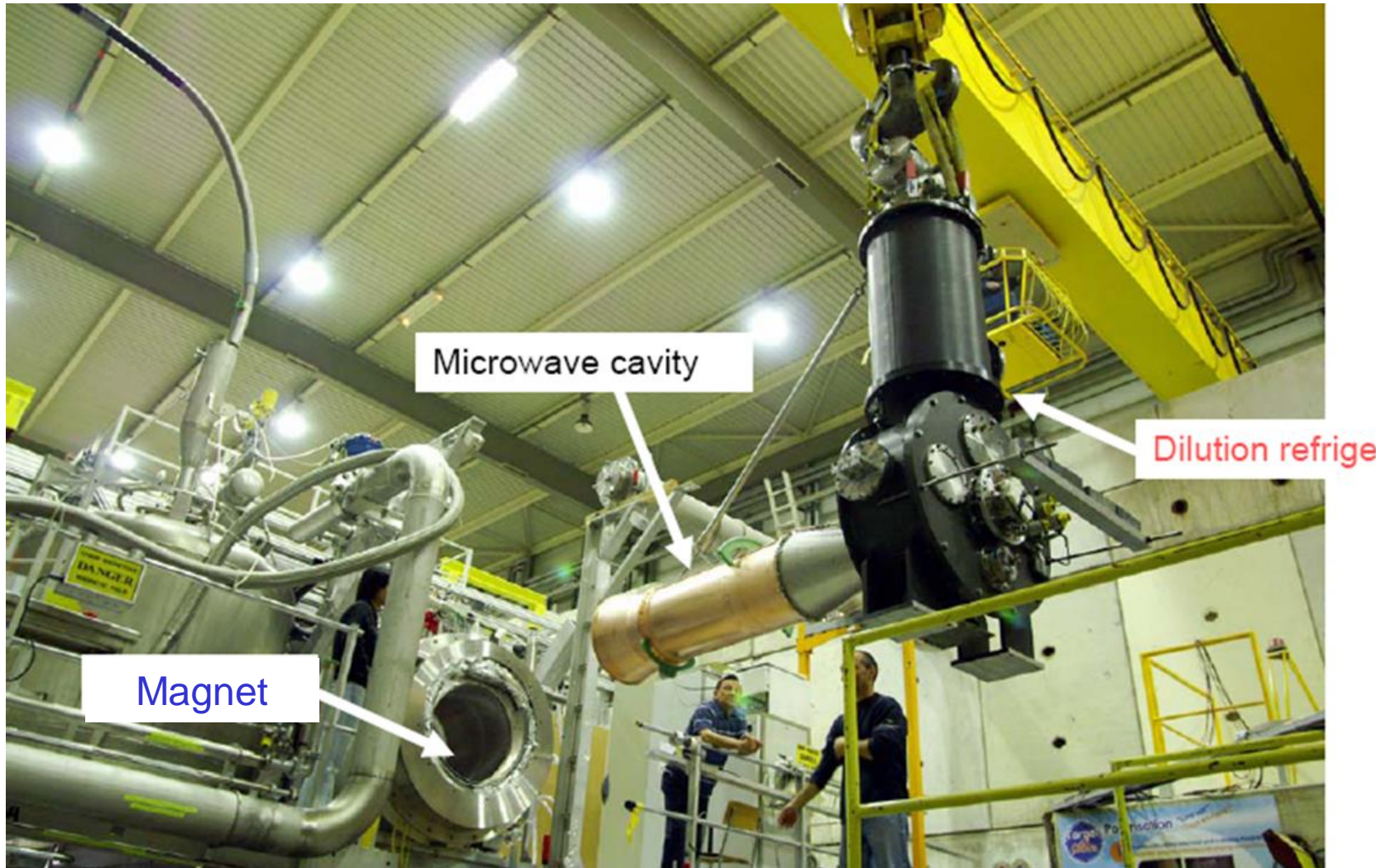
Nuclear target



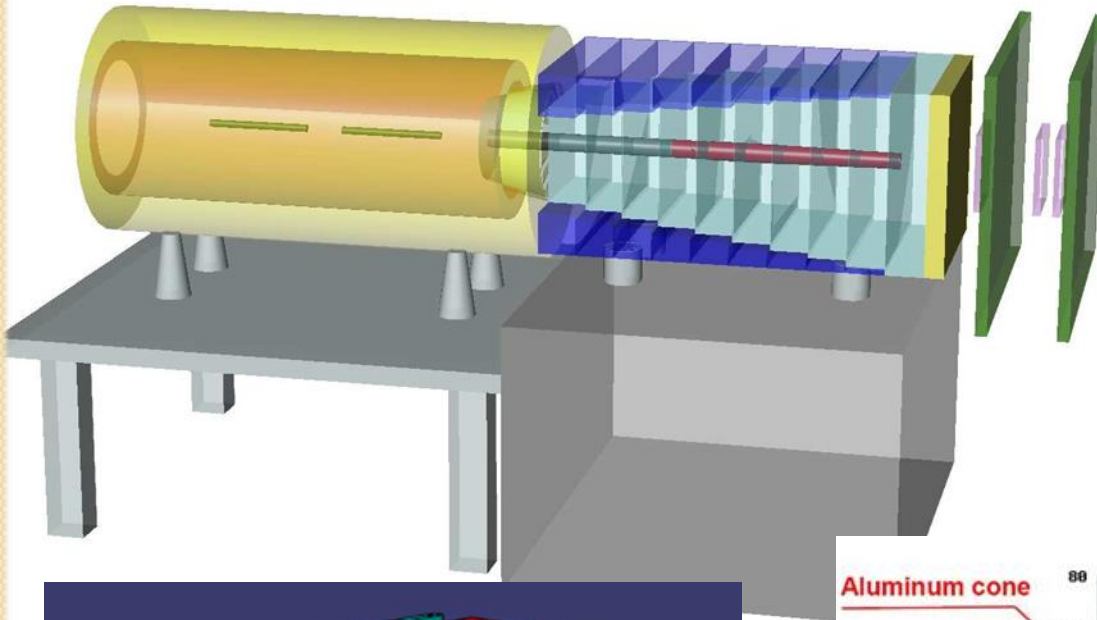
Polarized NH_3 Target



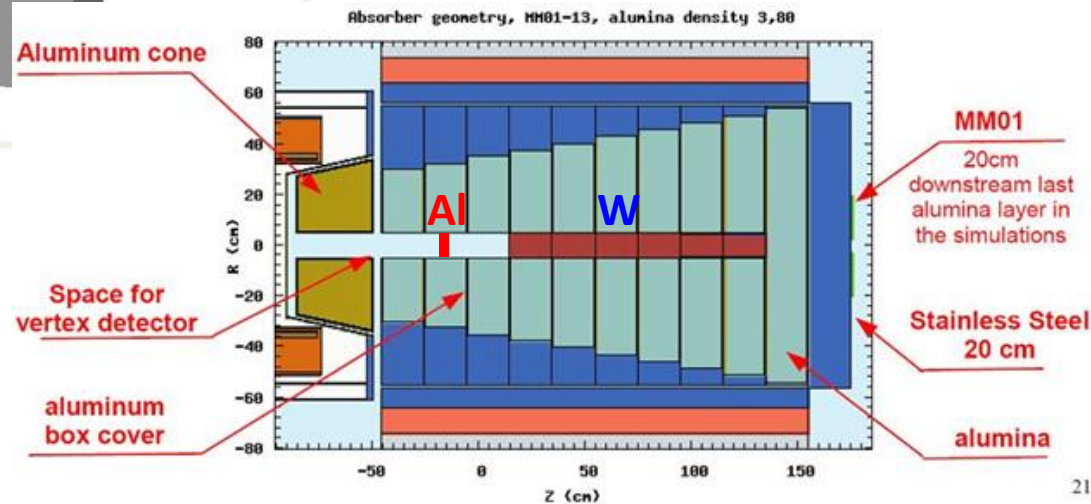
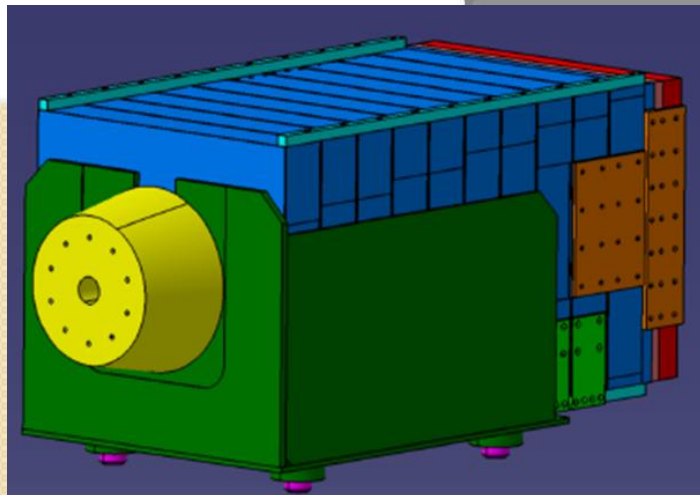
Polarized NH_3 Target



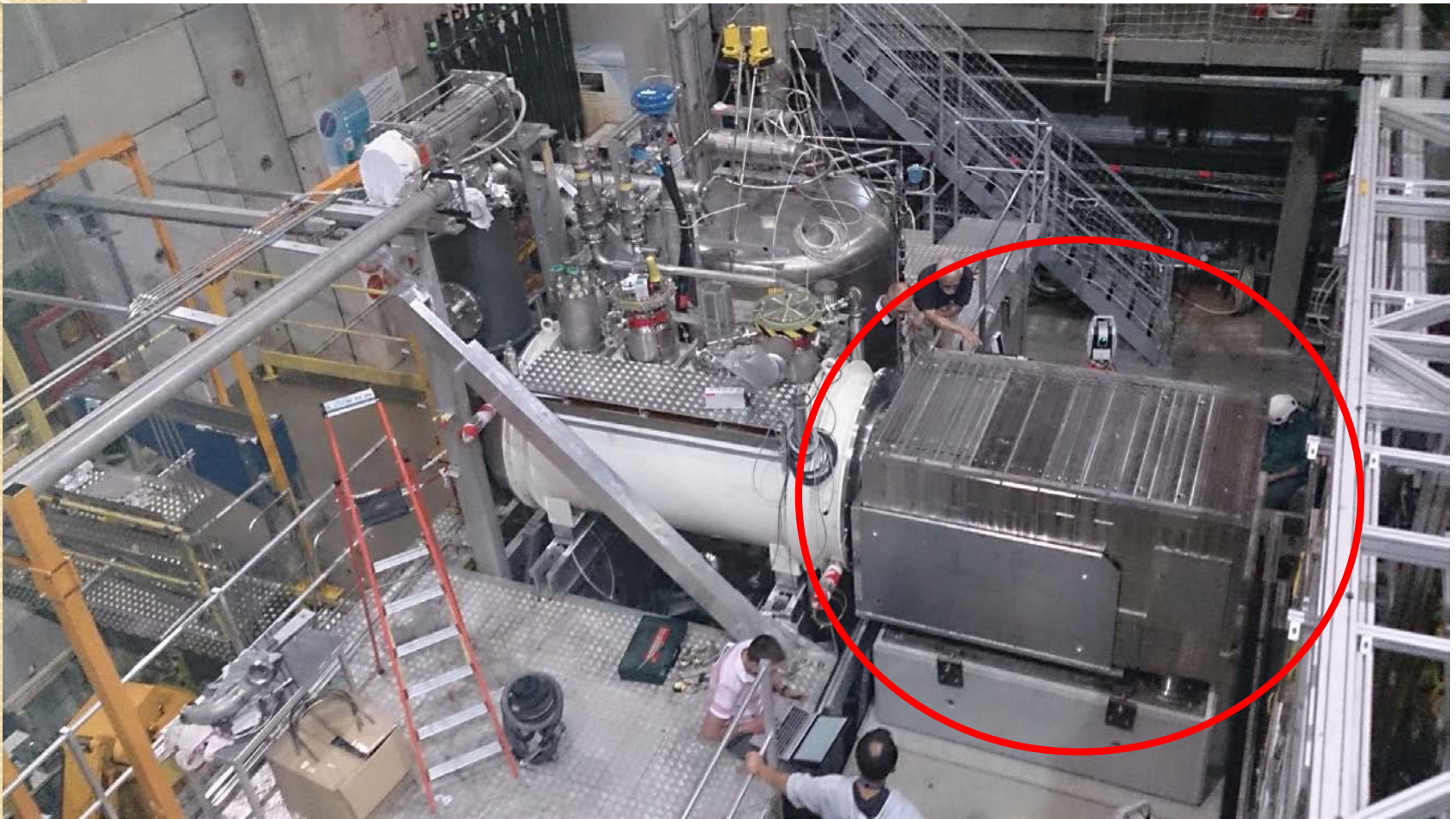
Hadron Absorber & Nuclear Targets



- Absorber: 236 cm long, made of Al_2O_3 .
- Beam plug: 120 cm long, made of tungsten.
- Radiation lengths (multiple scattering for μ): $x/X_0 = 33.53$
- Hadronic interaction lengths (stopping power for π): $x/\lambda_{\text{int}} = 7.25$
- 7cm Al target



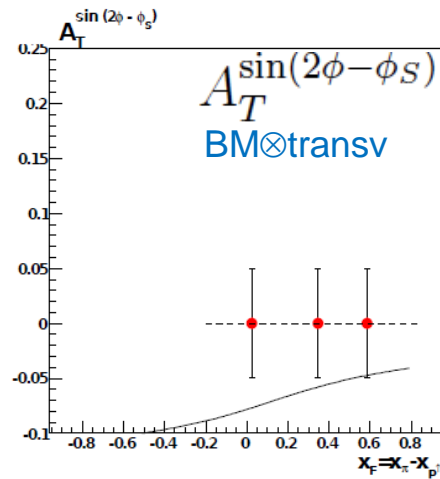
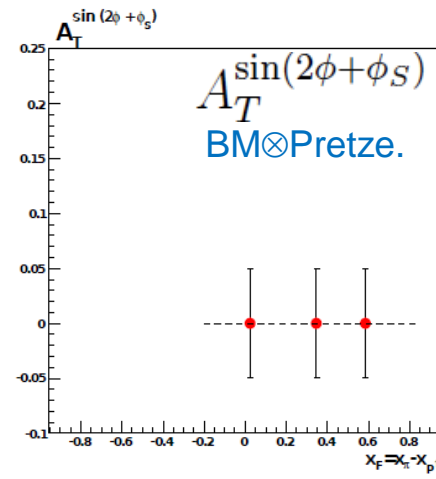
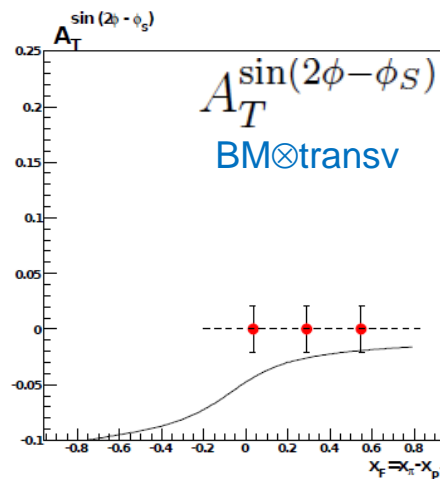
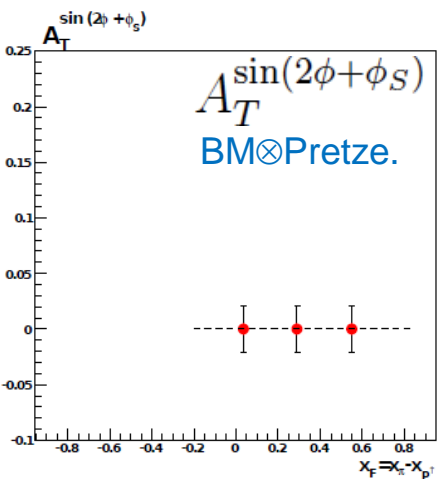
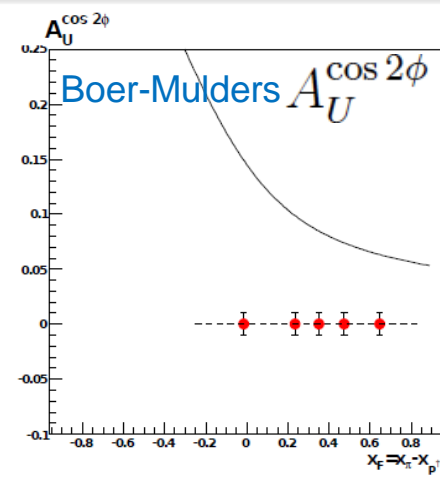
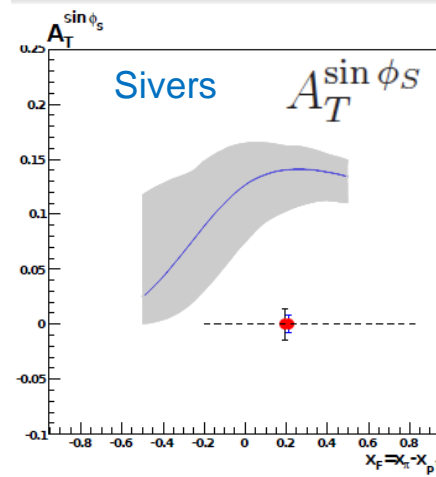
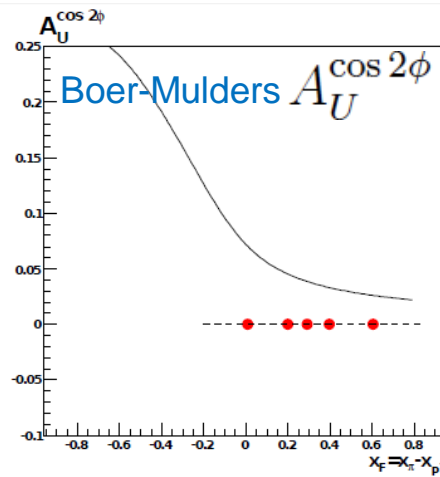
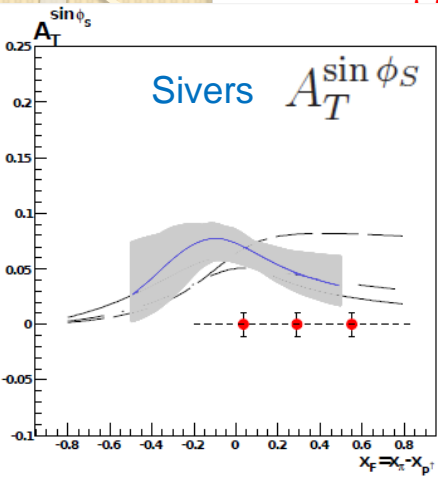
Hadron Absorber & Nuclear Targets



Theoretical Predictions vs. Expected Precision

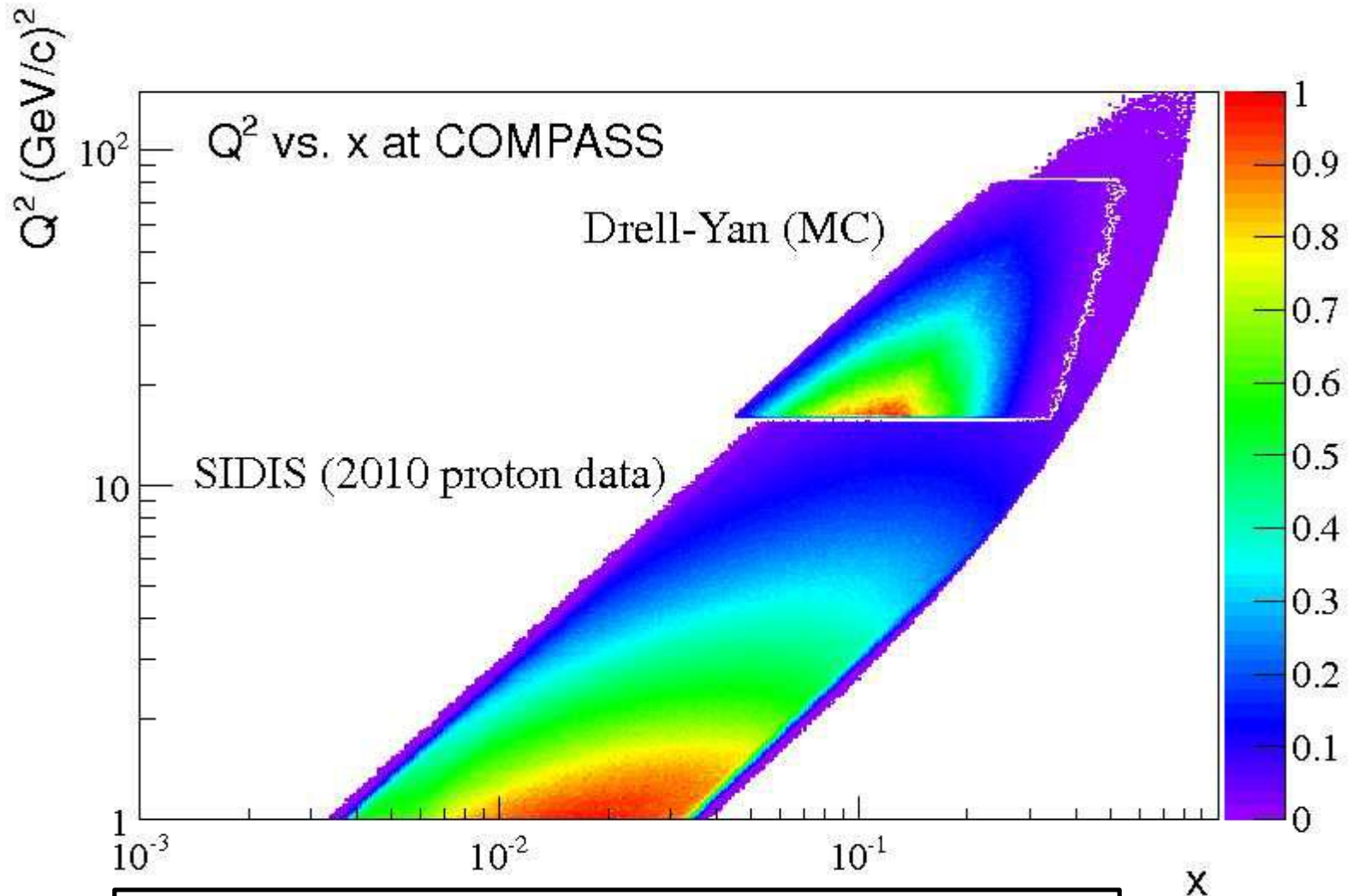
$$2 \leq M_{\mu\mu} \leq 2.5 \text{ GeV}/c^2$$

$$4 \leq M_{uu} \leq 9 \text{ GeV}/c^2$$



M. Anselmino et. Al, Eur.Phys.J.A39:89-100,2009.
 V. Barone et al., Phys. Rept. 359 (2002) I.
 B. Zhang et al., Phys. Rev. D77 (2008) 054011,

Overlapping Kinematic Region



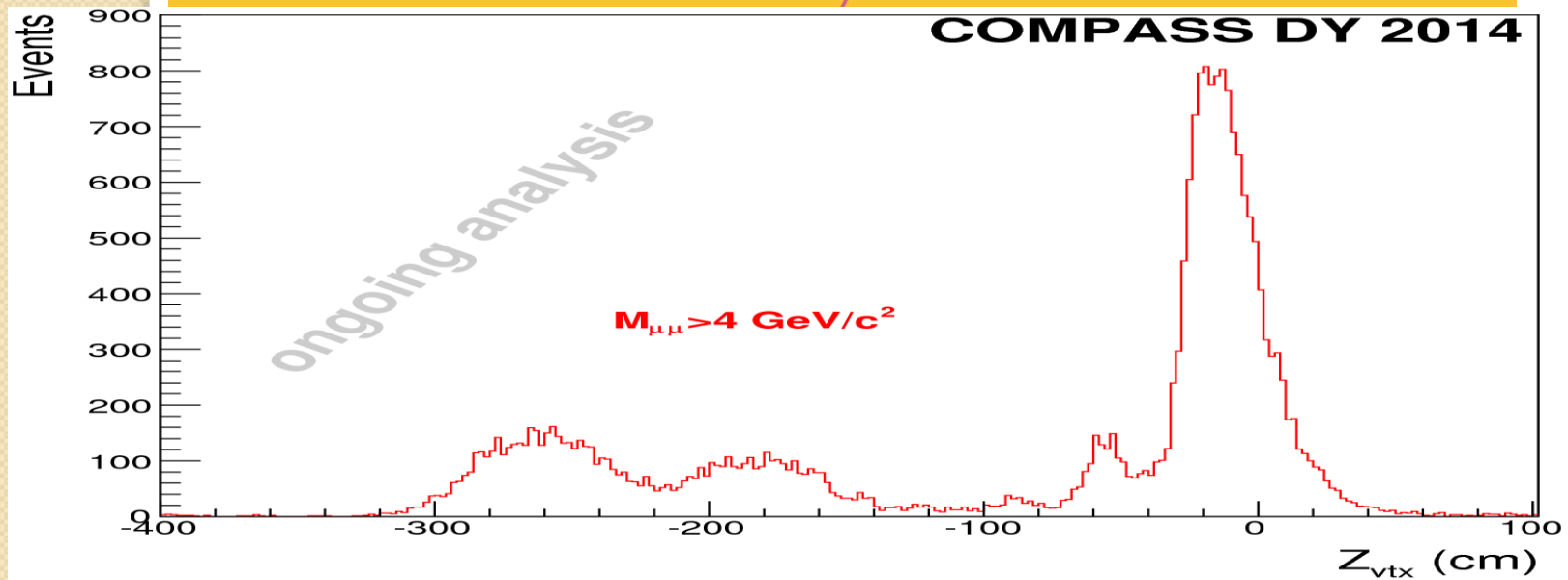
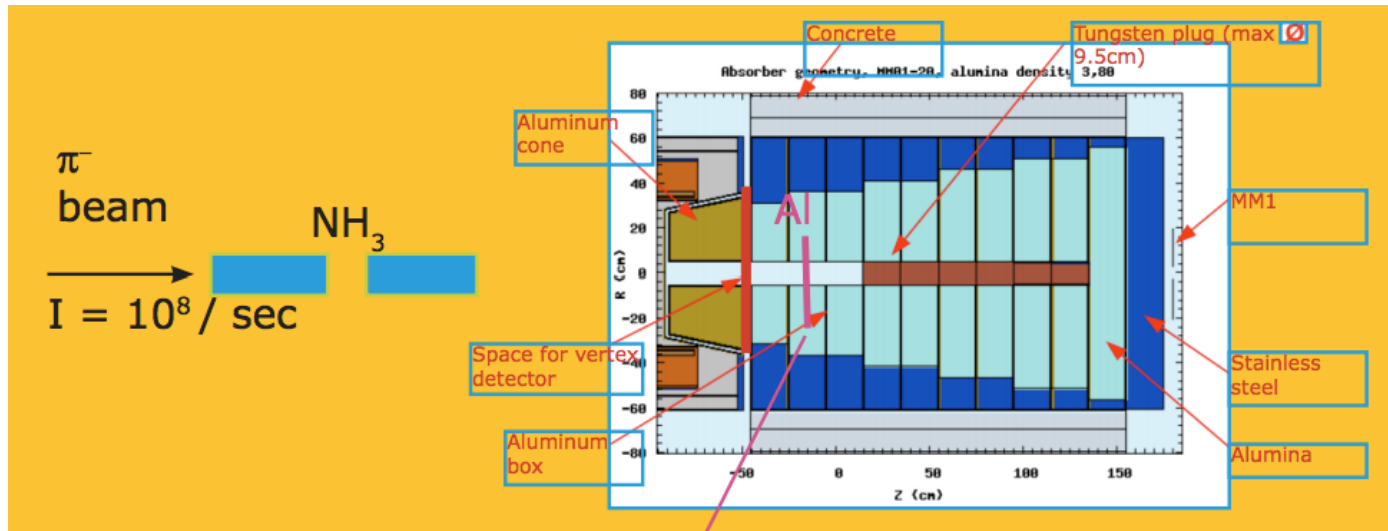
SIDIS and DY have overlapping acceptance at COMPASS

→ Consistent extraction of TMD PDFs in the same region.

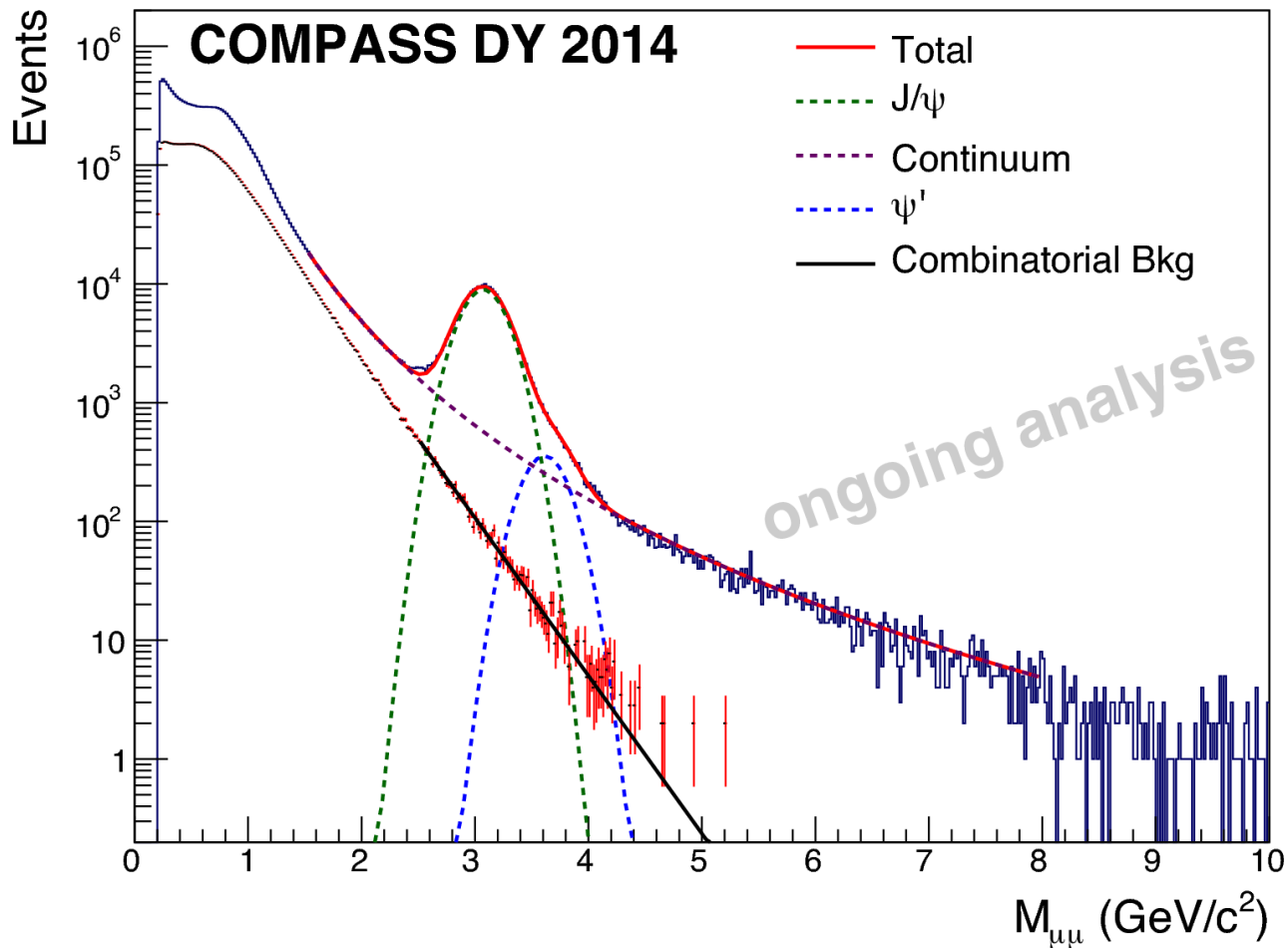
COMPASS DY Run Schedule

- **Oct – Dec 2014**: commission runs (completed).
- **May – Nov 2015**: polarized Drell-Yan measurement. Physics data-taking started from June.

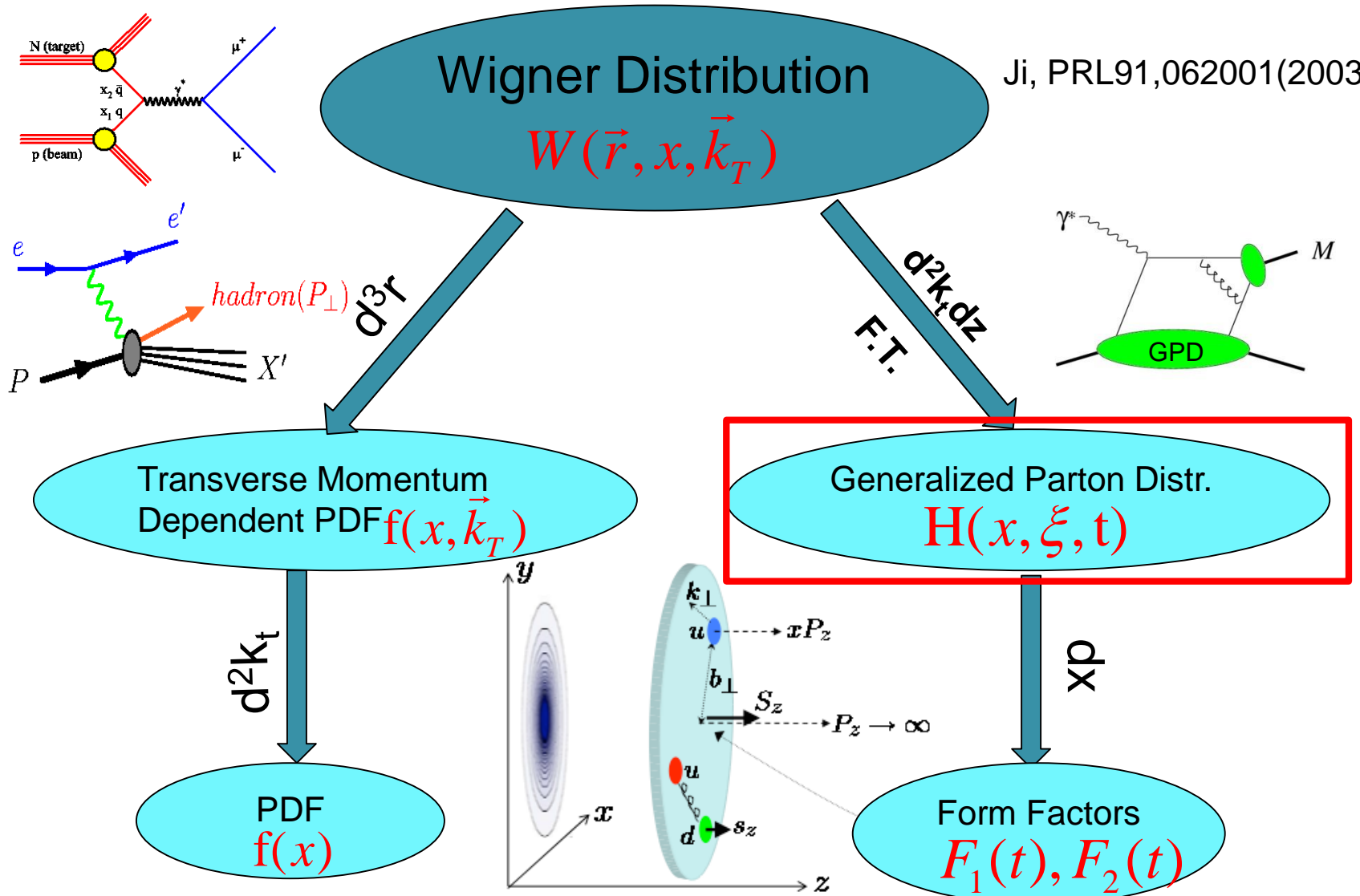
Dimuon Vertex Distributions (2014 DY)



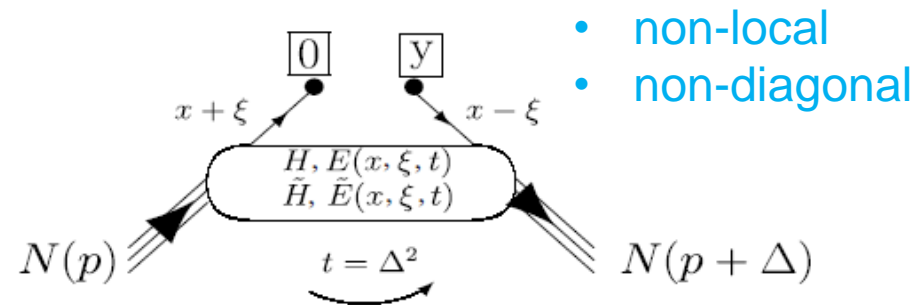
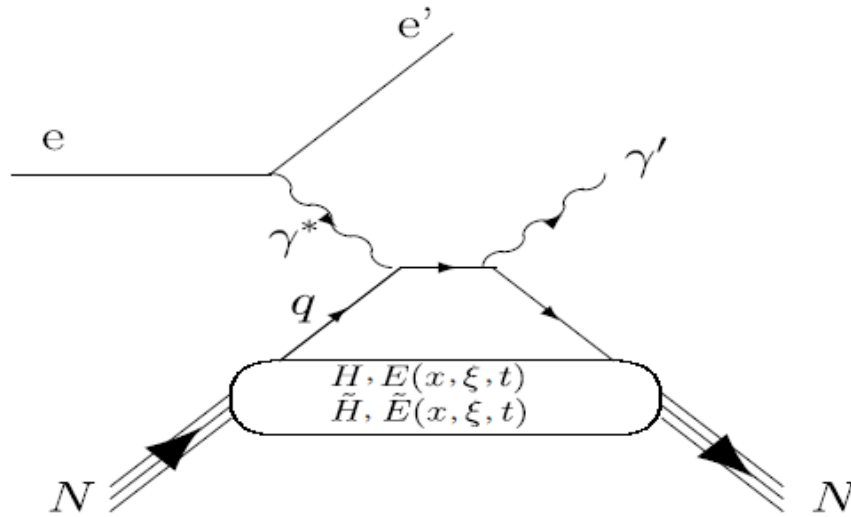
Dimuon Invariant-mass Distributions (2014 DY)



Nucleon Partonic Structure



Generalized Parton Distribution (GPD)



- non-local
- non-diagonal

Deeply virtual Compton scattering (DVCS)

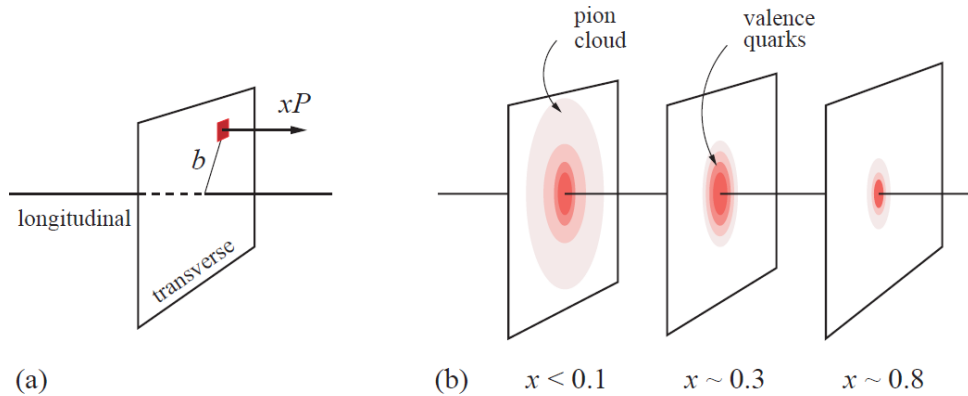
$$\frac{P^+}{2\pi} \int dy^- e^{ixP^+y^-} \langle p' | \bar{\psi}_q(0) \gamma^+ \psi_q(y) | p \rangle \Big|_{y^+ = \bar{y}_\perp = 0} \quad \frac{P^+}{2\pi} \int dy^- e^{ixP^+y^-} \langle p' | \bar{\psi}_q(0) \gamma^+ \gamma^5 \psi_q(y) | p \rangle \Big|_{y^+ = \bar{y}_\perp = 0}$$

$$= H^q(x, \xi, t) \bar{N}(p') \gamma^+ N(p) \quad = \tilde{H}^q(x, \xi, t) \bar{N}(p') \gamma^+ \gamma^5 N(p)$$

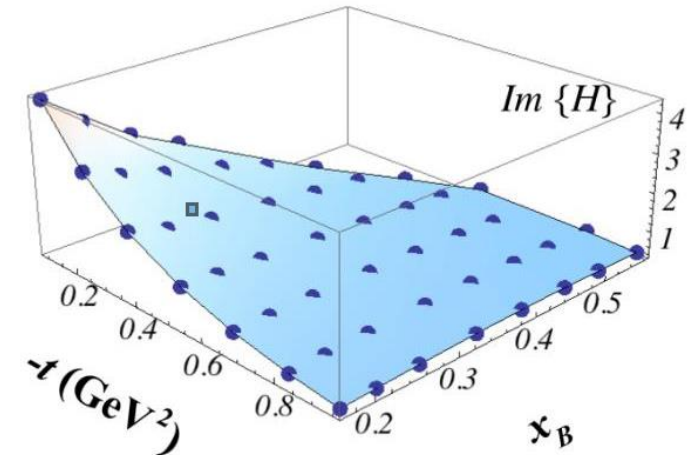
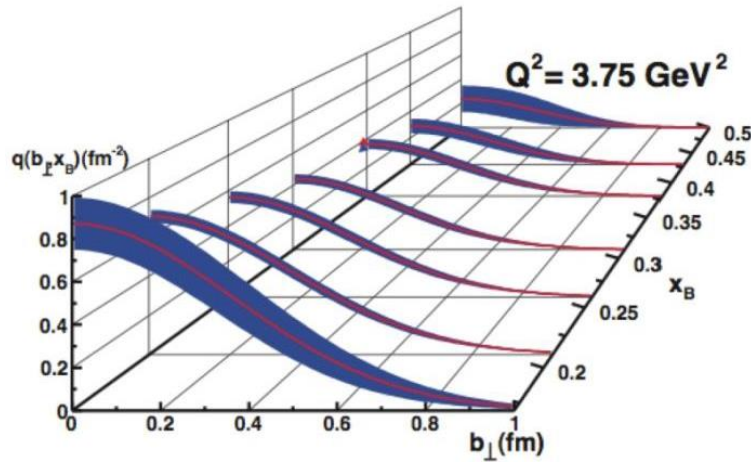
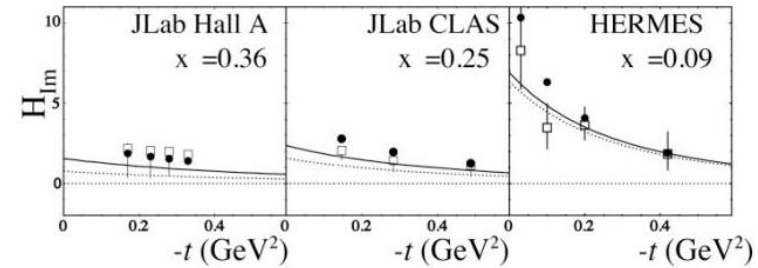
$$+ E^q(x, \xi, t) \bar{N}(p') i\sigma^{+\nu} \frac{\Delta_\nu}{2m_N} N(p), \quad + \tilde{E}^q(x, \xi, t) \bar{N}(p') \gamma^5 \frac{\Delta^+}{2m_N} N(p),$$

$$H^q, E^q, \tilde{H}^q, \tilde{E}^q(x, \xi, t)$$

Generalized Parton Distribution

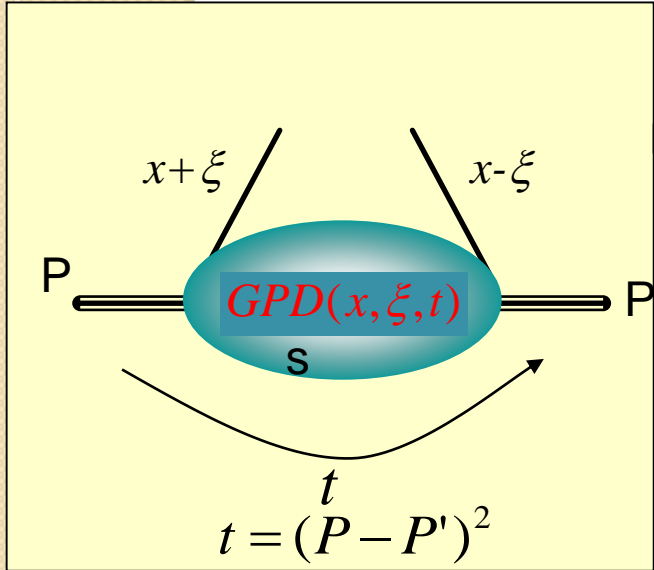


JLAB12 CDR, arXiv:1208.1244



- 1+2D description of the nucleon structure
- Correlations among longitudinal momenta and transverse positions
- Connection to quark orbital angular momentum

Generalized Parton Distribution (GPD)



$t = \xi = 0$

$$H_f(x, 0, 0) = q_f(x) = -\bar{q}_f(-x)$$

$$\tilde{H}_f(x, 0, 0) = \Delta q_f(x) = -\Delta \bar{q}_f(-x)$$

The first moments

$$\int_{-1}^1 dx \sum_f H_f(x, \xi, t) = F_1(-t)$$

$$\int_{-1}^1 dx \sum_f E_f(x, \xi, t) = F_2(-t)$$

$$\int_{-1}^1 dx \sum_f \tilde{H}_f(x, \xi, t) = G_A(-t)$$

$$\int_{-1}^1 dx \sum_f \tilde{E}_f(x, \xi, t) = G_p(-t)$$

The second moments

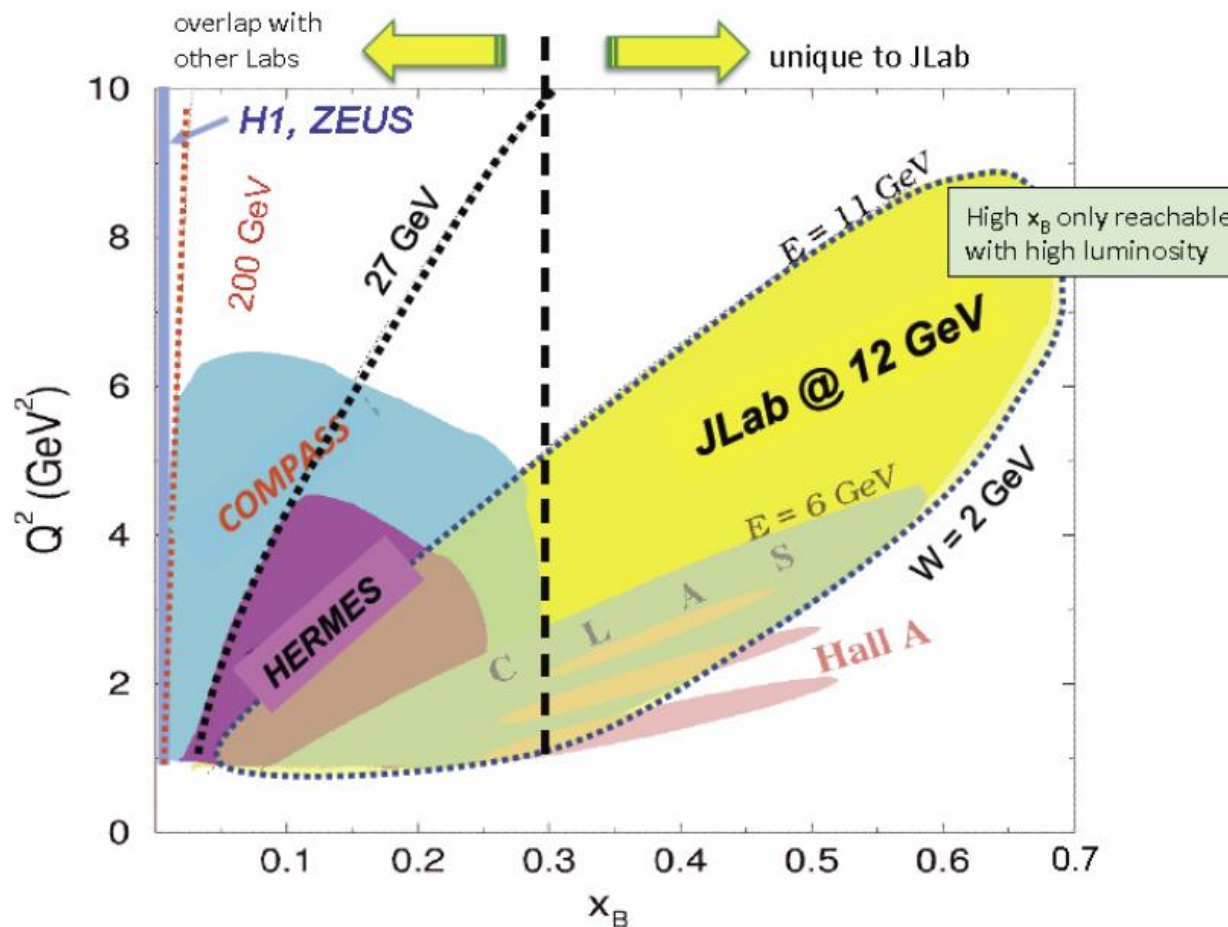
	γ^μ	$\gamma^\mu \gamma^5$
no spin flip	$H_f(x, \xi, t)$	$\tilde{H}_f(x, \xi, t)$
spin flip	$E_f(x, \xi, t)$	$\tilde{E}_f(x, \xi, t)$

Ji's sum rule

$$J_f = \frac{1}{2} \Delta \Sigma^f + L^f = \frac{1}{2} \int_{-1}^1 x dx [H_f(x, \xi, 0) + E_f(x, \xi, 0)]$$

The orbital angular momentum of quarks can be

Worldwide Activities for Measuring GPD



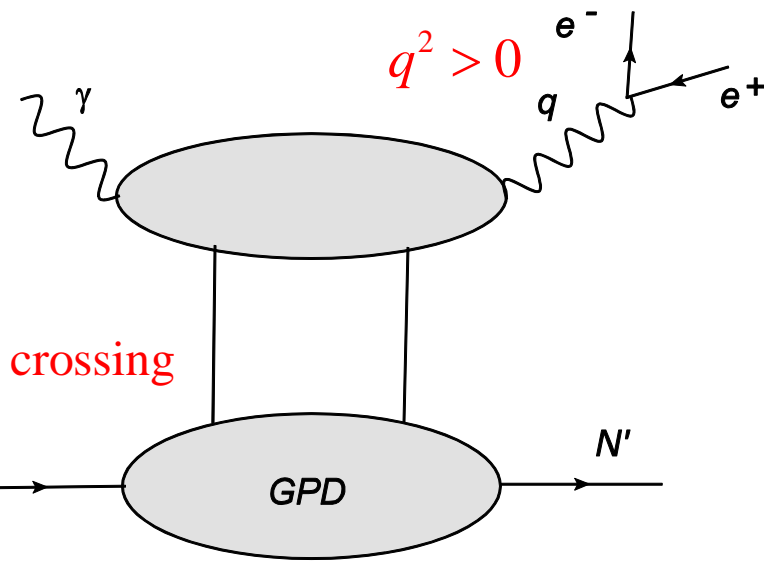
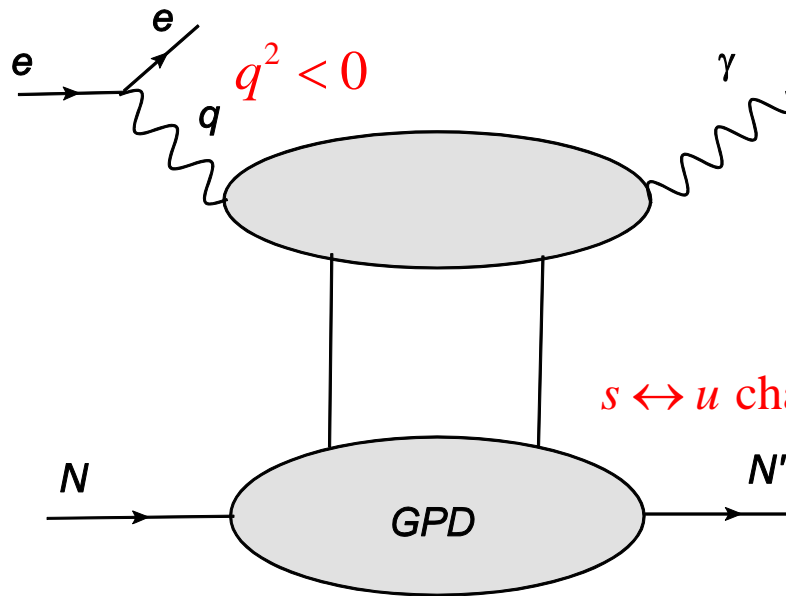
arXiv:1208.1244

Spacelike vs. Timelike Processes

Muller et al., PRD 86 (2012) 031502

Deeply Virtual Compton Scattering

Timelike Compton Scattering



$s \leftrightarrow u$ channel crossing

(a)

(b)

$$\mathcal{F}(\xi = \eta, t, Q^2) \stackrel{\text{SL} \rightarrow \text{TL}}{\Rightarrow} \mathcal{F}(\xi = -\eta, t, -Q^2),$$

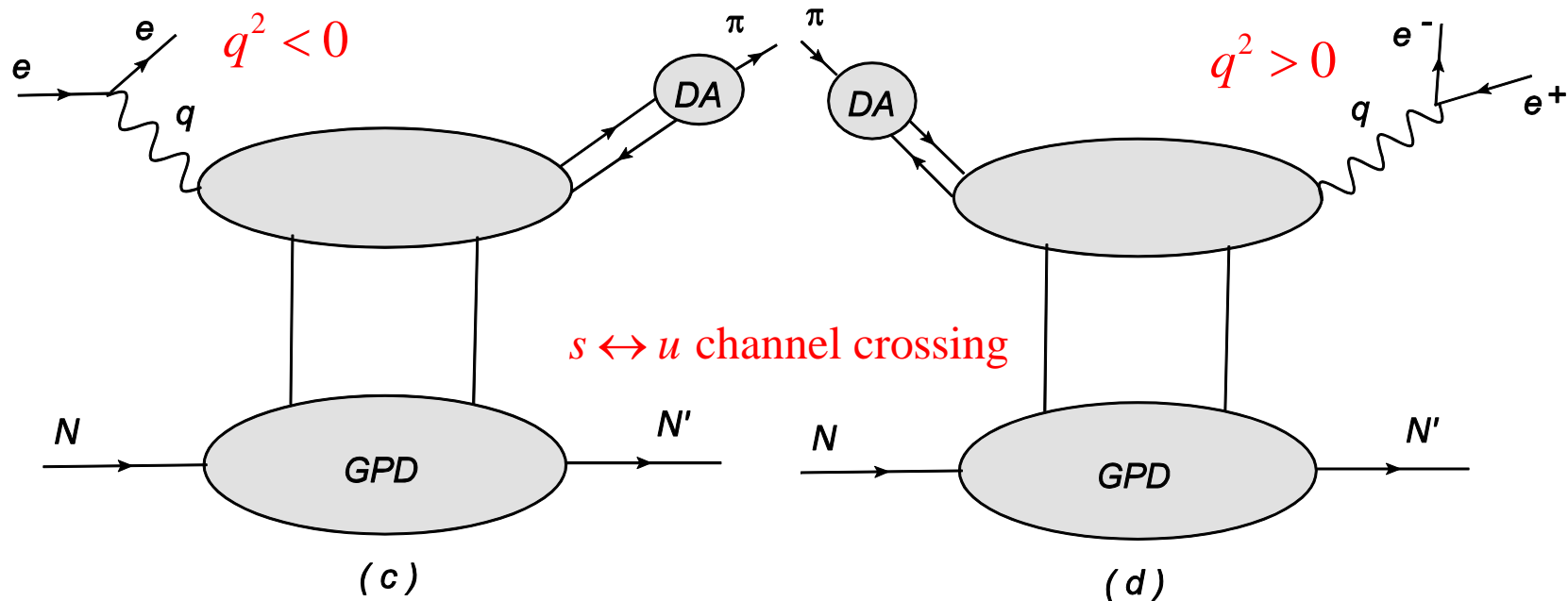
$$\mathcal{F}(\xi, t, Q^2) = \int_{-1}^1 dx \sum_{i=u,d,\dots,g} {}^S T^i(x, \xi) F^i(x, \xi, t, \mu^2),$$

Spacelike vs. Timelike Processes

Muller et al., PRD 86 (2012) 031502

Deeply Virtual Meson Production

Exclusive Meson-induced DY



**J-PARC Facility
(KEK/JAEA)**

South to North

**Experimental
Areas**

Linac

3 GeV
Synchrotron

Neutrino Beams
(to Kamioka) ←

**Materials and Life
Experimental Facility**

50 GeV Synchrotron

**Hadron Exp.
Facility**

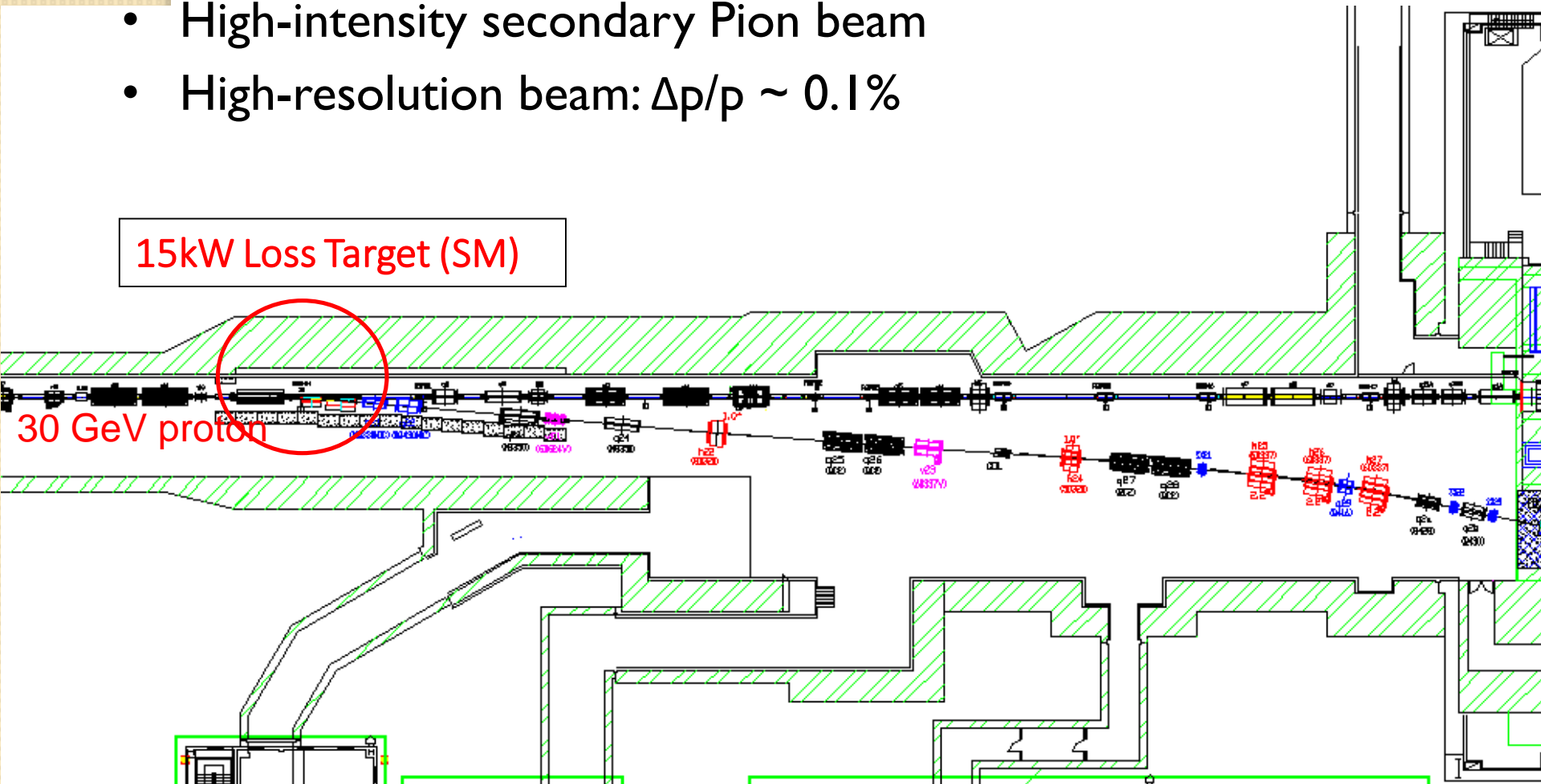
- JFY2007 Beams
- JFY2008 Beams
- JFY2009 Beams

Bird's eye photo in January of 2008

J-PARC High-momentum Beam Line (Hi-P BL)

- High-intensity secondary Pion beam
- High-resolution beam: $\Delta p/p \sim 0.1\%$

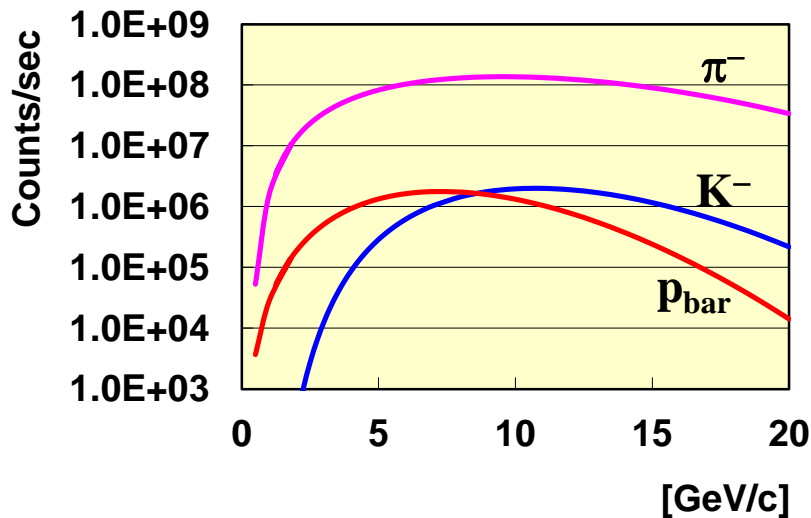
15kW Loss Target (SM)



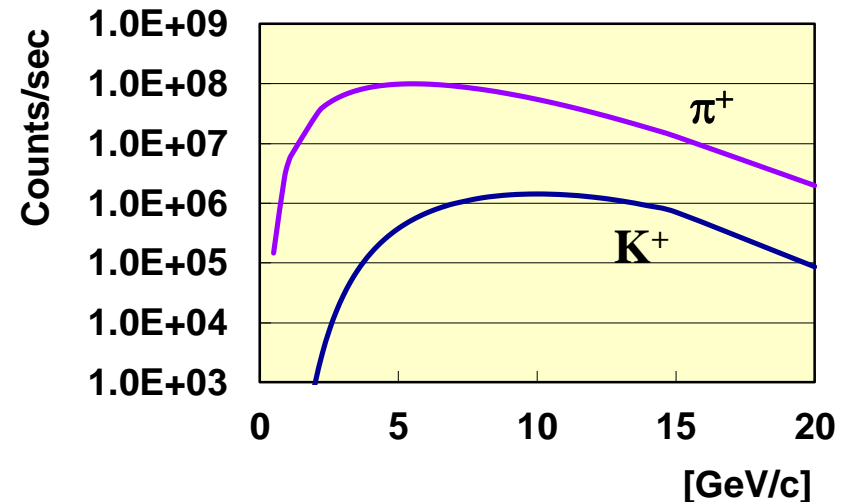
J-PARC High-momentum Beam Line (Hi-P BL)

- High-intensity secondary Pion beam
- High-resolution beam: $\Delta p/p \sim 0.1\%$

Negative Hadron Beams
(Prod. Angle = 0 deg.)



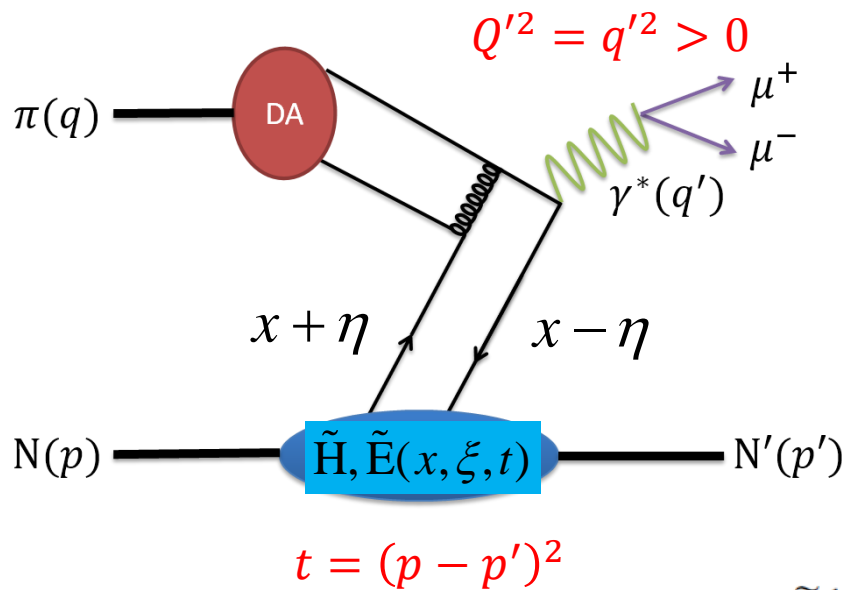
Positive Hadron Beams
(Prod. Angle = 3.1 deg.)



* Sanford-Wang: 15 kW Loss on Pt, Acceptance :1.5 msr%, 133.2 m

$\pi N \rightarrow \mu^+ \mu^- N$

E.R. Berger, M. Diehl, B. Pire, PLB 523 (2001) 265



$$\tau = \frac{Q'^2}{2pq} \approx \frac{Q'^2}{s - M_N^2} \quad \eta = \frac{(p - p')^+}{(p + p')^+}$$

$$\frac{d\sigma}{dQ'^2 dt d(\cos\theta) d\varphi} = \frac{\alpha_{em}}{256\pi^3} \frac{\tau^2}{Q'^6} \sum_{\lambda', \lambda} |M^{0\lambda', \lambda}|^2 \sin^2\theta,$$

$$M^{0\lambda', \lambda}(\pi^- p \rightarrow \gamma^* n) = -ie \frac{4\pi f_\pi}{3} \frac{1}{Q' (p + p')^+} \bar{u}(p', \lambda') \times \left[\gamma^+ \gamma_5 \tilde{\mathcal{H}}^{du}(-\eta, \eta, t) + \gamma_5 \frac{(p' - p)^+}{2M} \tilde{\mathcal{E}}^{du}(-\eta, \eta, t) \right] u(p, \lambda)$$

$$\tilde{\mathcal{H}}^{du}(\xi, \eta, t) = \frac{8}{3} \alpha_S \int_{-1}^1 dz \frac{\phi_\pi(z)}{1 - z^2} \times \int_{-1}^1 dx \left[\frac{e_d}{\xi - x - i\epsilon} - \frac{e_u}{\xi + x - i\epsilon} \right] \times [\tilde{H}^d(x, \eta, t) - \tilde{H}^u(x, \eta, t)],$$

Differential Cross Sections (Q^2, t, τ)

E.R. Berger, M. Diehl, B. Pire, PLB 523 (2001) 265

$$\begin{aligned} & \frac{d\sigma}{dQ'^2 dt} (\pi^- p \rightarrow \gamma^* n) \\ &= \frac{4\pi\alpha_{\text{em}}^2}{27} \frac{\tau^2}{Q'^8} f_\pi^2 \times \left[(1 - \eta^2) |\tilde{\mathcal{H}}^{du}|^2 - 2\eta^2 \text{Re}(\tilde{\mathcal{H}}^{du*} \tilde{\mathcal{E}}^{du}) \right. \\ & \quad \left. - \eta^2 \frac{t}{4M^2} |\tilde{\mathcal{E}}^{du}|^2 \right], \end{aligned}$$

$$t = (p - p')^2 \quad \tau = \frac{Q'^2}{2pq} \approx \frac{Q'^2}{s - M_N^2} = x_B$$

$$Q'^2 = q'^2 > 0 \quad \eta = \frac{(p - p')^+}{(p + p')^+} = \frac{\tau}{2 - \tau}$$

GPD $\tilde{H}(x, \eta, t)$ Double Integration

E.R. Berger, M. Diehl, B. Pire, EPJC 23, 675 (2002)

$$\begin{aligned} \tilde{H}^u(x, \eta, t) - \tilde{H}^d(x, \eta, t) \\ = [\tilde{h}^u(x, \eta) - \tilde{h}^d(x, \eta)] g_A(t) / g_A(0). \end{aligned} \quad (6)$$

We take the parameterization $g_A(t)/g_A(0) = (1 - t/M_A^2)^{-2}$ with $M_A = 1.06$ GeV from [17]. The functions

$$\begin{aligned} \tilde{h}^q(x, \eta) = \int_0^1 dx' \int_{-1+x'}^{1-x'} dy' \\ \times \delta(x - x' - \eta y') \Delta q_V(x') \pi(x', y'), \end{aligned} \quad (38)$$

$$\pi(x', y') = \frac{3}{4} \frac{(1-x')^2 - y'^2}{(1-x')^3}. \quad (39)$$

$\tilde{H}(x, \eta = 0, t = 0)$ = polarized valance distribution

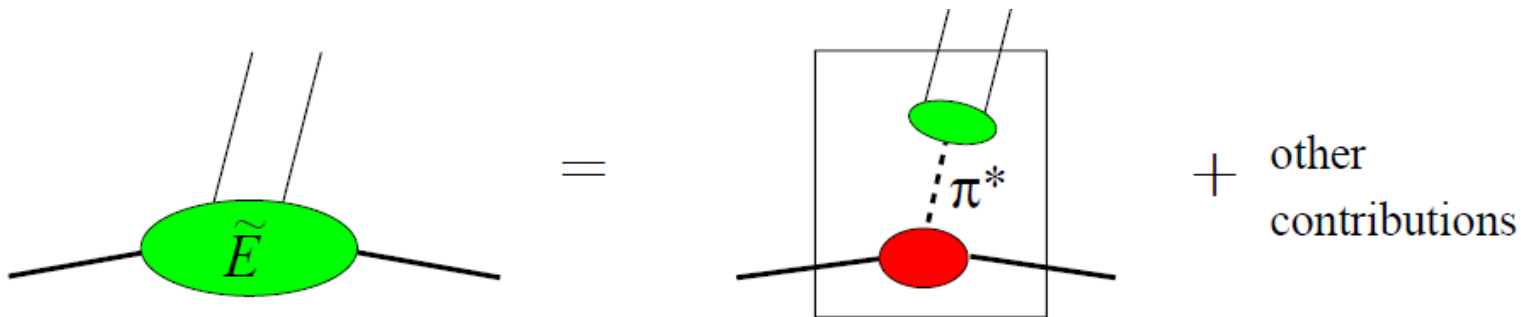
GPD $\tilde{E}(x, \eta, t)$ Pion-pole Dominance

E.R. Berger, M. Diehl, B. Pire, EPJC 23, 675 (2002)

$$\begin{aligned} & \tilde{E}^u(x, \eta, t) - \tilde{E}^d(x, \eta, t) \\ &= \Theta(\eta - |x|) \frac{1}{\eta} \phi_\pi\left(\frac{x}{\eta}\right) F(t) \end{aligned}$$

$$F(t) = \frac{4.4 \text{ GeV}^2}{m_\pi^2 - t} \left[1 - \frac{B(m_\pi^2 - t)}{(1 - Ct)^2} \right] \quad (8)$$

with $B = 1.7 \text{ GeV}^{-2}$ and $C = 0.5 \text{ GeV}^{-2}$. Note



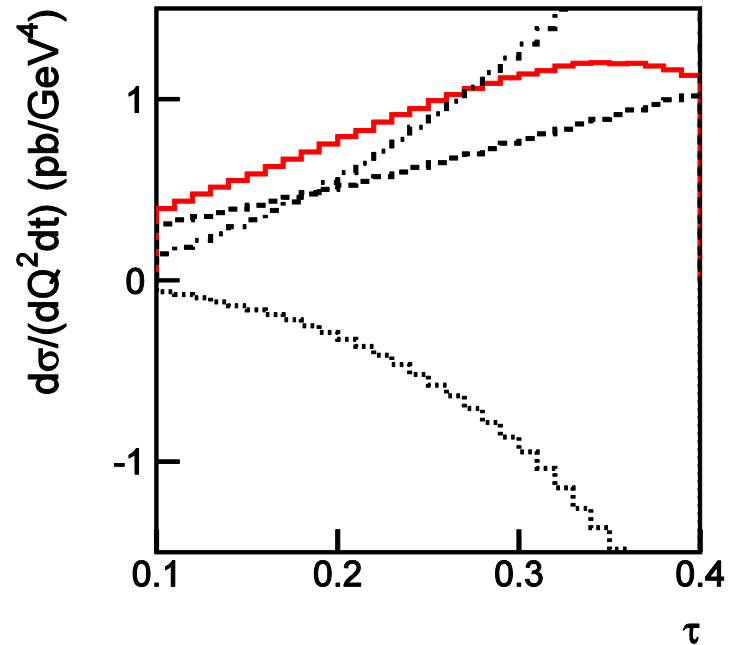
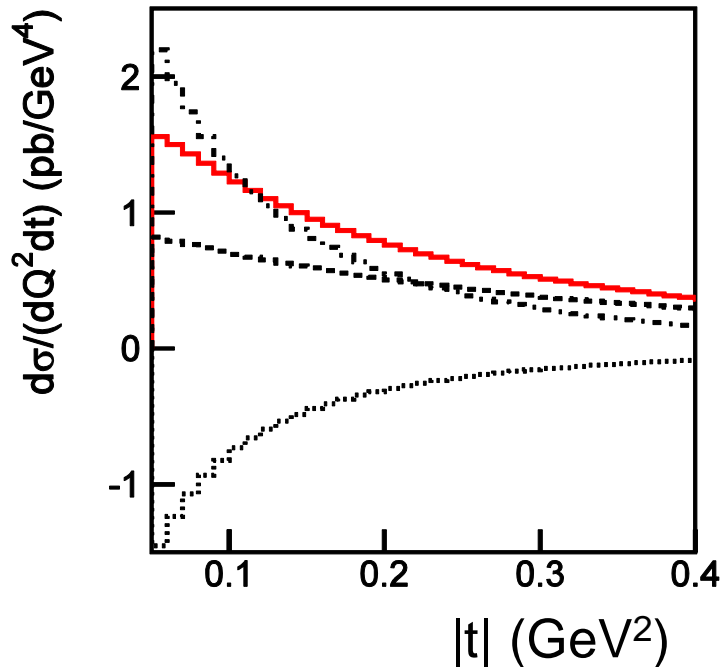
$$\tilde{E}^{u-d}(x, \xi, t) \xrightarrow{t \rightarrow m_\pi^2} \theta(|x| < |\xi|) \frac{1}{2|\xi|} \phi_\pi\left(\frac{x + \xi}{2\xi}\right) \frac{4m^2 g_A(0)}{m_\pi^2 - t}$$

$\pi N \rightarrow \mu^+ \mu^- N$

E.R. Berger, M. Diehl, B. Pire, PLB 523 (2001) 265

Cross sections increase toward small s !

$$Q'^2 = q'^2 = 5 \text{ GeV}^2$$

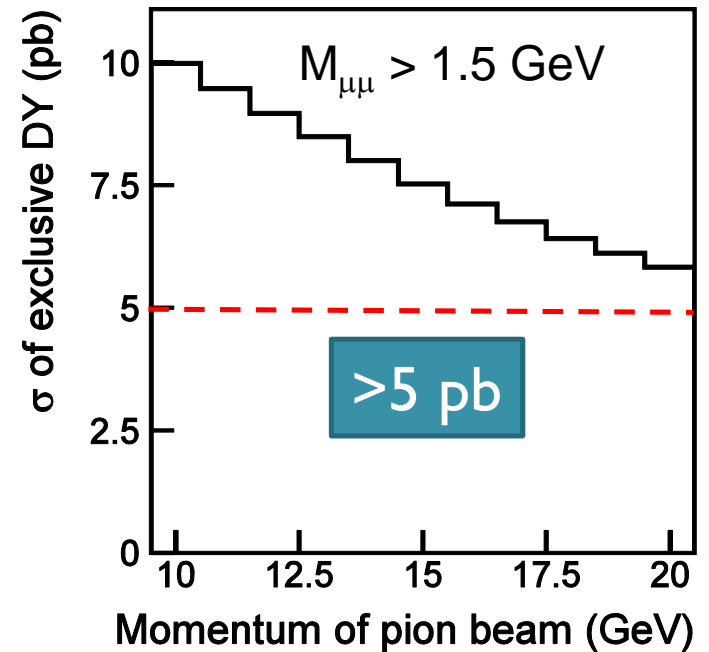
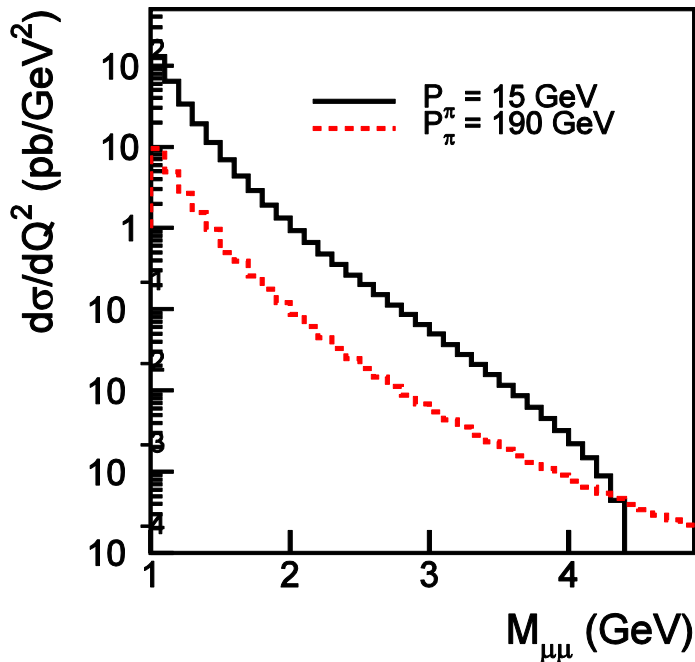


$$t = (p - p')^2 = -0.2 \text{ GeV}^2$$

$$\tau = \frac{Q'^2}{2pq} \approx \frac{Q'^2}{s - M_N^2} = 0.2$$

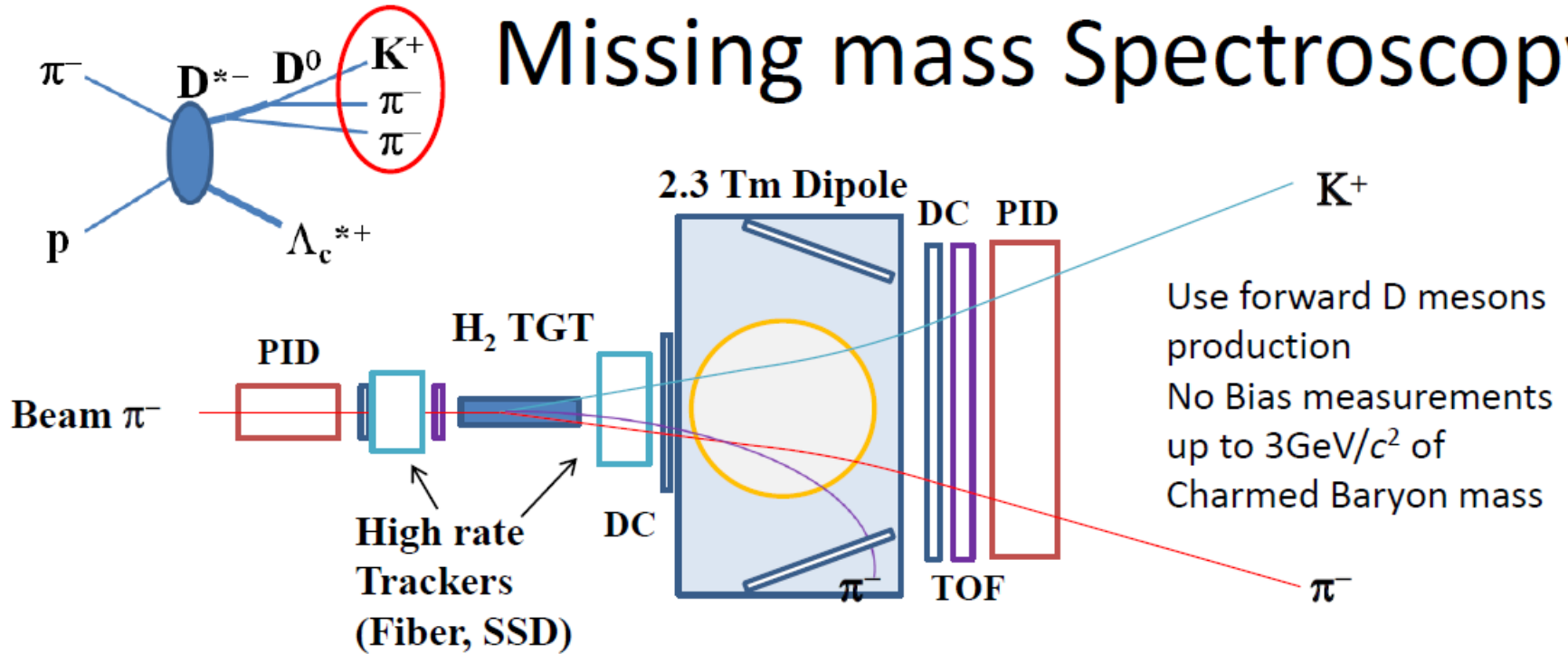
$\pi N \rightarrow \mu + \mu - N$:

CERN (190 GeV) vs. J-PARC (15 GeV)



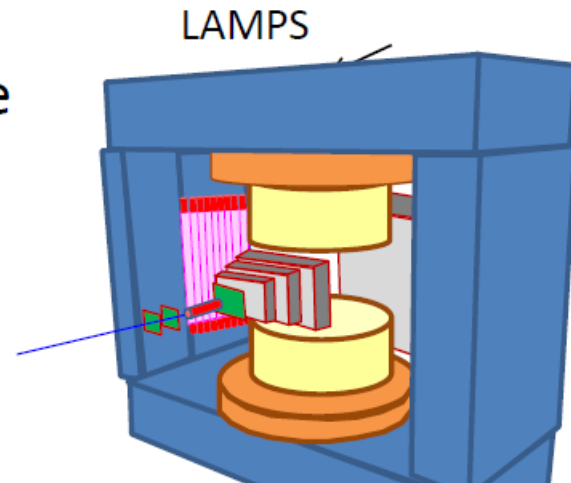
CERN, $P_{\pi} = 190$ GeV, $\sigma = 0.65$ pb

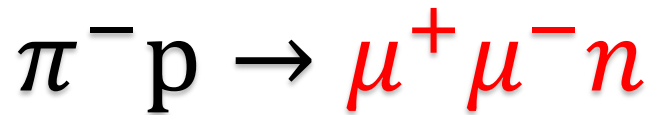
Missing mass Spectroscopy



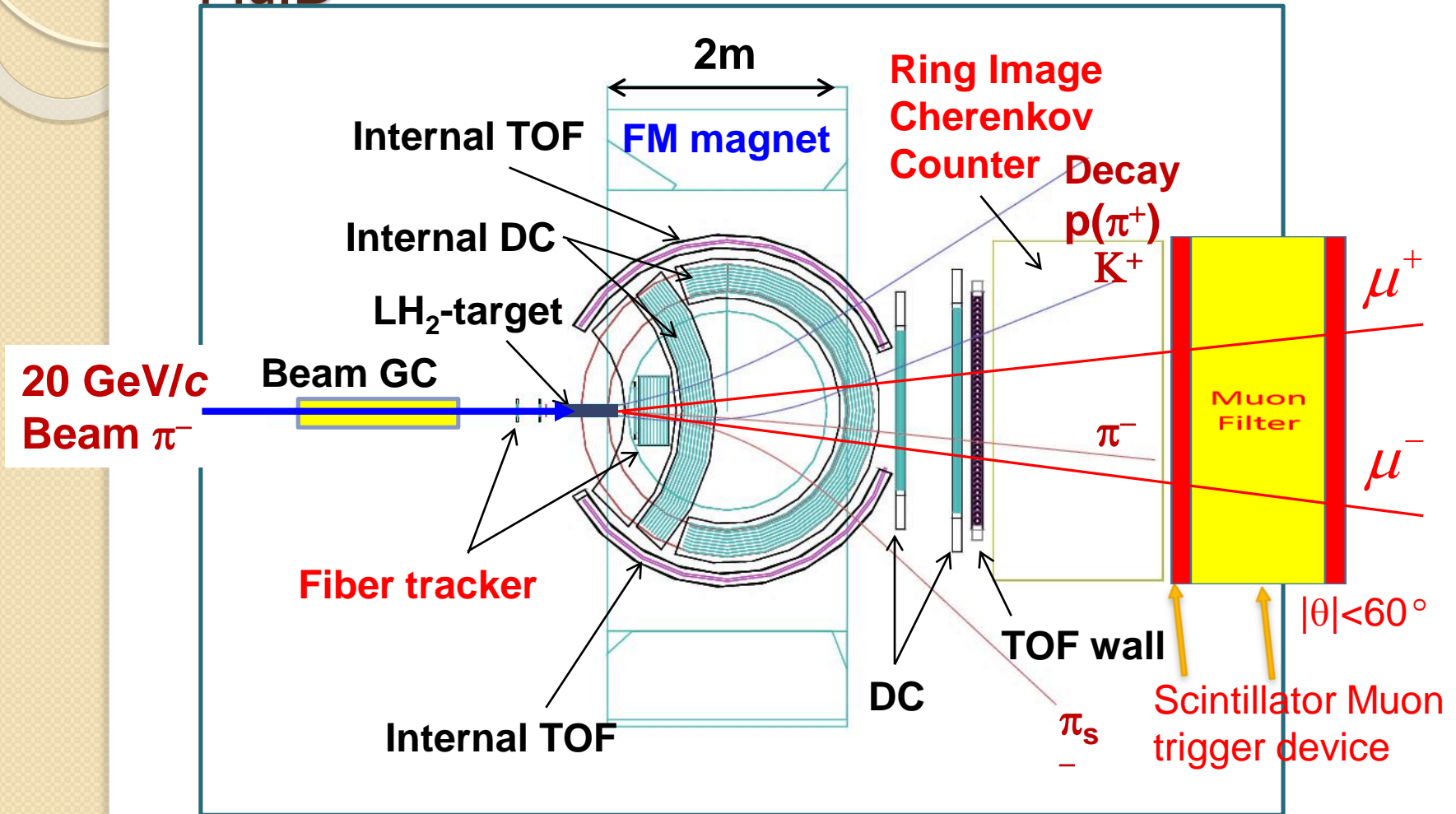
- Large Acceptance, Multi-Particle
 - K , π from D^0 decays
 - Soft π from D^{*-} decays
 - (Decay products from Y_c^*)
- High Resolution
- High Rate
 - SFT/SSD op. $>10\text{M}/\text{spill}$ at K1.8

- Good mass resolution is required
 - D^0 meson: 4.5 MeV , D^* meson: 0.7 MeV





Missing Mass Technique in E-50 Spectrometer + MuID



Acceptance: $\sim 60\%$ for D^* , $\sim 80\%$ for decay π^+

Resolution: $\Delta p/p \sim 0.2\%$ at ~ 5 GeV/c (Rigidity: ~ 2.1 Tm)

Experimental Conditions

- **Target** : 57cm LH₂ ($n_{TGT}=4 \text{ g/cm}^2$)
- **$\epsilon(\text{DAQ, Tracking, PID}) = 0.9*0.7*0.9$**
- **Beam momentum resolution**: $\Delta p/p = 0.1 \%$
- **Detector resolution**: $\Delta M/M = 1 \%$
- **Exclusive DY**: $\sim 1.2 \text{ events/day/pb}$ for $I_{\text{beam}} = 10^7 \text{ } \pi/\text{s}$
- **Beam Time**: 50 days

Yield Estimation

Event Generator

- Inclusive Drell-Yan

Pythia 6.4.26

- Exclusive Drell-Yan

GPD:

Pire 2001: EPJC 23, 675 (2002)

Kroll 2013: EPJC 73, 2278 (2013)

Kroll 2015: arXiv: 1506.04619

- Background

JAM 1.132

Particle Transportation + Detector

Geant 4.9.3

(E-50 spectrometer + Muon ID)

Total Cross Section

Inclusive Drell-Yan ($M_{\mu\mu} > 1.5 \text{ GeV}$)

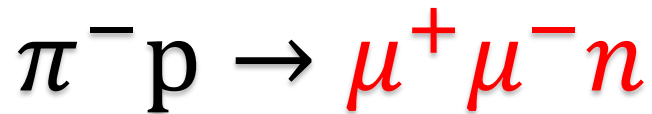
	π^-	π^+
10 GeV	2.11 nb	0.323 nb
15 GeV	2.71 nb	0.493 nb
20 GeV	3.08 nb	0.616 nb

Exclusive Drell-Yan ($M_{\mu\mu} > 1.5 \text{ GeV}$, $|t-t_0| < 0.5 \text{ GeV}^2$)

	π^- (Pire 2001)	π^- (Kroll 2013)	π^- (Kroll 2015)
10 GeV	6.28 pb	17.53 pb	140 pb
15 GeV	4.66 pb	10.64 pb	20 pb
20 GeV	3.69 pb	7.24 pb	

Hadronic Background

	π	π^+
10 GeV	26.9 mb	24.8 mb
15 GeV	25.8 mb	24.1 mb
20 GeV	25.1 mb	23.5 mb

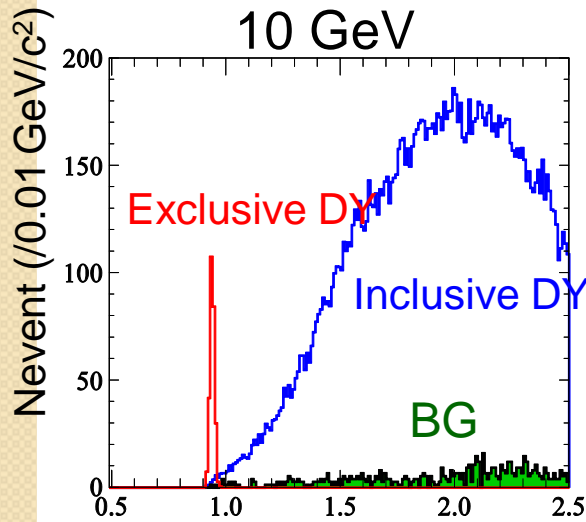


M_X In E-50 Spectrometer + MuID

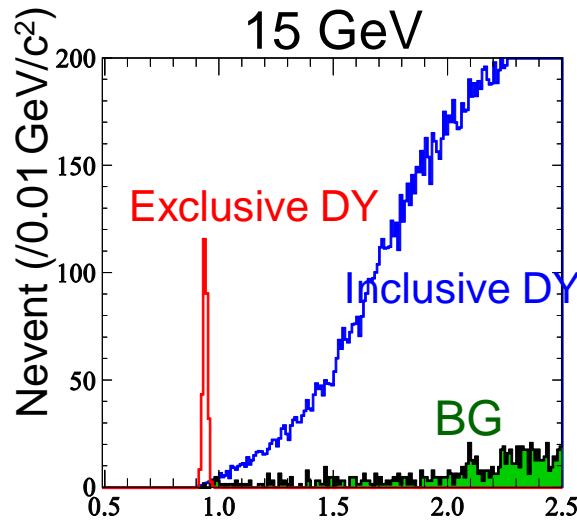
π^- beam 50 days

$$1.5 < M_{\mu^+\mu^-} < 2.9 \text{ GeV}/c^2$$

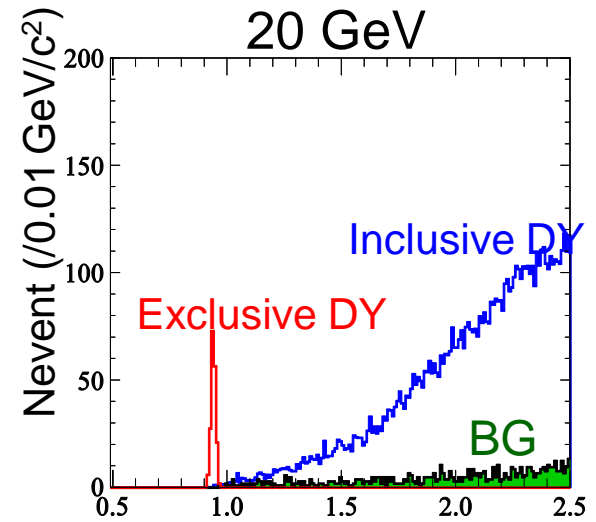
Beam Momentum



Missing Mass M_X (GeV/c^2)



Missing Mass M_X (GeV/c^2)



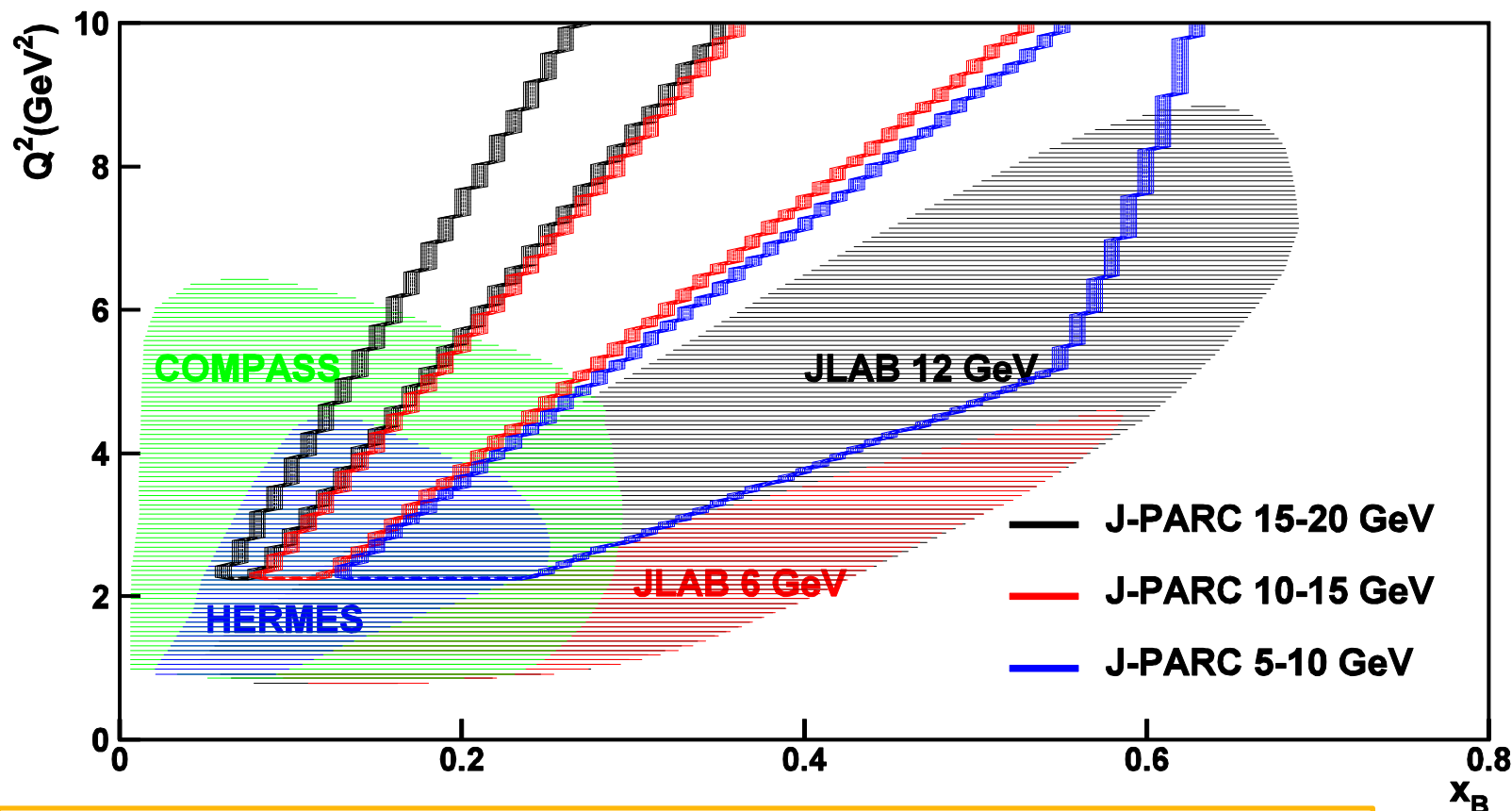
Missing Mass M_X (GeV/c^2)

S. Sawada (KEK)
 S. Kumano (KEK)
 J.C. Peng (UIUC)
 T. Sawada (AS)
 W.C. Chang (AS)

- The signal of exclusive Drell-Yan processes can be clearly identified in the missing mass spectrum of dimuon pairs.
- Because of the low event rate, this program could be accommodated into the E50 experiment.

GPD($x_B, t; Q^2$) from space-like and time-like processes

Large- Q^2 region



- J-PARC: time-like approach and large- Q^2 region.

Impacts of GPD measurements at J- PARC

- Information of GPD at large- Q^2 region.
- Test of universality of GPD in space-like and time-like processes.
- Test of QCD-evolution properties of GPD.
- Test of factorization of exclusive Drell-Yan process.

Summary

- Drell-Yan process, based on the EM annihilation of quarks and antiquarks from two hadrons, is a powerful experimental tool for exploring nucleon quark structures.
- Unique information of sea quark distributions has been obtained with Drell-Yan/W-boson experiments.
- The coming polarized Drell-Yan experiments will offer a clean ground for extracting TMD functions without the complication of fragmentation. A successful measurement of Sivers and Boer-Mulders functions in Drell-Yan process will mark a milestone of perturbative QCD and TMD physics.
- The measurement of exclusive meson-induced Drell-Yan process at J-PRAC will determine GPD in time-like process and large- Q^2 region.

References

- I. R. Kenyon, “*The Drell-Yan process*”, Rep. Prog. Phys. 45 (1982) 1261.
- T.M. Yan, “*Naive Drell-Yan and Its Successor*”, arXiv:hep-ph/9810268.
- W.C. Chang and D. Dutta, “*The pionic Drell-Yan process: a brief survey*”, Int. J. Mod. Phys. E 22 (2013) 1330020 [arXiv:1306.3971].
- J.C. Peng and J.W. Qiu, “*Novel phenomenology of parton distributions from the Drell-Yan process*”, Progress in Part. and Nucl. Phys. 76 (2014) 43 [arXiv:1401.0934].
- W.C. Chang and J.C. Peng, “*Flavor Structure of the Nucleon Sea* “, Progress in Particle and Nuclear Physics 79 (2014) 95 [arXiv:1406.1260].
- <http://users.phys.psu.edu/~cteq/schools/summer04/olness/olness.pdf>
- <http://users.phys.psu.edu/~cteq/schools/summer05/sterman/sterman.pdf>